THE DEVELOPMENT AND APPLICATION OF QUANTITATIVE REVERSE

TRANSCRIPTASE POLYMERASE CHAIN REACTION FOR

THE DETECTION OF AVIAN REOVIRUSES

Except where reference is made to the work of others, the work described in this dissertation is my own or was done in collaboration with my advisory committee. This dissertation does not include proprietary or classified information.

_____

Kejun Guo

Certificate of Approval:

_____

Sandra J. Ewald
Professor
Pathobiology and Poultry Science

_____

Joseph J. Giambrone, Chair
Professor
Poultry Science

_____

Vicky van Santen
Associate Professor
Pathobiology

_____

Richard C. Bird
Professor
Pathobiology

_____

George T. Flowers
Interim Dean
Graduate School

THE DEVELOPMENT AND APPLICATION OF QUANTITATIVE REVERSE TRANSCRIPTASE POLYMERASE CHAIN REACTION FOR THE DETECTION OF AVIAN REOVIRUSES

Kejun Guo

A Dissertation

Submitted to

the Graduate Faculty of

Auburn University

in Partial Fulfillment of the

Requirements for the

Degree of

Doctor of Philosophy

Auburn, Alabama
August 9, 2008

THE DEVELOPMENT AND APPLICATION OF QUANTITATIVE REVERSE TRANSCRIPTASE POLYMERASE CHAIN REACTION FOR THE DETECTION OF AVIAN REOVIRUSES

Kejun Guo

_____
Signature of Author

_____
Date of Graduation

VITA

Kejun Guo, son of Qing Guo and Xiaoqing Su, was born on September 17th, 1971, in Guiyang, Guizhou province, People's Republic of China. He graduated from Beijing Agricultural University (BAU) with the degree of Doctor of Veterinary Medicine (D.V.M.) in July, 1993. He went on to earn a Master's degree in Traditional Chinese Veterinary Medicine from China Agricultural University (the former BAU) in July, 1997. After working for Beijing Clever Educational Software Company as a professional programmer, he was admitted into the Department of Animal and Avian Sciences at University of Maryland and earned another Master's degree in 2004, in the area of mathematical modeling and optimizing nitrogen metabolism in dairy cattle to minimize nitrogen losses to the environment. In August 2004, he transferred and continued his graduate study for the degree of Ph. D. in the Department of Poultry Science at Auburn University.

DISSERTATION ABSTRACT

THE DEVELOPMENT AND APPLICATION OF QUANTITATIVE REVERSE TRANSCRIPTASE POLYMERASE CHAIN REACTION FOR THE DETECTION OF AVIAN REOVIRUSES

Kejun Guo

Doctor of Philosophy, August 9, 2008
(Master of Science, University of Maryland, 2004)
(Master of Science, China Agricultural University, 1997)
(Doctor of Veterinary Medicine, Beijing Agricultural University, 1993)

171 Typed Pages

Directed by Joseph J. Giambrone

We developed a TaqMan probe based real-time RT-PCR for qualitative and quantitative detection of avian reoviruses (ARVs). The primer-probe set was designed from the conserved region of ARV S4 genome segment. ARV strains S1133, 2408, CO8, 1733, JR1, ss412, and two vaccine strains (ChickVac™ and V.A. Vac®) were tested. Specificity tests indicated that the real-time RT-PCR had high specificity in the detection of 8 ARVs with no cross-reaction with other avian viruses. TaqMan real-time PCR successfully detected CO8 and ss412, which belonged in different serological subgroups compared with the other 6 strains. Full

-length ARV S4 gene was cloned and *in vitro* transcription performed to produce a pure ARV S4 RNA standard, which was used for sensitivity tests. Compared to traditional RT-PCR, real-time RT-PCR was about 150 times more sensitive. The detection limit of the real-time RT-PCR was approximately 25 ARV genome copies, which was equivalent to 5 copies/µl. Statistical analyses indicated excellent reproducibility.

Correlations between ARV genome copies and virus titer (EID_{50} and $TCID_{50}$) were determined using 7-day chicken embryos and chicken embryo kidney cell culture. Results indicated that for ARV strain 2408, 1 EID_{50} was equivalent to 3.9 ± 0.8 ARV genome copies, and 1 $TCID_{50}$ was equivalent to 2.9 ±0.3 ARV genome copies.

The TaqMan probe-based real-time RT-PCR developed was used to monitor ARV shedding in feces of commercial and specific-pathogen-free chickens infected with ARV 2408. ARV was detected in cloacal swabs at 1 day post-inoculation and throughout the tested period. Commercial chickens, which had high maternal ARV antibody titer, showed minimal clinical signs and low ARV excretion in the feces, whereas the SPF chickens had 30% mortality, more severe clinical signs, and higher virus shedding.

A SYBR-Green I based real-time PCR was developed to differentiate closely related ARV strains. Three primers sets were designed to amplify three partially overlapping regions, which covered a majority of mutation sites. Subsequently, melting curve analyses were performed to determine the unique melting peak temperature (T_m) of each region. Results indicated that each ARV strain had a

specific profile of T_m combination within the three regions. Strains CO8 and ss412 demonstrated more variations in T_m profiles than other tested strains, indicating that they may belong to different subgroups.

ACKNOWLEDGMENTS

I want to express my gratitude to Dr. Joseph Giambrone for his advice and guidance on my research and study in the past four years.

I would like to show my appreciation to Dr. Sandra Ewald, Dr. Vicky van Santen, and Dr. Richard Bird for help and directions in my research and the writing of this dissertation. Special thanks to Dr. Narendra Singh for reviewing this dissertation. I also want to thank Ms. Teresa Dormitorio and Shan-chia Ou for their help and friendship.

Most importantly, I want to express my deepest gratitude to my dearest wife Lin and our son Daniel for their unconditional support, encouragement, and love over the years.

Style or journal used: Journal of Virological Methods

Computer software used: Vector *NTI*® (*Invitrogen*), Microsoft Word®, Excel® 2007, SAS® 9.1, Windows XP Professional, KaleidaGraph 4.0

TABLE OF CONTENTS

LIST OF TABLES …… xi

LIST OF FIGURES ……. xiii

CHAPTER I: GENERAL INTRODUCTION …….. 1

CHAPTER II: LITERATURE REVIEW ……. 5

2.1 The history of avian reovirus ……. 5
2.2 The general biology of avian reoviruses ……..... 6
2.3 Characteristics of avian reovirus genomic RNA ……. 7
2.4 Avian reovirus protein coding assignments and their functions ….... 9
2.5 Genetic variation of avian reoviruses …….. 17
2.6 Avian reovirus replication ……... 19
2.7 Serological characteristics of avian reovirus …….. 24
2.8 Avian reovirus epidemiology …….. 25
2.9 Pathogenesis and molecular pathogenesis of avian reovirus …….. 27
2.10 Avian reovirus pathology …… 31
2.11 Avian reovirus immunology …… 34
2.12 The prevention and control of avian reovirus infections ……. 37
2.13 The detection and identification of avian reovirus ……..... 39
2.14 Polymerase chain reaction …….. 42
2.15 Real-time polymerase chain reaction …….. 44

CHAPTER III: DEVELOPMENT OF REAL-TIME RT-PCR FOR RAPID DETECTION OF AVIAN REOVIRUSES ……. 53

3.1 Introduction …….. 53
3.2 Materials and methods ……. 55

3.3 Results …….. 60
3.4 Discussion …… 62
CHAPTER IV: DETECTING AND MONITORING AVIAN REOVIRUS SHEDDING FROM CLOACAL SWABS USING REAL-TIME RT-PCR ……..…….. 82
4.1 Introduction …… 82
4.2 Materials and methods ……. 84
4.3 Results ……. 87
4.4 Discussion …… 89
CHAPTER V: DIFFERENTIATION OF NORTH AMERICAN AVIAN REOVIRUS STRAINS USING SYBR-GREEN I BASED TWO-STEP REAL-TIME RT-PCR WITH MELTING CURVE ANALYSIS ……... 103
5.1 Introduction ……. 103
5.2 Materials and methods …… 106
5.3 Results …… 110
5.4 Discussion ……..... 112
5.5 Conclusion ……. 115
DISSERTATION CONCLUSIONS …….. 127
BIBLIOGRAPHY …… 130
APPENDIX ……. 153

LIST OF TABLES

Table 2.1	The comparison of protein coding assignment and their locations between mammalian reovirus and avian reovirus.……	11
Table 3.1	Diseases associated with ARV strains ……..	69
Table 3.2	Real-time and conventional RT-PCR primers and TaqMan probe sequences ……..	70
Table 3.3	Intra-experimental reproducibility of real-time RT-PCR assay ……	71
Table 3.4	Statistics for standard curve and regression equations …….	72
Table 3.5	Correlation between strain 2408 viral genome copy number and titers ……..	73
Table 4.1	TaqMan real-time PCR primer and probe sequences ……...	96
Table 4.2	Disease in chickens infected with ARV strain 2408 ……...	97
Table 5.1	Disease association of different ARV strains ……...	120
Table 5.2	SYBR-Green based real-time PCR primer sequences …… ……	121
Table 5.3	Sites point mutations of different ARV strains discovered by multiple alignment analyses of the σC genes ……	122

LIST OF FIGURES

Figure 3.1 Multiple alignment analysis (partial) of ARV S4 genome segments and positions of primers …….. 74

Figure 3.2 Diagram of using restriction enzyme digestion to determine the orientation of blunt-end inserts ……. 75

Figure 3.3 Comparison of ARV infected chicken embryos and uninfected chicken embryos ……... 76

Figure 3.4 Specificity test of real-time RT-PCR …… 77

Figure 3.5 Limiting dilution assay determining the detection limit of real-time RT-PCR ……. 78

Figure 3.6 Electrophoresis photo of conventional RT-PCR of serial dilution of cloned ARV S4 gene ……. 79

Figure 3.7 Amplification curves of 10-fold serial dilutions of cloned ARV S4 RNA …….. 80

Figure 3.8 Standard curves of the current TaqMan real-time RT-PCR assay and regression equations ……. 81

Figure 4.1 Liver congestion and necrotic foci observed in a SPF chick, which died in first week of infection with ARV ……... 98

Figure 4.2 Gross lesions at 21 days in infected SPF chickens ……... 99

Figure 4.3 Comparison of infected footpad in an SPF chicken and a normal chicken …….. 100

Figure 4.4 Percentage of birds positive for ARV from fecal swabs detected by real-time RT-PCR of both commercial and SPF chicks …… 101

Figure 4.5 Amount of ARV detected in fecal swabs after infection monitored by real-time RT-PCR for both commercial and SPF chicks ……..….. 102

Figure 5.1 Schematic diagram of the experimental design ……..... 123

Figure 5.2 Mean melting peak temperature profiles of different ARV strains... 124

Figure 5.3 Multiple comparisons of mean ΔT_ms of different ARV strains at the three regions ……. 125

Figure 5.4 Phylogenetic analyses of North American ARVs..……..….…… 126

CHAPTER I: GENERAL INTRODUCTION

Reo-virus stands for "Respiratory Enteric Orphan virus", which was first isolated from the respiratory and intestinal tract of an apparently healthy individual in the 1950s. Reoviruses were so named because they were not related with any known disease at the time. Even though reoviruses have already been identified to be associated with various diseases, the original name is still used.

Reoviruses belong to the family of *Reoviridae*, which consists of 12 genera from a great variety of hosts, including mammals, reptilian and avian species (*Orthoreovirus*), human (*Rotavirus, Coltivirus, and Seadornavirus*), ruminants (*Orbivirus*), fishes (*Aquareovirus*); and invertebrates (*Cypovirus*, *Idnoreovirus*), plants (*Fijivirus*, *Oryzavirus*, and *Phytoreovirus*), even fungi (*Mycoreovirus*). There are more than 150 species of viruses in the *Reoviridae* family unified by one unique feature of their genetic makeup-segmented double-stranded RNA (dsRNA) genomes (Mertens, 2004; Nibert, 1998).

Avian reoviruses (ARVs) are one of the five members of *Orthoreovirus* genus, which contains several other distinctive groups, including non-fusogenic mammalian orthoreovirus, two fusogenic mammalian reoviruses (MRV) Nelson Bay virus and Baboon reovirus, and other reoviruses isolated from reptilian species. Reoviruses of mammalian and avian origin appear to be closely related in their protein-coding patterns of the dsRNA genome segments. Reassortments of genomic dsRNA segments can

occur both in laboratory and natural conditions. MRVs have no recognizable strict host preferences, and they can invade many different mammalian species. Similarly ARVs can infect a variety of avian species. The divergence between MRVs and ARVs is big enough to create enough barrier to separate them into distinct and orthoreovirus species (Mertens, 2004; Nibert, 1998).

Genomes of both MRVs and ARVs contain 10 dsRNA segments, which can be categorized into three classes corresponding to electrophoretic mobility: L (large), M (medium), and S (Small). There are three segments in the L-class (L1, L2, and L3), three segments in the M-class (M1, M2, and M3), and four segments in the S-class (S1, S2, S3 and S4), all of which are enclosed in a double-layer capsid of 70-80nm in diameter. Segment length ranges from 3.9kbp to 1.1kbp, and most encode a single protein, except for S1 gene, which encodes for 3 proteins (Joklik, 1983; Schnitzer et al., 1982). ARVs are different from most mammalian counterparts in their lack of hemagglutinating ability (Olson, 1978), their ability to cause cell-cell fusion (Kawamura et al., 1965; Kibenge and Wilcox, 1983), their diverse host range (Glass et al., 1973), and their distinct species-specific antigens (Olson, 1978).

Studies indicated that there are significant antigenic diversities among the Asian, European, Australian and American ARV isolates (Deshmukh et al., 1969; Hieronymus et al., 1983; Kawamura and Tsubahara, 1966; Robertson and Wilcox, 1986; Sahu and Olson, 1975; Sterner et al., 1989; Takase et al., 1987; van der Heide, 2000). From results of virus neutralization tests and serological assays, researchers were able to categorize the ARV isolates worldwide into 11 distinct serotypes (Wood et al., 1980). However, the heterogeneities in their pathogenicity and antigenicity are not absolute,

because there are considerable cross-reactions among different serotypes (Robertson and Wilcox, 1986). Phylogenetic analyses revealed that the European and Asian isolates were more dispersed in their attachment protein (σC) sequences than those from the US and Australia (Kant et al., 2003).

Although ARV was first isolated in 1954 from chickens with chronic respiratory diseases (Fahey and Crawley, 1954), it was not recognized as a distinct viral species until the discovery of viral arthritis-causing reovirus and their antigenic and pathogenic similarities in 1957 (Olson et al., 1957; Olson and Weiss, 1972). Since then, ARVs have been isolated from chickens with various disease conditions from many countries (Bagust and Westbury, 1975; Bains and MacKenzie, 1974; Dutta and Pomeroy, 1969; Glass et al., 1973; Olson and Kerr, 1966; Page et al., 1982a; Pradhan et al., 1987; Rosenberger et al., 1989; van der Heide et al., 1983). The ARVs have also been associated with many diseases in chickens, including viral arthritis/tenosynovitis (Kibenge and Wilcox, 1983; van der Heide and Kalbac, 1975), enteritis/runting stunting/malabsorption syndrome (MAS) (Goodwin et al., 1993; Hieronymus et al., 1983; Page et al., 1982a), inclusion body hepatitis (Mandelli et al., 1978; McFerran et al., 1976b), and myocarditis (Bains and MacKenzie, 1974; Jones, 1976).

Economic losses resulting from ARV infections are due to low hatchability, high mortality and morbidity, and poor growth and feed conversion. Viral arthritis also causes lameness, reduced weight gain caused by inability of reaching feed, as well as downgrading of carcasses at slaughter due to the unpleasant appearance of the affected hock joints. As for any infectious diseases, rapid, accurate, and highly sensitive detection of ARVs is critical for the effective prevention and control of ARV infections.

In addition, studies of the relationships between antigenicity, pathogenicity and genetic variations among the ARVs will yield essential knowledge and can be beneficial for effective vaccine development for the prevention and control of ARV infections and diseases.

The current study had the following objectives: 1) to develop a highly specific and sensitive method for the detection of ARVs using real-time reverse transcription (RT) polymerase chain reaction (PCR); 2). to study ARV (enteric form) infection progression and evaluate the real-time RT-PCR method by detecting and monitoring virus shedding in cloacal swab samples; 3). to understand the genetic diversities in the S1 genes and S4 genes among ARVs using nested RT-PCR, followed by nucleotide sequencing and phylogenetic analysis; and 4). to develop a SYBR-Green I real-time RT-PCR protocol and use melting curve analyses to differentiate ARV strains based on the nucleotide sequence variations in σC gene.

CHAPTER II: THE REVIEW OF LITERATURE

2.1 The history of avian reovirus

Knowledge about ARV was little until the accidental discovery made by Olson *et al.* in 1957 while studying *Mycoplasma synoviae*. An unknown agent produced similar synovitis signs and lesions in broiler chicken as *M. synoviae*; however, it did not respond to antibiotics (Olson et al., 1957). Additionally, unlike the *M. synoviae* infection, the synovitis-causing agent displayed an age-dependency in that only young chicks were susceptible to the infection (Kerr and Olson, 1964). These characteristics were consistent with a viral origin; therefore it was named "viral arthritis agent" (Olson and Kerr, 1966). In 1972, using electron microscopy, researchers determined that the virus had similar characteristics including virion structure, particle size, location in an infected cell as those of MRVs (van der Heide and Page, 1980). They determined that "viral arthritis agent" was a reovirus of avian origin.

Later, scientists found that viral arthritis was not the only disease associated with ARV infection. In fact, the "Fahey-Crawley virus", which was isolated from chickens with chronic respiratory diseases back in 1954 (Fahey and Crawley, 1954), had not only similar molecular structures with the viral arthritis-causing ARV, but had similar antigenicities, which put them in the same antigenic serotype (Olson and Weiss, 1972; Walker et al., 1972). By using experimental infection and virus isolation, researchers

associated ARV infections with an array of avian diseases, including enteritis and cloacal pasting (Dutta and Pomeroy, 1969), inclusion body hepatitis (McFerran et al., 1976a), myocarditis (Bains and MacKenzie, 1974), sudden increase of mortality because of lesions to the liver, kidney in young chickens (Bagust and Westbury, 1975), and so-called runting-stunting syndrome or malabsorption syndrome (MAS) (Goodwin et al., 1993; Page et al., 1982a; Pass et al., 1982; Vertommen et al., 1980) *etc.* ARVs have become recognized as important pathogens and research targets for disease prevention in the poultry industry.

2.2 The general biology of avian reoviruses

Avian reoviruses belong to the *Orthoreovirus* genus of the *Reoviridae* family (Mertens, 2004; Nibert, 1998), and are ubiquitous in nature. Reoviruses have a dual layer concentric capsid structure with a buoyant density of 1.37 g/ml, comprised of an outer capsid of ~85 nm in diameter, and an inner core of ~45 nm in diameter. The double capsid structure encloses a center cavity of 38nm in diameter, which accommodates the 10 segmented genomic dsRNA (Joklik, 1983; Luftig et al., 1972; Zhang et al., 2005) and many small, adenine-rich, single-stranded oligonucleotides of unknown function (Spandidos and Graham, 1976).

Avian reovirions are non-enveloped, which makes them resistant to adverse conditions. ARVs are stable between pH 3.0 and pH 9.0, and they can survive at ambient temperatures on common materials, such as feathers, wood shavings, glass, rubber and galvanized metal for up to ten days. They can even survive for ten weeks in water and at 4 $^{\circ}$C for three years without effect on their infectivity. However, they can be

inactivated at 56°C for less than an hour (Jones, 2000; Olson and Kerr, 1966). Some strains of ARVs have been reported to be resistant to proteolytic enzymes, such as trypsin, which makes them good candidates for vaccines administrated through drinking water (Al-Muffarej et al., 1996). ARVs can withstand certain disinfectants. Some strains can survive 2% formaldehyde at 4°C (Meulemans and Halen, 1982) and others were only partially inactivated after 24hr at room temperature in 2% phenol. They can be effectively inactivated by 0.5% organic iodine or 70-100% ethyl alcohol (Glass et al., 1973; Petek et al., 1967).

Although ARVs have similar structural and molecular composition as their mammalian counterparts, they also differ from MRVs in many aspects. ARVs do not hemagglutinate red blood cells (Glass et al., 1973), and they have the ability to cause cell-cell fusion (Duncan and Sullivan, 1998; Kawamura et al., 1965). In addition, ARVs only infect avian species and are associated with distinct pathological conditions, such as tenosynovitis (Robertson and Wilcox, 1986). MRVs are propagated on established murine and human cell lines. Most of the ARV strains only grow in primary culture of avian cells (Guneratne et al., 1982) with few exceptions, in which cases the ARV strains have been adapted to mammalian cell lines (Nwajei et al., 1988; Robertson and Wilcox, 1986).

2.3 Characteristics of avian reovirus genomic RNA

Avian reovirus genomes are double-stranded. Physicochemical analyses revealed that the base composition for both A/U and C/G ratios are identical and the genome segments are resistant to single-strand-specific nucleases, which indicated that the two strands of

each segment are collinear and complementary (Nibert and Schiff, 2001). The 10 dsRNA genome segments can be categorized into three groups, which are designated L (large), M (medium), and S (small), based on their size and electrophoretic mobility (Table 2-1). There are three segments in the L-class (L1, L2 and L3), three in the M-class (M1, M2 and M3), and four segments in S-class (S1, S2, S3 and S4). The molecular weight for each of the segments has been determined by polyacrylamide gel electrophoresis: 2.4-2.7x10^6 Da for the L-class segments, 1.3-1.7x10^6 Da for the M-class segments, 0.68-0.8x10^6 Da for S4 to S2 segments, 1.2x10^6 Da for the S1segment, respectively (Spandidos and Graham, 1976). The size of S1 segment is closer to the smallest M-class segment (M3) than to the largest S-class segment (S2), which makes it a better candidate for the M-class. However, historically, because the early studies on ARV were largely comparative to its mammalian counterpart, they also inherited the 3-group categorization of the genome segments. Since ARV S1 segment, similar to the MRV, encodes the cell attachment protein, it was categorized as one of the members of the S-class segments.

As for many viruses with segmented genomes, such as influenza virus and MRVs, reassortment can occur in both natural and laboratory conditions when two different strains of ARVs co-infect the same host; and thus progeny viruses may obtain genome segments from both parent strains (Liu et al., 2003; Roner et al., 1990). Reassortment provides viruses advantages in mutation and evolution. Studying the recombinant (reassorted) viruses is very helpful for determining the functionality and phenotypic characteristics of genome segments. It can also reveal important information such as the evolution patterns and genetic lineage of a particular ARV strain (Liu et al., 2003).

Martinez-Costas *et al.* (1995) uncovered the nucleotide sequences of ARV S1133 genome except for the L2. Subsequent sequence analyses revealed that with the exception of S1 segment, all other genome segments encode only one primary translation product. The plus strand of each segment is identical to its own mRNA transcript, which is equipped with a type-1 cap structure at its 5' end, and a pyrophosphate group at the complementary position of the minus strand (3' end). The 5' cap is formed by viral capping enzyme (encoded by L3). It is recognized by cellular translation initiation factor eIF-4E, which is essential for efficient protein translation. 5' cap structure also improves the stability of the free plus strand viral RNAs and mRNA transcripts by protecting them from 5'exonucleases (Nibert and Schiff, 2001). Nucleotide sequence analyses indicated that all positive strands start with 7 bases: GCUUUUU, and end with 5 bases: UCAUC at their 5' and 3' end, respectively.

2.4 Avian reovirus protein coding assignments and their functions

The 10 genome segments encode for at least 12 primary translation products, among which segment S1 is a tricistronic gene, which expresses 3 protein products. Among all 12 viral proteins, there are 8 structural proteins that are incorporated into the newly formed virions. On the other hand, the other four viral proteins are nonstructural, and are only expressed in the processes of replication, but not in the mature progeny viral particles (Martinez-Costas et al., 1997; Varela and Benavente, 1994). Following the convention and the nomenclature of the MRV, ARV proteins are divided into three size classes L, M, and S corresponding to their encoded genome segments. The L-class proteins are designated lambda (λ), whereas the M-class proteins mu (μ), and the S-class sigma (σ) (Table 2-1). To avoid confusion with MRV, within each size class, instead of

using numbers, the structural proteins are designated with alphabetical subscripts, such as (σA, σB, etc.). There are at least 10 structural proteins in ARV virions, among which 8 of them are the primary translation products from their corresponding encoded genome segments: λA, λB, λC, μA, μB, σA, σB, and σC. On the other hand, the other two structural proteins μBN and μBC are the post-translational cleavage products of the N-terminus and C-terminus of their precursor μB, respectively (Varela et al., 1996). The nonstructural proteins are named with their own group designation and "NS", such as μNS and σNS. Similar to structural protein μB, μNS goes through post-translational modification, which results in a truncated or cleaved form μNSN and μNSC (Touris-Otero et al., 2004b). Recent studies discovered two more nonstructural proteins P10 and P17, and they are encoded by the first two open reading frames (ORF) of the only multi-cistronic segment in ARV genome-S1gene (Bodelon et al., 2001; Shmulevitz et al., 2002).

The association between the ARV proteins and their encoding segments were determined by *in vitro* translation assay using denatured genome segments (Varela and Benavente, 1994). Results indicated that the molecular weights of the polypeptides were proportional to the size of their encoding segments with the exception of the S1 gene. Although S1 is the largest of the S-class segments, the dominant protein it encodes, σC, is the smallest among all S-class polypeptides. Sequence analyses showed that S1 has a unique tricistronic structure, which includes three out-of-phrase and partially overlapping ORFs. Two of the ORFs located at 5'-proximal encode two nonstructural proteins P10 and P17 and the last ORF at 3'-proximal encodes the ARV cell attachment protein σC (Shapouri et al., 1995). The functions and the distributions of each viral protein are summarized in Table 2-1.

Table 2.1. Comparison of protein coding assignments and locations between mammalian reovirus and avian reovirus.

Genome Segment	MRV[a] Proteins	ARV[b] Proteins	Distribution (ARV)	Function (ARV)
L1	λ1	λA	Inner Core	Core shell scaffold
L2	λ2	λB	Inner Core	Putative transcriptase
L3	λ3	λC	Turrets	Capping enzyme
M1	μ2	μA	Inner Core	Putative transcriptase co-factor
M2	μ1/μ1C	μB/ μBN /μBC	Outer capsid	Penetration
M3	μNS	μNS	Nonstructural	Formation of viral factories and protein recruitment
S1	σ1 & σ1NS	σC P10 P17	Outer capsid Nonstructural Nonstructural	Cell attachment Fusogenic protein Unknown
S2	σ2	σA	Inner core	dsRNA binding, anti-interferon activity
S3	σNS	σB	Outer capsid	Unknown
S4	σ3	σNS	Nonstructural	ssRNA binding

a. Protein coding assignments proposed by McCrae and Joklik, 1978; Nibert and Schiff, 2001.
b. Protein coding assignments and functions proposed by Benavente and Martinez-Costas, 2007; Varela and Benavente, 1994.

Viral protein λA is encoded by the largest of L-class segments L1. Similar to the λ1 of MRV, this protein is considered to be a major protein that forms the inner core shell, which accommodates the virus genome segments and the viral RNA polymerase. The inner core shell then serves as the scaffold for the virus core assembly. Therefore, the expression of λA is started in the early stage of the replication cycle, and upon expression it can associate with the ARV viral factories in infected cells. In co-expression experiment with μNS, instead of diffusing evenly through the cytoplasm as when expressed alone, λA tends to aggregate around the globular inclusions (viral factories),

which suggests that μNS may be involved in recruiting of λA to the viral factories (Touris-Otero et al., 2004a).

Viral protein λB, which is encoded by L2 segment, is one of the minor components of the viral core. The actual function of this polypeptide is unknown, because L2 is the only segment that has not been fully sequenced. Comparison of the size and copy numbers within the virion with those of other members in the *Reoviridae* family suggested that λB might possess the RNA polymerase activity. However, the hypothesis is yet to be tested until the full sequence analysis is performed.

Viral protein λC is encoded by the L3 gene, and the polypeptide expands and connects both inner core and the outer capsid. The λC pentamers form turret structures, which project from the five-fold axes of the cores towards the outer capsids (Zhang et al., 2005). λC is not only a structural component of the ARV capsid, but also functions as the guanylyltransferase, which adds the 5' type-1 cap structure to the plus-strand RNAs. *In vitro* experiments revealed that λC binds with GMP with a phosphoamide linkage, and subsequently transfers the GMP moiety to GDP and GTP acceptors, which form the cap structures (Martinez-Costas et al., 1995). Multiple alignment analyses comparing the λC protein sequences of ARV with that of MRV and grass carp reovirus suggested that the GMP binding ability of λC was facilitated by two lysine residue at position 169 and 198, and the RNA-capping function of λC was conserved across different reovirus species (Hsiao et al., 2002).

Viral protein μA is another minor component of the inner capsid, which is encoded by the largest M-class segment M1. The nucleotide sequences and deduced amino acid

sequences have been reported. However, no study has elucidated the function and properties of this protein. Since the mammalian form of M1encoded protein- μ2 was shown to functionally interact with M-class nonstructural protein μNS, it is also hypothesized that μA might function similarly with μNS (Martinez-Costas et al., 1997). Using electron cryomicroscopy and image reconstruction, Zhang and coworkers (2005) discovered that μA proteins are located in the transcriptase complexes (likely formed by λB RNA polymerase) within the inner core, which indicate that functionally μA protein maybe a co-factor for transcriptases. However, another bioinformatic study indicated that μA possessed a sequence motif NH2-Leu-Ala-Leu-Asp-Pro-Pro-Phe from position 458 to 464, which was characteristic for the N-6 adenine-specific DNA methyltransferases. Furthermore, such sequence motifs were conserved in all 12 ARV strains tested (Su et al., 2006; Timinskas et al., 1995).

Viral protein μB and μBC: μB is the primary translation product of the M2 genome segment, and μBC is the product of μB after post-translational cleavage at the N-terminal side. In fact, a majority of the μB proteins in an infected cell undergo the modification, which cleaves the μB protein between residues Asn and Pro at position 42 and 43 resulting in a smaller N-terminal fragment (μBN) and a larger μBC protein (Martinez-Costas et al., 1997). Both μB and μBC are major components of the ARV outer capsid, and they also form complex with σB protein in the cytoplasm of the infected cells (Touris-Otero et al., 2004a). In addition, μBC was shown to play a critical role in virus penetration and internalization at the initiation of the infection and subsequent uncoating to release the virus core from lysosome to the cytoplasm. Such functions are facilitated

by two polypeptides δ and δ′, which are products of sequential cleavages of μBC close to its C-terminal (Duncan et al., 1996).

Viral protein μNS has a MW of 70KDa. It is a nonstructural protein encoded by the smallest M-class segment M3 (Varela and Benavente, 1994). Similar to protein μB, some μNS molecules are also cleaved near the N-terminus resulting in a smaller μNSN (15KDa) and a larger μNSC fragment (55KDa). However, the function and properties of these truncated forms of μNS are still unknown. When ARV proteins are expressed in transfected cells individually, μNS is the only protein that can form inclusions (viral factories) in the infected cells. This suggested that μNS was critical in the early stage of the virus replication cycle (Touris-Otero et al., 2004b). When μNS was co-expressed with other viral proteins in transfected cells, it displayed specific noncompetitive binding with σNS and λA, but not with other viral proteins. This may indicate a mechanism for selectively recruiting σNS and λA to the viral factories (Touris-Otero et al., 2004a).

Viral protein σC, P10, and P17. ARV S1 gene is the only non-monocistronic segment within the whole genome. Encoded by the 3'-proximal cistron of S1 gene, σC is one of the most important and most studied polypeptides among ARV proteins, because it is the only viral protein present in the soluble extract of infected cells that can attach to avian cells. Additionally, σC is the only protein that can induce ARV-specific neutralizing antibodies, which makes it a target and marker in studies on ARV genetic variations as well vaccine development (Martinez-Costas et al., 1997; Shapouri et al., 1995). σC is a minor outer capsid protein. Its native state - homotrimer- forms spike-and-knob structure from the turret and sticks out of the surface of the virion. The

distribution of σC on the surface of the ARV virion is the basis of its cell attachment activity. However, one study showed σC was active for attachment of avian cells in its oligomeric state. The mechanism by which σC protein converts from homotrimer to its monomer state is unknown (Grande et al., 2002; Martinez-Costas et al., 1997). Host cell receptors are the determinant of host range and infectivity of many viruses, and same is true for ARV. Saturation-binding experiment indicated that on the surface of a single chicken embryo fibroblast (CEF) cell, there were $2.2x10^5$ receptor units for ARV σC protein (Grande et al., 2000). Amino acid sequence analyses also revealed a receptor-binding domain at the C-terminal (residues 151-326) end, which was comparable to the head domain of the MRV cell attachment protein (Guardado Calvo et al., 2005).

The first ORF of ARV S1 segment encodes a small (10.3kDa) and yet important nonstructural protein P10. Using a P10-specific monoclonal antibody, it has been shown present in ARV infected cells (Bodelon et al., 2001; Shmulevitz et al., 2002). The expression of P10 in transfected cells has been reported to increase plasma membrane permeability, and subsequently cause extensive cell-cell fusion, thus suggested that P10 play a key role in ARV fusogenic activities. Amino acid sequence analyses confirmed that P10 had the structure of a typical type-1 transmembrane protein, which consisted of a center transmembrane domain and two intervening sequences separate the endodomain and ectodomain at each end (Bodelon et al., 2001; Shmulevitz and Duncan, 2000).

The third primary translation product expressed by S1 gene (the second ORF) is another nonstructural protein-P17 that has no sequence homology with other known viral proteins and cellular proteins. Mutation analyses revealed a functional nuclear localization signal at its carboxyl-terminal, which was further confirmed that P17 is

accumulated in the nuclei of both infected cells and transfected cells (Costas et al., 2005). A recent study indicated that P17 increased the expression of $p21^{cip1/waf1}$ and P53 and caused retardation in cell growth, when expressed in transfected mammalian cells. Results suggested that P17 may function as a nucleo-cytoplasmic shuttling protein to adjust host cell proliferation through the $p21^{cip1/waf1}$/ P53 pathway (Liu et al., 2005).

Viral protein σA is encoded by the S2 gene and it is another component of the ARV virion inner core (Martinez-Costas et al., 1997). Unlike other viral proteins, σA possesses unique sequence-independent dsRNA binding activity. It displays very high affinity to dsRNA molecules, and the σA-dsRNA complex stays stable even under high salt concentration (Martinez-Costas et al., 2000; Touris-Otero et al., 2005; Yin et al., 2000). σA was reported to have anti-interferon activity by blocking the activation of dsRNA-dependent protein kinase PKR, which helped ARV resist the host antiviral activity of interferon (Gonzalez-Lopez et al., 2003; Martinez-Costas et al., 2000). Moreover, recent study indicated that σA played another important role in ARV morphogenesis by stabilizing the core shell protein λA and promoted coating of the outer shell proteins (Xu et al., 2004).

Viral protein σB, which is a major component of the ARV outer capsid, is encoded by the S3 segment (Varela et al., 1996). Aside from its structural role, σB has no known function as compared to its MRV form σ3, which possesses similar anti-interferon activity as ARV σA (Touris-Otero et al., 2005). However, σB has been shown to bind with μB and μBC in the cytosol of the infected cells, and form a ternary complex, which

subsequently incorporated into early stage of the outer shell (Touris-Otero et al., 2004a; Touris-Otero et al., 2004b).

Viral protein σNS is encoded by the smallest segment of ARV genome-S4 (Varela and Benavente, 1994), and under RNA-free condition forms homodimer or trimer. The σNS has relatively high affinity with ssRNA such that it forms complexes with ssRNA in a sequence-independent manner. On the other hand, sequence analyses indicated that the ssRNA binding domain does have minimum length restriction of 10-20 nucleotides for mRNAs. Additionally, σNS aggregates in large ribonucleoprotein complexes in the cytoplasm and inclusions, which suggests that it may be involved in viral RNA packing and ARV replication (Touris-Otero et al., 2005).

2.5 Genetic variation of avian reoviruses

The dsRNA genome gives ARVs slight advantages over other viruses with ssRNA genomes in terms of the stability of the genetic materials. However, because of the lack of proof-reading, RNA polymerases have higher chances of mismatching during virus replication, which in turn causes higher rate of mutations. As one of the RNA viruses, ARVs also benefit from elevated mutation rate, such that they can evolve to cope with adversities. In addition, the segmented genome also gives ARV advantage of rapidly generating new recombinant strains via reassortment. In this section, several recent phylogenetic studies on ARV genome are summarized.

The *Orthoreovirus* genus consists of members with extremely diverse characteristics, and the virus species are further categorized into subgroups based on their host range and ability to induce cell-cell fusion. The genus is classified into three subgroups, non-

fusogenic MRV, fusogenic ARV and fusogenic MRV, with the last subgroup only consisting of two species (Nelson Bay virus and baboon reovirus) (Duncan et al., 1995). Cross-species phylogenetic analyses indicated that non-fusogenic MRV, ARV, Nelson Bay virus, and Baboon reovirus are four distinct species. These four species were further divided into three clades, in which ARV and Nelson Bay virus were included in the same clade and MRV and Baboon reovirus each in their own clade based on the similarity of their genetic makeup (Duncan, 1999).

Avian reovirus as one of the subgroups for *Orthoreovirus* genus includes a variety of reovirus sub-species from different avian species. There is only limited similarity in terms of nucleotide sequences and amino acid sequences. Results of phylogenetic analyses, which compare the S-class genome segments (S1 and S3) and their encoded proteins from chicken origin reoviruses with those from turkey, goose and Muscovy duck, indicated similarity of nucleotide sequences and amino acid sequences were ~53% and ~55%, respectively. Researchers suggested that non-chicken origin viruses, especially turkey reovirus should be considered in a separate subgroup (Banyai et al., 2005; Day et al., 2007; Kapczynski et al., 2002; Sellers et al., 2004). Therefore, it is important to mention that within this dissertation, unless mentioned, all ARVs stands for chicken origin reoviruses.

Various nucleotide and amino acid sequence analyses of ARVs excluding the non-chicken origin species have revealed the existence of genetic diversity (Hsu et al., 2005; Kant et al., 2003; Liu et al., 2003; Liu and Huang, 2001; Su et al., 2006). Since, σC protein is the antigenic determinant that induces neutralizing antibodies and its encoding gene is known to have higher divergence than other ARV genes, most sequence

comparisons studies were conducted on σC-encoding gene and their protein products. (Liu et al., 2003). All of the phylogenetic studies resulted in classifying the ARV isolates tested into various groups and lineages; however, meta-analytically there is no identical pattern. Such results suggested that different ARV genome segments may evolve in an independent manner (Hsu et al., 2005; Liu et al., 2003). Phylogenetic studies also provided evidences showing frequent reassortments among the circulating lineages were responsible for the topological variation in the ARV genome segments. Most importantly, all studies concluded that diversity is not correlated with the serotypes or pathotypes of the ARV isolates; instead, the time and geographic location of the isolation has more deterministic influence on ARV genetic divergence (Hsu et al., 2005; Kant et al., 2003; Liu et al., 2003).

2.6 Avian reovirus replication

The complete replication cycle of a typical ARV consists of following milestone steps: virus encounter with and attachment to the host cell, virus internalization by endocytosis, uncoating to remove the outer capsid proteins and release the inner core, viral genome transcription to produce mRNA and mRNA translation to produce viral proteins, the assembly of the progeny inner core and recruitment of ssRNA to replicate the genome, morphogenesis (recoating) – the addition of the outer capsid proteins to the completed new inner core, and lastly, the lysis of the host cell to release the progeny viruses.

2.6.1. Virus attachment, internalization and uncoating

The attachment of ARV to host cell is mediated by the specific interactions of the minor outer capsid protein σC and host cell surface receptors (Grande et al., 2000;

Shapouri et al., 1995). The information regarding the structure, identity and the properties of the host cell receptors is not available; however, some unpublished results from Martinez-Costas's group provided interesting insights. The attachment process of ARV, unlike its mammalian counterpart, was not inhibited by glycosidases, lipases, or EDTA, instead, it is only affected by exposing to proteases. This indicates that ARV attachment utilizes a novel (unknown) mechanism, which does not involve sialic acid-based receptors (Benavente and Martinez-Costas, 2007). ARV was reported to attach and replicate in mammalian cell lines, but not the other way around, suggesting that the receptors responsible for ARV attachment are ubiquitous and the lack of MRV receptors on avian cell surface created the host-specific barrier for MRV infection (Barton et al., 2001; Robertson and Wilcox, 1986). In addition, saturation-binding assay determined that there are $1.8x10^4$ receptors sites for ARV particles per cell (Grande et al., 2000). As a non-enveloped virus, ARV is internalized by receptor-mediated endocytosis, and the outer capsid proteins are removed by lysosomal proteases within the vacuoles. Uncoating processes are believed to be mediated by proton-ATPase driven endosomal acidification, which promotes the partial or total removal of the outer capsid and generates the subviral particles that are capable of crossing the membrane (Carrasco, 1994). In the proteolytic uncoating processes, ARV major outer capsid protein μBC is sequentially cleaved at its carboxyl-terminal, which generates two truncated polypeptides δ and δ′. The first cleavage product-δ appears to be homologous to the MRV form of cleaved μ1C, which is known to play a critical role in MRV entry and uncoating. However, the function and properties of the second cleavage product- δ′and its role in

ARV uncoating process require further investigation (Duncan, 1996; Nibert and Fields, 1992).

2.6.2. Viral gene expression

Viral gene expression processes include the transcription of the viral genome to produce viral mRNA, and subsequent production of viral proteins utilizing the cellular machinery. Because of the dsRNA nature of the ARV genome, the transcription process relies on the catalytic activity of ARV built-in RNA-dependent RNA polymerase, which utilizes the negative strand as the template to generate all 10 viral mRNAs. Although the actual identity of the ARV RNA polymerase and its encoding gene in the genome are still not clear, experimental evidence suggests its association with the core components, because the inner core and the intermediate subviral particles (ISVPs) are capable of catalyzing the transcription of all 10 full length mRNAs *in vitro* (Martinez-Costas et al., 1995).

Mature ARV mRNAs are identical to the positive strand of their encoding genes, which makes them serve both in translation for production of viral proteins and in replication as the templates for generating complementary negative strands. All transcripts are equipped with a type-1 cap structure at their 5' terminal, but with no 3' polyadenylation. There are short untranslated regions at both 5' and 3' ends (Martinez-Costas et al., 1995). Electron cryomicroscopy analyses revealed that ARV protein λC, whose pentamer mode forms the turret structure extended from inner core to the outer capsid, has mRNA capping enzyme activity (Zhang et al., 2005). It is believed that viral mRNAs are synthesized with the virus core, and a type-1 cap is added when they are exiting the viral core through the channel inside the turrets into the cytoplasm. This

model is consistent with the fact that viral cores or ISVPs are required for effective *in vitro* transcription of ARV viral mRNAs (Martinez-Costas et al., 1995; Zhang et al., 2005).

Since viruses utilize cellular machinery to translate viral mRNAs and produce viral proteins, their viral transcripts are mimicking the valid cellular mRNAs, so that they can be recognized by the ribosomes. This is also true for ARVs that all their viral mRNAs except for S1 segment are monocistronic and the translation processes for these viral transcripts follow the rule of standard cellular mRNAs. On the other hand, the mechanism for translating the tricistronic S1 mRNA to produce three different polypeptides is still under investigation. Nucleotide sequence analyses revealed relatively weak contexts surrounding the start codons of the first and second cistrons, which result in low translational efficiency for these two ORFs. Experimental optimization of the leading sequence of the first cistron increased the production of P10 without affecting the expression of distant σC (Shmulevitz et al., 2002). Scientists proposed that the translation of the first two cistrons might follow the "leaking scanning" scheme, so that while a subset of ribosome subunits are translating the weak cistron, the other subunits slide along the transcript looking for the downstream start codon to initiate alternative translation processes (Kozak, 1991). In any case, a multicistronic gene is beneficial in improving the coding capacity within the limited genome size. It may as well serve as mechanism to regulate the expression of the downstream cistrons, since the requirement for σC protein is relatively small. Additionally, the regulation of the expression of ARV genes appears to be translational, because even though the amount of

the viral proteins expressed within infected cells varies, yet, the original viral transcripts were produced in similar amounts (Nibert and Schiff, 2001).

2.6.3. Morphogenesis and virus exit

The morphogenesis processes involve recruiting newly synthesized viral proteins into the viral factories and incorporating them onto the viral cores to build the new viral particles. After assembling the progeny virions, they are released to the surrounding cells, thus concluding the replication cycle. ARV forms inclusions (also known as the viral factories), which are globular shaped, contain no organelles, and are so named because they are the location for manufacturing new viral particles (Fields et al., 1971; Silverstein and Schur, 1970; Touris-Otero et al., 2004a; Touris-Otero et al., 2004b).

The M-class nonstructural protein μNS is the only ARV protein known to form inclusion in infected cells when expressed individually. In addition, μNS also mediates the selective recruitment of viral proteins σNS and λA, but not other proteins (Touris-Otero et al., 2004a; Touris-Otero et al., 2004b). By combining the metabolic pulse-chase labeling technique with cell fraction and antibody immunoprecipitation assay to study the recruitment of newly synthesized viral proteins into viral factories, Touris-Otero and co-workers (2004a) revealed that the ARV morphogenesis occurred exclusively within the globular inclusions and unlike its mammalian counterparts, it is not microtubule-associated. The morphogenesis processes are regulated in a timely manner, so that it takes about 30 min for the assembly of the viral core after the expression of the viral proteins and another 30 min is needed for assembling the outer capsid. The mechanism by which newly formed ARV progeny exit the host cell is still unknown, but the discovery of the fusogenic protein P10 and its permeablizing activity suggested that P10

plays an important role in ARV exiting (Bodelon et al., 2001; Shmulevitz and Duncan, 2000).

2.7 Serological characteristics of avian reovirus

Phylogenetic studies on the nucleotide and amino acid sequences of ARV genome have shown diversity among the ARV isolates around the world, and serological studies are in agreement that great variations exist and as such resulted in complex serological classification of ARVs (Deshmukh et al., 1969; Hieronymus et al., 1983; Kawamura and Tsubahara, 1966; Robertson and Wilcox, 1986; Sahu and Olson, 1975; Sterner et al., 1989; Takase et al., 1987; van der Heide, 2000). The heterogeneity in sequences and serological classifications may be due the relatively high mutation rate of RNA viruses, and the reassortment or recombination of the segmented genome (Rekik et al., 1991). Because of the high frequency of mixing and matching (reassortment) of the genome segments, most of the isolates share the similar genome segments. As the result, there are cross reactions for serological classification between ARV isolates and all US ARVs belong to the same serotype.

Avian reovirus subtypes are determined by cross virus neutralization (VN) assay that measures percentage of plaque-reduction in primary chicken kidney cell culture (Wood et al., 1980). With this test, which measures the level of cross reactivity and relatedness, virologists categorized an array of ARV isolates into multiple subtypes. Among these studies, Kawamura *et al.* (1965) and Takase *et al.* (1987) reported similar results by classifying a large numbers of Japanese ARV isolates into 5 subtypes, whereas Wood *et al.* (1980) identified 11 subgroups among isolates from many countries. In Australia, 10 isolates were grouped into 3 subtypes (Robertson et al., 1984) and in the US, all the ARV

isolates were closely related (van der Heide, 2000). Although no unified classification resulted from these studies, they are in agreement with results from phylogenetic studies, which show greater diversities in ARV lineages in the Netherlands, Germany, and Asia, especially Taiwan, than in the US and Australia (Kant et al., 2003).

Serological tests for the classification of ARVs are losing their importance because of the significant cross reactivities among isolates. Furthermore, current classification methods including both serological and phylogenetic subtyping all failed to correlate to specific disease conditions, which is more important for the prevention and control of ARV infections.

2.8 Avian reovirus epidemiology

Transmission of ARVs can be vertically from eggs or horizontally from other chicks that are infected. Jones and Onunkwo (1978) experimentally injected a group of day-old chicks with arthrotropic ARV and subsequently mixed them (in-contact) with uninoculated birds from the same hatch. All chicks with virus injection developed viral arthritis (VA) within 7 days, and other in-contact (uninoculated) birds gradually developed VA as well after 6 - 7 weeks. In the duration of the experiment, ARV was recovered from trachea, intestine, and hock joint tissues from both groups indicating fecal-oral route transmission of the virus. In addition, ARV can also gain entry via respiratory tract or damaged skin and establish itself in the hock joint (Al-Afaleq and Jones, 1990). In reality, the source of ARV infections is more likely from chicks hatched from contaminated eggs. Experimentally infected breeders can pass ARV on to their eggs in a period of 1 to 3 weeks post inoculation (Menendez et al., 1975b; van der Heide and Kalbac, 1975), and subsequently with young chicks hatched carrying the virus

(Al-Muffarej et al., 1996; Menendez et al., 1975b; van der Heide and Kalbac, 1975). Although these studies showed relatively low incidences of ARV vertical transmission, the ARV-infected young chicks can act like "seed" for further spreading of the virus to other uninfected birds through horizontal routes. In addition, low percentages of congenitally infected chicks are difficult to rapidly diagnosis, which contributes to the persistency of ARVs.

Avian Reoviruses can invade multiple tissues and persist in some of them for a long period of time. Two studies indicated that VA-producing ARV were recovered from the spleen or hock joint of laboratory infected chickens up to 285 and 91 days post-inoculation, respectively (Jones and Onunkwo, 1978; Kerr and Olson, 1969). The persistent viruses even though most of time do not cause disease, some physiological events, such as sexual maturation can reactivate the virus, which may explain some reoccurrences of the ARV infections in breeder flocks (Jones et al., 1975).

Avian reovirus susceptibility in chickens is age-dependent. In multiple experimental infection studies, researchers compared the susceptibilities of chickens of different ages. The results indicated that chickens are most susceptible to ARV infection and disease at hatch, and the susceptibility drops rapidly thereafter. The severity of the disease, including the gross and microscopic lesion development in the various tissues, in the thymus, trachea, intestine, liver, *etc.* as well as the virus shedding from the feces for chickens older than 1 week are less than those of younger birds. This indicates much more resistance for ARV infection in older chicks, which may correlate to the maturation of the immune system (Jones and Georgiou, 1984; Montgomery et al., 1986; Roessler and Rosenberger, 1989). Interestingly, the susceptibility of ARV infection also varies

because of the breed of the chickens. Lighter breed and white Leghorn layers are more resistant than heavier breeds like broilers. Broilers tended to have more severe gross lesions, longer virus persistency and spreading to more tissues and organs, and delayed seroconversion than the lighter breeds and layers infected with the same virus (Jones and Kibenge, 1984). These results may help explain that VA form of ARV disease is predominantly reported in broilers and only occasionally in layers (Schwartz et al., 1976).

2.9 Pathogenesis and molecular pathogenesis of avian reovirus

Avian reoviruses are associated with many disease conditions, including tenosynovitis (viral arthritis) (Kibenge and Wilcox, 1983), enteritis related MAS or runting-stunting syndrome (Page et al., 1982a), chronic respiratory diseases (Fahey and Crawley, 1954), inclusion body hepatitis (McFerran et al., 1976a), myocarditis (Kerr and Olson, 1969), hydropericardium (Bains and MacKenzie, 1974) *etc*. The most severe cases of ARV infections can cause acute hepatic necrosis and early death within a week (Jones and Guneratne, 1984). In experimental studies, ARVs were reisolated from essentially most of the tissues and organs in the host within a relatively short time post-inoculation (PI), such as liver in 6 hr PI, bursa of Fabricius in 12 hr PI, plasma, red blood cells, and monocyte fractions in 30 hr PI, bone marrow in 3-5 days PI, hock joint, respiratory, enteric, and reproductive tracts in 4 days PI (Kibenge et al., 1985; Menendez et al., 1975a).

In the early pathogenesis progression of ARV infection, the viruses were detected in the blood in 24 to 48 hr PI, indicating viremia which rapidly spread the viruses throughout the body. Viral distribution pattern suggested that the epithelium of the intestine and bursa of Fabricius is the primary site for ARV entry and replication (Jones

et al., 1989; Kibenge et al., 1985). The exception to the virus distribution timeline is liver, isolation of virus within 6 hr was reported; however, the time was not adequate for sufficient replication and redistribution via viremia, which suggested that the virus may be absorbed into the liver through portal blood (Kibenge et al., 1985). Under experimental condition, usually at 14-15 days PI, most of the viruses are eliminated from the host or no longer detectable, except for hock joint and oviduct, within which ARV can persist for at least 285 days (Kerr and Olson, 1969). The prolonged existence of ARV in the reproductive system confirmed the source and possibility of ARV vertical transmission.

Host cell surface receptors determine the virus host range and the conditions affect viral entry. In case of ARV, the identity and properties of the host cell receptor are unknown. However, it has been reported that ARV receptor, unlike the mammalian counterpart, is ubiquitous, and exists on the mammalian cells (Barton et al., 2001). Such wide availability of receptors gives ARV great advantages in terms of host range, and it may explain its multi-tissue tropism characteristics. Although ARVs are capable of invading many tissues and organs, they do demonstrate preferences in some tissues or organs. Epithelia of small intestine and bursa of Fabricius are the primary site of entry and replication. In addition, studies suggested the liver as a "favorite" target for ARV infection, because laboratory infection with high dosage commonly resulted in mortality with hepatitis in ten days (Jones et al., 1989; Jones and Guneratne, 1984; Kibenge et al., 1985). *In vitro* infection with an MAS related ARV isolate (ARV-CU98) of avian cells, including macrophages, B and T cells, liver cells from both chicken and turkey origin demonstrated a selective infection by ARV of liver cells (Heggen-Peay et al., 2002). The

prominent viral arthritis to tibiotarsal-tarsometatarsal (hock) joint is another site where virus replication can cause serious consequences (Jones et al., 1989; Jones and Kibenge, 1984; Sahu and Olson, 1975).

Tenosynovitis or viral arthritis is the only disease condition that can be definitively reproduced by experimental infection ARV. In fact, some studies strongly suggested that almost all ARV strains have the potential to cause viral arthritis (Jones and Guneratne, 1984; Sahu and Olson, 1975). On the other hand, the pathogenesis of MAS, the second most frequently noticed disease condition associated with ARV infection, is still not understood. The generally accepted hypothesis is that ARV caused disease in the digestive system, such as, enteritis, hepatitis, pancreatitis, and proventriculitis, which can disrupt normal feed digestion and nutrient absorption resulting in a nutrient deficiency (Songserm et al., 2003; Sterner et al., 1989; van der Heide et al., 1981). Attempts to reproduce MAS by ARV infection were not all successful, because several MAS studies resulted in isolation of other pathogens, such as enterovirus (McNulty et al., 1984), parvovirus (Kisary et al., 1984), calicivirus (Wyeth et al., 1981), and bacteria (Kouwenhoven et al., 1978b), suggesting that the cause for MAS may be multi-factorial. Another MAS reproduction study demonstrated that ARV combined with intestinal homogenate from healthy birds or formalin treated intestinal homogenate from MAS birds can lead to MAS. This suggested that ARV infection in combination with some unknown agents or substances in the intestine caused MAS in chickens (Songserm et al., 2002).

Molecular aspects of ARV pathogenesis are related to its fusogenic and apoptosis-inducing activities. All ARVs have the ability to induce cell-cell fusion during

replication. ARV-induced cell fusion is initiated by a so-called fusion-associated small transmembrane protein- viral protein P10, which is encoded by the first cistron of S1segment (Bodelon et al., 2001; Shmulevitz et al., 2002). Within ARV replication cycle, nonstructural protein P10 is expressed and serves as viroporin, which permeabilizes host cell membrane and cause extensive syncytium formation. The fusogenic activity and membrane permeabilizing ability are located at different domains of P10 protein (Bodelon et al., 2002; Shmulevitz et al., 2004). The cell-cell fusion can promote the transmission of the virus without exposure to immune defense of the host, as well as enhance subsequent systemic dissemination of progeny viruses from apoptotic syncytium cells (Salsman et al., 2005).

Another important molecular weapon of ARV, which may directly relate to its pathogenesis or virulence, is its ability to induce host cell apoptosis (Lin et al., 2007). The ARV σC protein, which is encoded by the third ORF of S1 genome segment, is a viral apoptin responsible for proapoptotic function of ARV. Studies indicated that σC could initiate apoptosis via P53-dependent pathway in many cell types, including both mammalian and avian cells (Lin et al., 2006; Shih et al., 2004). A recent study by Liu *et al.* (2005) demonstrated that P17, another viral protein encoded by S1 segment may play a role in ARV pathogenesis. The expression of P17, although it does not cause cell death or apoptosis, can activate P53 and CDK inhibitor $P21^{cip1/waf1}$, thus causes cell growth retardation and reduced cell proliferation in culture. All S1 segment encoded viral proteins play important roles in ARV pathogenesis, therefore, it is not surprising to see that studies using mono-reassortment technique concluded S1 was the determinant of ARV virulence (Duncan and Sullivan, 1998; Ni and Kemp, 1995). Some other viral

proteins have been reported to participate in ARV pathogenesis, such as σA, which has demonstrated anti-interferon activity by irreversibly binding with dsRNA and blocking the activation of interferon-induced, dsRNA-dependent enzymes, such as PKR and 2', 5'-oligoadenylate synthetase, which play important role in regulating protein synthesis in virus-infected cells (Clemens, 1997; Martinez-Costas et al., 2000; Rebouillat and Hovanessian, 1999).

The ability of ARV to sustain prolonged infection in joints and tendons is due to the relatively sequestered anatomical structure, which does not come in direct contact with blood and lymphatic fluid, therefore protecting virus from elimination by host immune system (Roessler and Rosenberger, 1989). *In vitro* infection using primary chicken embryo tendon cells (CET) revealed that ARV replication in CET displayed a tissue (or cell)-specific manner. CET can support ARV infection with no visible cytopathic effect (CPE) for up to 16 days with low amount of progeny virus shedding as compared to CEF culture. The initiation of infection, ssRNA transcription, and viral protein expression in CET cells are much slower. Since the same CET culture supported normal replication of Newcastle disease virus, it is likely that the CET restriction to ARV is virus-specific. The slow and prolonged ARV replication cycle in CET generated much less antigen than in other cell types, which provided ARV advantages of evading host immune system, therefore, the virus may sustain infection for long periods (Huang, 1995).

2.10 Avian reovirus pathology

Avian reoviruses cause chicken tenosynovitis (or VA) and are associated with runting-stunting (or MAS) syndrome, which are major diseases in chickens (Robertson and Wilcox, 1986). Other conditions, such as chronic respiratory disease (Fahey and

Crawley, 1954), enteritis, proventriculitis, myocarditis, pericarditis, hepatitis, and brittle bone syndrome may be secondary conditions or a part of the VA or MAS (Kerr and Olson, 1969; Page et al., 1982a; Page et al., 1982b; Sahu and Olson, 1975; Vertommen et al., 1980).

Viral arthritis/tenosynovitis is a disease in heavy-type broilers, however, occasionally, an outbreak can occur in the lighter breeds (Schwartz et al., 1976). Visible signs of VA are varying degrees of lameness starting at 4 to 7 weeks PI with mortality as high as 12-16% (Johnson and van der Heide, 1971). Progression of VA begins with soft swelling of joints, which results from hypertrophy and/or hyperplasia of the synovial membrane and surrounding tissues. Excess clear or turbid (if bacterial or mycoplasma infection is involved) fluid can be seen in the joints. Later, hemorrhagic foci may be seen in the synovial membranes with developments of erosions on articular cartilage. Most loose connective tissues surrounding the tendon sheaths are replaced by granulomatous and fibrous connective tissues, which thicken and harden tendon sheaths. Granulomatous tissues may also invade the tendon, which cause firm adhesion of tendon to its sheaths and difficulties for movement of infected joints. Shanks may become swollen when digital flexor tendons are affected. Finally in most severe cases, especially in heavy broilers, the diseased birds may exhibit black and blue thighs, which are caused by ruptured gastrocnemius tendon and blood vessels and digital flexor tendon can also be ruptured because of the disease. In chronic cases, the tendons are gradually "fixed" by fibrosis and adhesion to the sheaths, which can lead to stilted walking (McNulty, 1993; van der Heide, 1977).

Histological examinations revealed that the pathological changes in the thickened tendon sheath are due to edema, hypertrophy and hyperplasia of the synoviocytes, and synovial membrane villous proliferation. The infiltration of the inflammatory cells, such as lymphocytes, plasma cells, macrophages, and a small numbers of heterophils play a role in the destruction of the tendon (McNulty, 1993; van der Heide, 1977). Lesions and disease signs caused by ARV related VA are not specific for ARV. They are close to those of *Staphylococcus aureus* and *Mycoplasma synoviae*, which are commonly isolated along with ARV. Researchers suggested there are differences in degree of pathological changes (Kibenge and Wilcox, 1983), whereas, others indicated that the ARV typically caused diffuse lymphocytic inflammation, while *S. aureus* infections were more likely causing focal purulent synovitis (Hill et al., 1989). Birds suffering from ARV related VA were also shown to have microscopic lesions in the liver, spleen, and bursa of Fabricius; in addition, pericarditis and myocarditis were commonly reported (Hill et al., 1989; Kerr and Olson, 1969; Roessler and Rosenberger, 1989; Tang et al., 1987). The severity of the disease depends on the strains or isolates, since most ARV strains have the potential to cause VA (Jones and Guneratne, 1984; Sahu and Olson, 1975).

Malabsorption syndrome, also known as runting-stunting syndrome or pale bird syndrome is an important disease in poultry, which is associated with ARVs. Signs of MAS include stunted growth, elevated feed conversion, depression, poor feathering, erratic feather development, diarrhea, discoloration of the shank, paleness of the skin, brittle bones, femoral head necrosis, osteoporosis, and increased lameness (Hieronymus et al., 1983; Kouwenhoven et al., 1978b). In the present research, four of the strains, 1733, 2408, ss412 and CO8 were isolated from MAS related conditions.

Malabsorption syndrome affected flocks were reported to have 5-20% of birds showing stunted growth by one week of age; increased incidence of lameness, and poor pigmentation as early as 2 weeks of age. Gross lesions seen in MAS affected chicks include increased pericardial fluid, enlargement of proventriculus with hemorrhagic foci in proventricular glands, decreased size of gizzard with atonic muscle, pancreas atrophy, swollen and friable intestinal tracts with orange-tinged mucus-like fluid, and poor calcification of the skeletal system, which can easily lead to broken femur head (Kouwenhoven et al., 1978a; Page et al., 1982a). Necrosis development in the cartilage of the femur growth plate has been reported (Robertson and Wilcox, 1986).

Histological lesions in enlarged proventriculus are due to hyperplasia or hypertrophy of the glandular epithelium and the development of edema or fibrosis, whereas pancreatic atrophy is caused by diffuse vacuolar degeneration with loss of functional acinar cells and subsequent fibrosis. Lesions in the liver exhibit as hypertrophic hepatocytes, dilated sinusoids blood vessels and the development of fibrosis in the capsule. These pathological changes in the digestive system may disrupt nutrient uptake and lead to nutrient deficiency. Microscopic lesions have been observed in the femur growth plate, periosteum, and ossification groove, which may be associated with deprived bone calcification. Lesions in the bursa of Fabricius indicate follicular lymphocyte depletion and atrophy, which may obliterate the immune system, leading to immunosuppression (Page et al., 1982a; Robertson and Wilcox, 1986).

2.11 Avian reovirus immunology

Avian reovirus infection can lead to an array of diseases, and the types and severities of disease conditions and the final outcome of the disease are determined by

combinations of multiple factors, such as, virulence infective dosage (Gouvea and Schnitzer, 1982), route of infection (Kibenge et al., 1987), breed of chicken (Jones and Kibenge, 1984), and age at infection (Jones and Georgiou, 1984). Outcomes of the ARV infection are influenced by the active host immunity, and interaction between host and virus.

Kibenge *et al.* (1987) utilized a compartmentized approach by obliterating T-cell and B-cell producing capability individually or together to determine the roles that different parts of the immune system played in the defense against ARVs. Chickens were divided into five groups by different immunosuppressive treatments: surgical thymectomy (Tx), surgical bursectomy (Bx), cyclophosphamide (Cy, chemically destroys the adaptive immune system), or Cy+Tx, and untreated group. All birds were inoculated with arthrotropic ARV strain at one-day old, and subsequently observed for 5 weeks. All Cy treated groups (Cy, and Cy+Tx) had significantly increased mortality, incidence of leg gross lesions, and severity of microscopic lesions as compared to the untreated group. The Bx group showed a marked increase in mortality and had similar severity of gross or microscopic lesion as the untreated group, whereas Tx group displayed mild microscopic lesions and rarely gross lesions. Virus was continuously recovered from cloacal swabs from Tx and untreated group for 2 weeks, Bx group for 3-4 weeks, and persisted in the Cy treated group (Cy, and Cy+Tx). Serum antibody was determined by gel precipitation and VN, which revealed a strong positive response in untreated and Tx group, a delayed positive response in Bx group, and was absent in all Cy treated groups. They concluded that both humoral immunity and cell mediated immunity played important roles in protection against ARV infection, however, humoral immunity (specific antibody

production) played the more dominant role. This may be explained by the early pathogenesis aspect of ARV, which developed plasma viremia shortly after infection (Jones et al., 1989), and the primary defense for viremia caused systemic infection were circulating antibodies. This was consistent with the increased mortality and severity of gross lesions in humoral immunity deficient groups Bx, Cy and Cy+Tx.

On the other hand, T-cell mediated immunity determined the type of cells infiltrated into the tendon tissues, which affected the development and severity of lesions (Kibenge et al., 1987). T-lymphocytes and plasma cells are the predominant inflammatory cells in the synovia of the ARV caused arthritic joints. Commonly, in the acute phase of the infection, only a small number of $CD8^+$ lymphocytes present in the synovia, gradually, increased number of $CD4^+$ and $CD8^+$ lymphocytes aggregate, as well as some IgM positive B-cell, and plasma cells. If the infection persists, $CD4^+$ T-cells eventually become the dominant cell type along with some IgM positive B-cells and plasma cells. These types of lymphocytes and the activation level present in the ARV infected joints are similar to those reported in rheumatoid arthritis in humans. Therefore, ARV arthritis has been considered as a animal model for human rheumatoid arthritis (Marquardt et al., 1983; Pertile et al., 1996).

While circulating antibodies (mostly IgG) are important for eliminating systemic infection, its isotype IgA, which is secreted to mucus secretion on the surface of the mucosal membrane, such as epithelium of the respiratory and intestinal tract, is also important for mucosal immunity against infection. Experimental infections revealed that IgA production was determined by age at infection, route of infection, and the trypsin-resistance ability of the ARV strain. Birds cannot produce IgA isotype if they were

infected orally before week of age, and when subcutaneous route was used, birds can only produced IgA if they were infected after 3-weeks of age. There was no difference in IgG production in different age groups and different routes of infection. Trypsin-resistance enables ARV survival in the harsh environment of digestive or respiratory tract, thus it induces sufficient IgA production (Mukiibi-Muka and Jones, 1999).

2.12 The prevention and control of avian reovirus infections

Avian reoviruses are ubiquitous in the environment and avian hosts, and are relatively resistant to the environmental conditions and chemical and physical agents, which makes the notion of maintaining commercial flocks free of ARV infections impossible. Especially in breeder flocks, there is no detectable seroconversion that can prevent viruses being transmitted vertically through eggs to newly hatched progeny chicks. Therefore, the common measure of ARV prevention and controls is vaccination with inactivated virus in breeders and live vaccine in their progeny.

Since chicks are most susceptible to ARV infection once hatched till at least a week-old (Jones and Georgiou, 1984; Roessler and Rosenberger, 1989), the basic protocol of vaccination is to protect birds at an early age, preferably from day one. In practice, vaccines are given to the breeder flocks, so that the maternal antibodies can be passively passed to the newly hatched chicks via egg yolk. Maternal antibodies and their protective capability to the progeny birds was first studied in 1975 using inactivated Connecticut isolate S1133, however, inactivated virus did not induce adequate antibody titer to yield protection to the progenies (Cessi and Lombardini, 1975; van der Heide et al., 1976). Attempts to use live vaccines in day-old young chicks were not very

successful because of the immature mucosal immunity (Mukiibi-Muka and Jones, 1999). Therefore, the development of new live vaccines or vaccination protocols occurred.

An attenuated strain of S1133 was developed after adapting and passaging in chicken embryo seventy-four times. This live vaccine was administrated to 10-15 week old broiler breeder flocks via drinking water, which resulted in protection against subsequent oral or subcutaneous challenge of homologous virus in progeny chickens (Eidson et al., 1979; van der Heide and Page, 1980). However, the vaccine did not protect the chicks from the challenge of virus from a different serotype (Rau et al., 1980). Giambrone (1985) proposed a multiple vaccination protocol, which used live attenuated vaccine as a primer in the early life of the breeders, followed by an inactivated vaccine at 6-weeks of age and again prior to the egg production; this primer-booster vaccination scheme resulted in strong titers in breeders (Giambrone, 1985).

Avian reovirus vaccines are administrated via oral, subcutaneous, or intratracheal routes, which are labor intensive, and are limited to vaccination of breeders. Giambrone and Hathcock (1991) developed a novel route of vaccination using virus suspension coarse-spray. Subsequently, this method was evaluated by administration of S1133 derived live vaccine directly into day-old chicks, and resulted in effective protection (Giambrone et al., 1992; Giambrone and Hathcock, 1991). *In ovo* vaccination involves injection of vaccine into an embryo before hatch. It can be performed using an automated injector to minimized labor costs and time, therefore, ensures the precise and uniform dosage of vaccine delivery into hundreds of eggs per minute. In fact, approximately 80% of broilers in the United States and more than 30 countries on six continents are vaccinated *in ovo* against Marek's disease virus (Guo et al., 2003a; Toro et

al., 2007). A new experimental *in ovo* ARV vaccine has been developed and tested safe for specific-pathogen-free (SPF) embryos and provided adequate protection in newly hatched chicks against ARVs (Guo et al., 2003b).

Advances in molecular biology opened a new arena for vaccine development. A new generation of vaccines - subunit vaccine - has become popular. The DNA/RNA that encodes immunogenic epitope(s) of the target pathogen is extracted and manipulated and introduced into a production system, such as, bacteria, fungi or even transgenic plants, so that the immunogenic proteins can be produced in large scale. Modified fungi or transgenic plants can also be used as probiotic additive or feed, or better yet, edible vaccine (Huang et al., 2006; Wu et al., 2005). A recent study reported that a yeast-derived ARV σC protein induced effective protection against ARV infection (Wu et al., 2005).

Although it is impossible to maintain commercial flocks free of ARV infection, sound management, carefully executed biosecurity measures, effective vaccines and proper vaccination schemes can minimize risks of developing ARV related diseases.

2.13 The detection and identification of avian reovirus

Avian reovirus is commonly seen in birds concomitantly infected with other pathogens that cause similar disease. e.g. *S. aureus* and *M. synoviae* co-existence in VA tendon tissues. Such combinations make diagnoses based on external signs impossible. Therefore, the confirmation of ARV infection requires laboratory examination to verify the presence of virus.

Virus isolation (VI) assay involves propagation of samples in live hosts, such as embryos or primary cell cultures, and observation of possible development of

pathological changes in these hosts. VI is very sensitive, although time consuming and laborious, and is still considered as the "gold standard" for virus detection. Sample materials are injected into the yolk sac of an embryonated SPF egg followed by 3-6 day incubation. ARV typically kills the embryo within 3-5 days after inoculation, and embryos are hemorrhagic with yellowish necrotic foci on the liver. When propagating ARV in cell cultures, typical CPEs are formation of giant syncytium cells, and within 3 to 4 days, monolayer cells peel off from the cell culture flask. If samples have low virus titer, extended incubation time or multiples passages may be required before pathological changes in embryos or CPEs in cell culture can be observed. There are arrays of detection methods that are used for the detection of ARV, and these detection methods can be categorized into three groups: antigen detection, antibody detection, and molecular detection methods, which target specifically certain genetic markers (viral RNA).

Antigen detection utilizes ARV-specific antibody, which can be polyclonal or monoclonal (sometimes conjugated with a "visible" reporter unit), to bind with ARV in tissues or samples. Antigen-antibody reaction can be visualized by precipitation in agar gel [e.g. agar-gel precipitin assay (AGP)], or visibility of reporter [e.g. fluorescent antibody assay (FA)]. FA assay is used to localize ARV antigen in tissues of infected chicken (Menendez et al., 1975a), whereas AGP test is used to detect group-specific antigen (Adair et al., 1987; Kawamura and Tsubahara, 1966). Western blotting, which utilizes highly specific monoclonal antibody to recognize a particular protein of ARV, is commonly used (Endo-Munoz, 1990). Monoclonal antibodies have been used in immunoperoxidase staining to detect ARVs from paraffin-embeded tissues (Liu et al., 1999). Commonly used antibody detection methods include VN test and enzyme-linked

immunosorbent assay (ELISA). While both of the tests can be used for quantitative measurement of ARV-antibody titers, cross-VN test can be used to determine ARV serotypes (van der Heide, 1977). Because of widespread ARV infections, detection results are difficult to interpret. Nevertheless, it remains convenient for evaluating vaccine protection. An indirect immunofluorescence (IIF) assay has been used for serum ARV antibody detection (Ide, 1982).

New methods have been developed for the detection of pathogens. The focus of these techniques is the genetic material of the pathogens, in case of ARV, the dsRNA genome. Molecular-based techniques including reverse transcriptase (RT)-PCR (Bruhn et al., 2005), nested PCR (Liu et al., 1997), multiplex RT-PCR (detecting multiple targets in the same reaction) (Caterina et al., 2004), real-time RT-PCR (Ke et al., 2006), PCR followed by restriction fragment length polymorphism (RFLP) (Lee et al., 1998), and *in situ* hybridization (ISH) (Liu and Giambrone, 1997), have been used to detect of ARVs.

Although all the methods are used to detect ARV infections, different inferences can be drawn based on the target of the method. Antigen detection methods focus on the ARV-specific antigens in the tissues, which could be either from live viruses or virus debris. Antibody detection measure circulating antibodies in the serum and molecular-based methods detect viral RNA, which could arise from either virus debris or viruses. Therefore, when interpreting results, both antigen detection methods and molecular-based methods only suggests the existence of the virus, but have no indication of the viability and infectivity of the virus. Antibody detection suggests that the host has been infected sometime in its life, and does not indicate the existence of virus at the time of sampling. VI is the only test in which a positive result denotes presence of viable ARV.

2.14 Polymerase chain reaction

Polymerase chain reaction (PCR) is an indispensible technique that is widely used in molecular biology, biology, medicine, genetics, and criminal investigation, *etc*. It is considered as a monumental scientific technique. Nowadays, PCR is one of the basic research methods in these areas. PCR was invented by Dr. Mullis in 1983 when he was conducting research on oligonucleotide synthesis in Cetus Corporation, and he was awarded a Nobel Prize in chemistry in 1993 because of the invention (Rabinow, 1996).

An array of PCR variations have been developed, such as: 1) Hot-start PCR. This is type of PCR includes an initiation step, which start the reaction at denaturation temperature (~95˚C) to reduce non-specific amplification. The DNA polymerase used is bound with an antibody or by covalent bound inhibitors, which only dissociate from the polymerase after a high temperature activation step. 2) Multiplex PCR involves multiple specific primer sets within a single PCR tube to amplify multiple PCR products of different sizes from different DNA sequences. All the primers have to be extensively optimized, so that they all have similar annealing temperature and amplicons of different sizes, which can be differentiated by gel electrophoresis. 3) Nested PCR, in which two sets of specific primers are used in two consecutive PCR reactions. The primers used in the second PCR are located inside of the amplicon sequence of the first PCR, so that nested PCR can further reduce non-specific amplifications. 4) Real-time PCR is a combination of fluorescent reporter with regular PCR, which allows monitoring the real-time accumulation of the amplicons in the reaction. Real-time PCR will be explained in detail later.

Since RNA cannot be recognized by most DNA polymerases, it is not able to serve as a template for PCR. Therefore, in order to study and amplify RNAs, they have to be converted to complementary DNA (cDNA) first, and such conversion is called reverse transcription (RT), which is catalyzed by specialized RNA dependent DNA polymerase or reverse transcriptase (RTase). There are two commonly used RTases: avian myeloblastosis virus reverse transcriptase (AMV-RTase) and Moloney murine leukemia virus RTase (MMLV-RTase). AMV-RTase has higher thermostability than MMLV-RTase, and it can retain its activity at as high as 53˚C. Higher RT temperature can reduce the formation of the secondary structures, therefore facilitates the recognition of RNA by RTase (Freeman and Vrana, 1996). On the other hand, MMLV-RTase has significantly less RNAse H activity than AMV-RTase, which makes it a better choice for reverse transcribing long full-length cDNA (Gerard et al., 1997). Unlike PCR, besides specific primers, the RT process can also be primed by random hexamers or oligo-dT primers. While specific primers decrease unspecific priming, random hexamers maximize the number of RNAs that can be reverse transcribed, whereas oligo-dT primers actively hybridize with any RNAs with a poly-A tail (most likely mRNAs). After reverse transcribing, newly synthesized cDNA is then amplified by a regular PCR process. Depending on the preferences and experimental conditions, RT-PCR can be performed in one-step (two enzymes in one tube) or two-step (two enzymes in two tubes) fashion, or even "one enzyme in one tube" with a special DNA polymerase with intrinsic RT capability, such as *Tth* DNA polymerase.

2.15 Real-time polymerase chain reaction

2.15.1 Real-time PCR basics

Real-time PCR, which is also known as real-time quantitative PCR or kinetic PCR, is a relatively new molecular technique derived from conventional PCR, which allows simultaneous detection and quantification of target DNA molecules. Given a standardized DNA control, real-time not only can be used to relatively quantify target DNA concentration, but also to estimate the absolute copy numbers of target DNA in the tested sample. Real-time PCR is commonly abbreviated as "RT-PCR", which is easily confused with reverse transcription PCR (also abbreviated as "RT-PCR"). Therefore, herein this dissertation, to avoid the confusion, real-time PCR will not be abbreviated and "RT-PCR" exclusively denotes reverse transcription PCR.

The basic mechanism of real-time PCR follows the conventional PCR. In addition, it also includes a fluorescence reporter, which is excited by the light source of real-time PCR instrument during the PCR process and emits a fluorescent signal corresponding to the amplification of target DNA. During the initial few cycles the fluorescent signal is too weak to be distinguished from the background noise. However, as the amount of the PCR products accumulate exponentially at the early stage of PCR, the signal strength increases accordingly. Later on, the signal plateaus as the major ingredients in the reaction, such as primers, fluorescent reporter, or nucleotide triphosphates (dNTPs), are running out. The fluorescent signal is detected by fluorimeter, which is usually computerized and with specialized software program. The quantitative measurements are acquired instantaneously.

During a real-time PCR, the computer program measures the fluorescence signal and the fluorescence signal intensity ratio change ΔRn is calculated as:$\Delta Rn = (Rn^{+}) - (Rn^{-})$. (Rn^{+}) is the fluorescence emission intensity ratio at any given cycle, and (Rn^{-}) is the initial emission intensity ratio prior to the amplification in the same reaction tube. The software plots ΔRn (y-axis) against the PCR cycles (x-axis), generates a typical "S" shaped curve, namely amplification curve. At the early stage of the amplification curve, ΔRn remains low and not distinguishable from the background. As the PCR generates substantial amount of amplicons, it in turn increases the intensity of fluorescence emission by the reporters. The number of cycles at which fluorescence signal level reaches a certain threshold (generally set as 10 standard deviations above baseline) is defined as C_T value. The C_T values of a given experiment decrease linearly with the increasing quantity (in log scale) of initial target DNA (Heid et al., 1996). Therefore, the mathematical relationship between C_T values and log concentration of the target DNA is used in relative or absolute quantification. On the other hand, the C_T is an arbitrary value, which can be changed manually according to experimental conditions. Thus, the comparison of individual C_T values between experiments should be avoided; instead C_T can only be used to distinguish samples within the same experiment.

In real-time PCR, the basic equation describing PCR amplification is:

$$N_C = N_0 \times (1 + E)^C$$

in which, C is a given cycle number, N_C and N_0 represent the number of templates in the reaction tube at C cycles and 0 cycle, respectively; and E is the efficiency of the PCR assay. Therefore, by rearranging of equation above, the initial amount of the template of a given C_T value can be calculated as following:

$$N_0 = \frac{N_{c_T}}{(1+E)^{C_T}}$$

Thus the comparison between any two C_T values (relative quantification) within the same experiment equals:

$$\frac{[N_0]_A}{[N_0]_B} = (1+E)^{(C_T B - C_T A)}$$

Whereas $[N_0]_A$ and $[N_0]_B$ are the initial input of target molecule in sample A and B, respectively, and C_TA and C_TB are the corresponding C_T values of A and B. Assuming under optimal experimental condition, the efficiency is 100%, thus, the difference between *n* cycles reflects a 2^n difference in template concentration between two samples. On the other hand, absolute quantification is usually achieved by measuring the above relationships between the C_T values and their known initial concentration (or amount) of serially diluted purified target DNA templates, which can be produced by cloning. The plot of regression relationship between C_T values and the log transformed initial amounts of the standard is called standard curve, with which a regression equation can be as follows:

$$\log(N_0) = -\log(1+E) \cdot C_T + \log\left(N_{C_T}\right)$$

thus: $Slope = -\log(1+E)$ and $intercept = \log\left(N_{C_T}\right)$ (Rutledge and Cote, 2003). Since most real-time PCR software can estimate the slope automatically, therefore the PCR efficiency is readily assessable.

At the designing stage of development of a real-time PCR protocol, the size of target amplicon may vary depending on the types of fluorescence reporters applied. Although amplicons as long as ~400 bp has been reported for probe-based system (Bustin et al., 1999; Shmulevitz et al., 2004), generally it is recommended to limit the amplicon size

under 200 bp. Shorter amplicons have lower melting temperatures (T_m), which allow them to be denatured within shorter time as in the common real-time PCR denaturation step. They can more efficiently bind with their complementary primers, thus higher PCR efficiency. Real-time PCR primers usually about 15 to 30 bases in length and 20-70% in G/C contents, are expected to have a relatively higher T_m (58-60 $^{\circ}$C) than conventional PCR primer. The difference of the T_m of any primer pair should be less than 1-2 $^{\circ}$C. Real-time PCR probes usually about 30 bases in length, are designed to have a T_m 5-10 $^{\circ}$C higher than the corresponding primer set, which ensures their binding with target prior to the primers and competing efficiently against primers that are much more abundant for the targets. The selection of fluorescence reporter and the characteristics of each common reporter are explained in detail in following section.

2.15.2 Fluorescent reporters

There are two major forms of fluorescent reporters that are distinguished by their chemistry and are used in real-time PCR: sequence –specific probe based and non-specific DNA dyes. In sequence-specific probe group, most commonly used are TaqMan probe and hybridization probe, whereas in DNA dye group, SYBR-Green I is most popular. As the development of real-time PCR, more and more novel fluorescence reporter systems have been invented in the past decade, such as the following, 1) probes with only one fluorescence dye attached: displacement probes (Li et al., 2002) and Light-Up probes (Svanvik et al., 2000); 2) Some probes are modified to improve affinity with target DNA, thus the length can be as short as 10-12 bases: Light-Up probes and MGB-probes (Kutyavin et al., 2000). 3) Fluorescence dye can also be directly attached to primers with slight modifications: Scorpion primers (Whitcombe et al., 1999), LUX

primers (Nazarenko et al., 2002), and Ampliflour primers (Uehara et al., 1999). Nevertheless, despite the various chemistries of these different fluorescence reporter systems, they share the basic role in a real-time PCR, which is emitting fluorescence signal upon binding with target DNA templates. Therefore, in the current review, efforts will be concentrated on the most commonly used systems: TaqMan probe, hybridization probe, and SYBR-Green I.

a. TaqMan probe

TaqMan probe is also known as the hydrolysis probe for it is hydrolyzed by the 5' to 3' exonuclease activity of DNA polymerase after hybridizing with the target amplicon during PCR amplification. The emphasis on the exonuclease activity makes *Taq* or *Tth* the primary DNA polymerases of choice, other DNA polymerases, such as *Tfl* can also be used (Gut et al., 1999). A TaqMan system consists of two sequence-specific primers and the added specificity of a dual-labeled sequence-specific probe. The TaqMan probe contains a fluorescent reporter dye (such as fluorescein) at its 5' end and a second fluorescence dye, known as the quencher, at its 3'end, which is capable of absorbing the fluorescence emission spectrum from the first dye when they are at close proximity. Additionally, the exonuclease activity of the DNA polymerase is specific to double-stranded DNA. Therefore, when TaqMan probe is in its free (unbound, single-stranded) state, it remains intact and no fluorescence emission is detected (Heid et al., 1996). TaqMan probe hybridizes with the target region on the template and forms a double-stranded probe-DNA hybrid after the denaturation step. The binding of TaqMan probe and the target DNA remains until the extension stage, during which DNA polymerase extends the newly formed nucleotide sequence from the primers and reaches the

hybridized probe. Because of the double-stranded structure, the hybridized probe is subject to hydrolyzing and cleaving by the DNA polymerase exonuclease activity, which results in release of the fluorescein reporter from the quencher. Therefore, the fluorescence emission from the reporter dye is no longer absorbed by the quencher, and with the accumulation of emissions from the "freed" reporter, eventually, the signal is strong enough (the threshold) to be detected by the real-time PCR instrument (Heid et al., 1996; Lyamichev et al., 1993). The first fluorescence dye and quencher pair used in real-time PCR was FAM (6-carboxyfluorescein) and TAMAR (6-carboxy-tetramethyl-rhodamine), which are still popular choices for the TaqMan system. However, today, there are much more choices for the fluorescence dyes and quenchers, such as at 5' end using FAM, HEX™, TET™, Cy3™, Cy5™, TEX™-163, JOE NHS Ester, or ROX NHS Ester as the fluorescence reporter; in combination of 3' end Iowa black™ FQ, Black Hole Quencher®, TAMRA, or TAMRA NHS Ester as the quencher (http://www.idtdna.com/Catalog/DualLabeledFluorescentProbes/Page1.aspx). The important criteria for fluorescence dye selection are, first of all, the quencher must be able to absorb the emission spectra from the fluorescence reporter; and secondly, the wavelength of the emission from the reporter has to match the wavelength that can be detected by the sensor of the real-time PCR instrument.

b. Hybridization probe

The hybridization probe system, which was first developed on Roche LightCycler®, involves two single-labeled probes to maximize specificity (Wittwer et al., 1997). The 5' proximal probe carries a fluorescein donor at its 3' end, and the 5' end of the 3' proximal probe is attached with a fluorophore acceptor. The two fluorescence components are

selected so that the emission spectra of the donor overlap with the excitation spectra of the acceptor. In addition, the 3' of the acceptor probe has been modified by phosphorylation to prevent further extension by DNA polymerase. Both of the probes are sequence-specific that are designed to bind to complementary region of the target amplicon at a head-to-toe formation with less than 5 bases (recommended) in between. When both probes are hybridized to their target regions, they are close enough, so that the emission from the fluorescein donor can be efficiently transferred to the fluorophore acceptor, thus stimulating the emission from the acceptor. The two emission spectra from donor and acceptor have different wavelengths, which when strong enough (cross the threshold) can be detected by two different channels of the real-time PCR machine. The donor emission signal, which has shorter wavelength, serves as the background, and the intensity of the acceptor emission is then compared to the background. Therefore, the fluorescence intensity changes are measured and calculated as the changes of signal/background ratios.

In the hybridization probe system, a fluorescent signal is detected when both probes are hybridized to the correct locations, thus improving the specificity. In addition, because of the modified structures, 3' end probe is blocked for extension and protected from exonuclease hydrolysis, so that, further melting curve analysis is possible.

c. SYBR-Green I dye

SYBR-Green I is one of the most popular asymmetric cyanine dyes used in real-time PCR (Zipper et al., 2004). Asymmetric cyanine dyes consist of two nitrogen-containing aromatic components, of which one of them is positively charged. Thery are connected via a methine bridge and because of the vibration and rotation of the two

aromatic components, which dissipate the electronic excitation energy to the surrounding solution. Therefore, asymmetric cyanine dyes emit a minimum amount of fluorescence in their free state. As the dye binds to the minor groove of a double-stranded DNA, which inhibits the rotation of the aromatic components, thus these asymmetric cyanine dyes start to emit a bright fluorescence (Nygren et al., 1998).

As with all asymmetric cyanine dyes, SYBR-Green I is a sequence non-specific reporter in real-time PCR. It emits strong fluorescence signals upon binding with any double-stranded DNA, including false-primed primer-template complexes and unspecific primer-dimers. Therefore, strictly minimized primer-dimer formation is an important concern at primer designing stage for SYBR-Green based real-time PCR. In addition, SYBR-Green's binding with double-stranded DNA molecule is not in one to one ratio. In fact, multiple dye molecules can bind to the same DNA molecule simultaneously; therefore, the fluorescence intensity of SYBR-Green is also determined by the mass of DNA, which means longer sequences have stronger fluorescence than shorter ones. These draw backs have limited SYBR-Green based real-time PCR as the best choice for absolute quantification. However, there are also advantages using SYBR-Green base systems because of its cost-effective characteristics and possibility of performing melting curve analysis.

2.15.3 Melting curve analysis

Melting curve analysis is performed after the completion of the PCR for the determination of the T_m profile of real-time PCR products, which can provide additional specific identification of the product. Both hybridization probe and SYBR-Green I based real-time PCR allow further analyses with melting curves. In the process, temperature is

gradually increased and the fluorescence emission is continuously measured. When the temperature reaches the specific T_m of the amplicon, hybridization probes separate from the target (hybridization-based real-time PCR). And for SYBR-Green based real-time PCR, when the reaction reaches the T_m, the DNA strands separate, which dissociates the SYBR-Green molecules. As the result, the fluorescence drops abruptly (Ririe et al., 1997). The temperature is known as the melting temperature or melting peak. The fluorescence intensity is then plotted as a function of temperature as the amplicons or hybridization probes dissociate. Results can be converted to melting peaks, by plotting the first negative derivative of fluorescence (-dF/dT) with respect to temperature. Under optimal condition, the melting peak of each amplicon is represented by a single sharp peak, which is determined by factors, such as amplicon length, sequence, and GC content. Since the T_ms for primer-dimers are usually lower, represented by lower and broader melting curve, they can be readily distinguished from the distinctive sharp transition of the amplicons. Melting curve analysis is highly sensitive, and can be used to differentiate amplicons with differences of only a few base pairs (Espy et al., 2002).

CHAPTER III: DEVELOPMENT OF REAL-TIME RT-PCR FOR RAPID DETECTION OF AVIAN REOVIRUSES

3.1 Introduction

Avian reoviruses (ARVs) may cause tenosynovitis and are associated with diseases, such as viral enteritis related malabsorption syndrome, or runting and stunting syndrome, chronic respiratory disease, inclusion body hepatitis, myocarditis and hydropericardium etc. in chickens (Bains and MacKenzie, 1974; Fahey and Crawley, 1954; Kerr and Olson, 1969; Kibenge and Wilcox, 1983; McFerran et al., 1976; Page et al., 1982). These disease conditions can lead to economic losses due to mortality and morbidity, stunted growth, and poor feed conversion. Viral arthritis also causes downgrading of carcasses at slaughter due to the unsightly appearance of hock joints.

ARVs belong to the genus of *Orthoreovirus* and the family of *Reoviridae* (Mertens, 2004; Nibert, 1998). They have a non-enveloped, double-layer concentric capsid of 70-80 nm in diameter, enclosing the segmented double-stranded RNA (dsRNA) genome (Spandidos and Graham, 1976). The 10 dsRNA segments are categorized into three groups, which are designated L (large), M (medium), and S (small), based on their size and electrophoretic mobility. There are three segments in the L-class (L1, L2 and L3), three in the M-class (M1, M2 and M3), and four in S-class (S1, S2, S3 and S4) (Joklik, 1983; Schnitzer, 1985). For the standard ARV strains S1133 and 1733, all genome segments (except the L2 segment) have been sequenced. The 10 genome segments code

for at least 8 structural proteins (λA, λB, λC, μA, μB/μBC, σC, σA and σB) and 4 non-structural proteins (μNS, P10, P17, and σNS) (Benavente and Martinez-Costas, 2007; Varela and Benavente, 1994).

Virus isolation (VI), serological methods, such as virus neutralization (VN), and histopathological assays are common detection techniques for ARV infection (Robertson and Wilcox, 1986). VI and VN require propagation of the viral samples in chicken embryos or cell culture for 3-5 days to observe pathological changes. Serological methods, such as agar-gel precipitin assay (Adair et al., 1987), fluorescent antibody assay (Menendez et al., 1975), and enzyme-linked immunosorbent assay (Slaght et al., 1978), although fast, lack sensitivity for detection of ARVs. Therefore, it is necessary to develop a simple, rapid, and highly sensitive and specific method to detect ARV infections. Polymerase chain reaction (PCR) is widely used in laboratories due to its high sensitivity and specificity for target nucleotide sequences. In recent studies, reverse transcriptase (RT)-PCR (Bruhn et al., 2005), nested PCR (Liu et al., 1997), multiplex PCR (detecting multiple targets in the same reaction) (Caterina et al., 2004), and PCR followed by restriction fragment length polymorphism (RFLP) (Lee et al., 1998), have been used to detect ARVs.

Real-time PCR allows real-time detection and quantification of target DNA molecules as they proceed through amplification cycles. By incorporating fluorescent reporters, real-time PCR can measure and monitor target DNA amplification during the exponential phase, resulting in more accurate readings compared to conventional PCR. The current study developed a rapid, specific, and sensitive real-time RT-PCR assay

targeting the ARV S4 genome segment. This is the first reported TaqMan probe based real-time RT-PCR for detecting ARVs.

3.2 Materials and methods

Avian reovirus strains

Eight ARV strains, including S1133, 2408, CO8, 1733, JR1, ss412, and two vaccine strains: ChickVac™ and V.A. Vac® (Fort Dodge Animal Health, Fort Dodge, IA) were tested (Table 3.1). Both ChickVac™ and V.A. Vac® were developed from the standard strain S1133. They are used for prevention of tenosynovitis in broiler chickens. ChickVac™ is used for young chicks at 1-10 days of age and V.A. Vac® for older chickens between 3-8 wks of age. Strain JR1, which is known to be trypsin-resistant, was provided by Fort Dodge Animal Health, Inc. (Overland Park, KS).

Virus propagation and preparation

All strains were propagated in primary chicken embryo kidney (CEK) cell cultures. Flasks were stored at -70 ℃ after 48 to 72 hrs of incubation when 75%-85% cytopathic effect (CPE) was observed.

Cell cultures were frozen and thawed three times to rupture the cell membrane and release virus particles. Subsequently cell culture materials were transferred into 30 ml centrifugation tubes, which contained 3 ml of 40% sucrose. Centrifugation was at 100,000 x*g* using Type 30 rotor with Beckman® (Fullerton, CA) ultracentrifuge L8-70 for 1.5 hr. The bottom phase, which contained concentrated virus and cell debris, was collected into cryopreservation vials and stored in -70˚C until use.

Viral RNA extraction

Viral RNAs were extracted using Qiagen RNeasy® Mini Kit (Valencia, CA) with slight modifications. Briefly, 250 µl of concentrated virus-cell suspension were mixed with 3.5 volumes (875 µl) of lysis buffer RLT and 20 U Proteinase K (Sigma-Aldrich, St. Louis, MO) and incubated at 37˚C for 10 min. Two and half volumes (625 µl) of cold 100% ethanol were added and mixed well. Seven hundred microliters of the mixture was transferred to an RNeasy column and centrifuged at 9,000xg for 15 sec, then the flow-through was discarded. Remaining mixture was filtered through the same column and subsequently, the column was washed once with 700 µl of buffer RW1 and twice with 500 µl buffer RPE. The column was transferred to a new 2 ml collection tube and centrifuged at 14,000xg for 2 min to remove excess reagents from the column filter. Finally, total RNA was eluted in 30 µl of nuclease-free water.

Primer and probe design

The S4 gene sequences of nine pathogenic ARV strains: 2408 (GenBank accession number AF213468), 1733 (AF294772), 176 (AF059724), 601SI (AF294773), OS161(AY573913), 750505 (AF213470), 919 (AY573912), T6 (AF213469) and S1133 (U95952) were aligned using AlignX® (Fig. 3.1) from Vector NTI™ Sequence analysis and data management software v10.3 (Invitrogen Corporation, Carlsbad, CA). One set of gene-specific primers and hydrolysis probe combination, which generates a 139-nucleotide PCR product, was designed from the conserved region of S4. Another set of primers that encompassed the full length of S4 gene for conventional RT-PCR was also selected. The target nucleotide sequence was searched using BLAST service with the GenBank nucleic acid database. Results indicated that positive sequences were from

ARV isolates only. Thus, the primer-probe set we developed and the resulting PCR amplicons demonstrated high specificity. All custom-designed probes and primers (Table 3.2.) were manufactured by Integrated DNA Technologies®, Inc. (Coralville, IA).

Real-time RT-PCR and conventional RT-PCR

Real-time RT-PCR was performed on a LightCycler® (Roche Applied Science, Indianapolis, IN) with a 20 µl reaction volume, within which were 5 µl sample viral RNA and 15 µl of reaction mixtures. The Qiagen One-Step RT-PCR Kit (Valencia, CA) was used for making reaction mixtures, which contain 4 µl of 5x buffer, 3.75 mM of $MgCl_2$, 325 µM of dNTPs (each), 0.5 µM of each primer (R-S4F and R-S4R), 20 U of RNase inhibitor, 0.8 µl of Enzyme Mix, and 0.25 µM of probe S4-P. Reverse transcription was carried out at 45˚C for 30 min, and subsequently the reaction was heated at 95˚C for 15 min to deactivate the reverse transcriptase. The PCR stage was subjected to 40 cycles at 95˚C denaturation for 0 sec, 59˚C annealing for 20 sec, and 72˚C extension for 10 sec.

Conventional two-step RT-PCR was conducted in GeneAmp® PCR System 9700 (Applied BioSystems, Foster City, CA) with GeneAmp® RNA PCR Core Kit (Applied BioSystems, Foster City, CA) following recommended reagent concentrations and RT-PCR protocol from the manufacturer with modifications. In the reverse transcription (RT) step, 1 µl of primer S4-FF (100 µM) was mixed with 2 µl of each RNA sample in a MicroAmp® tube (Applied BioSystems, Foster City, CA), and subsequently the mixture was subjected to 99˚C for 5 min for denaturation in the thermocycler. Reaction tubes were rapidly cooled on ice for 5 min to promote annealing between primers and target sequence (S4). For each reaction, 8 µl of RT reaction mixture with final concentrations of 4.55 mM of $MgCl_2$, 1 µl of 10x PCR buffer II, 0.9 mM of dNTPs each, 10 U of RNase

inhibitor, and 25 U of MuLV reverse transcriptase were added. The RT reaction was performed at 42˚C for 60 min and 72˚C for 15 min. In the PCR step, 40 µl of reaction mixture containing the final concentrations of 2 mM of $MgCl_2$, 4 µl of 10x PCR buffer II, 2 µM of primer S4-FR, and 2.5 U of AmpliTaq® DNA polymerase were dispensed into each reaction tube. The PCR step was subjected to a 95˚C initial denaturation for 5 min and 35 cycles of 95˚C denaturation for 1 min, 55˚C annealing for 1 min, and 72˚C extension for 1 min, and followed by 72˚C final extension for 7 min. PCR products were detected following 1.5% agarose gel electrophoresis.

Construction of ARV σNS RNA standard

Full length (1104 bp) ChickVac™ S4 cDNA was obtained by conventional RT-PCR with primers S4-FF/S4-FR and cloned into NovaBlue Singles™ competent (*Escherichia coli*) cells via T7Blue-3 vectors, which was supplied by a blunt-end cloning kit (Novagen, Darmstadt, Germany), according to the manufacturers' instruction.

To verify successful insertion, recombinant plasmids were extracted from small-volume liquid cultures using Wizard® Plus SV kit (Promega, Madison, WI). Plasmids were digested with restriction enzymes *Sna*bI and *Hin*dIII (Promega, Madison, WI) to select the plasmids with inserts of correct size, and with restriction enzymes *Hin*dIII and *Mfe*I (Roche, Penzberg, Germany) to determine correct orientation (Fig. 3.2).

Plasmids with correct inserts were sequenced using T7 primer to confirm the full length sequence. Finally, plasmids were linearized with *HindIII* and transcribed with RiboMAX™ Large Scale RNA Production System-T7 (Promega, Madison, WI) to produce high quantity viral RNA in accordance with the kit instructions. Transcribed

RNA products were purified with Qiagen RNeasy Mini Kit (Valencia, CA), and concentrations were measured by the NanoDrop® ND-1000 UV-Vis Spectrophotometer.

Copy number of the S4 RNA was calculated by the following formula (Ke et al., 2006):

$$S4\ RNA(copies/\mu l) = \frac{6.022 \times 10^{23}\left(\frac{molecules}{mole}\right) \times concentration\left(\frac{g}{\mu l}\right)}{Molecular\ weight\ \left(\frac{g}{mole}\right)}$$

The specificity of real-time RT-PCR protocol

To examine the specificity of real-time RT-PCR, all 8 ARV strains, non-template negative controls, and other avian pathogens, including avian influenza virus (AIV) matrix, H5 and H7 genes, and infectious bursal disease virus (IBDV) strains (VarE and APHIS) were tested.

The detection limit

A limiting dilution assay was used to determine the detection limit of the assay (Ke et al., 2006; Taswell, 1981). Cloned full length ARV S4 RNA was diluted into 50, 30, 20, 5, and 1 copies per reaction tube. Ten replicates for each dilution were examined using real-time RT-PCR. Fraction of negative reactions was plotted against number of copies within the reaction tube. As for standard Poisson distribution, number of copies that can be detected with this assay corresponded to 37% negative reactions (Slaoui et al., 1984).

Viral titers

50% embryonic infective dosage (EID_{50}) and 50% tissue culture infective dosage ($TCID_{50}$) of the ARV reference strain 2408 determined as follows. Nine 10-fold serial dilutions of virus stock were made in PBS.

EID_{50}: Four 7-day chicken embryos were used per dilution and each embryo was inoculated with 200 µl of virus dilution via yolk sac route. Embryos were checked for typical pathological changes (hemorrhagic embryo, Fig. 3.3) after incubation for 72 hrs. The viral titer (EID_{50}) was calculated using Reed-Muench method (Reed and Muench, 1938).

$TCID_{50}$: 10^{-2} to 10^{-9} virus dilutions were inoculated to chicken embryo kidney (CEK) cell culture on 96-well cell culture plates. Five wells on each row for each dilution and two replicates on each plate were used. After incubation for 48 hrs, plates were examined under an inverted microscope for CPE and $TCID_{50}$ was calculated using Reed-Muench method (Reed and Muench, 1938).

3.3 Results

Specificity of the real-time RT-PCR assay

Real-time RT-PCR amplified ARV RNAs. All 8 ARVs strains were positive. No significant fluorescence signal was detected with non-template control. All non-ARVs, IBDV strains, AIV (H7, H5 and matrix genes) were negative (Fig. 3.4).

Detection limit

To determine the end point of sensitivity of real-time RT-PCR assay, serial dilutions at low concentrations between 50 and 1 genomic copies were analyzed. Detection limit of real-time RT-PCR was determined by extrapolating the point of 37% negative samples intersecting with the x-axis (number of copies) on the linear regression graph of limiting dilution assay. Results indicated that the detection limit of the real-time RT-PCR was approximately 25 ARV genome copies (Fig. 3.5).

Sensitivity comparison of real-time RT-PCR and conventional RT-PCR

Sensitivity of real-time RT-PCR assay was compared with conventional RT-PCR using cloned S4 RNA standard and identical primers (R-S4F/R-S4R). Conventional RT-PCR with the same primer set appeared able to detect as few as $3.8x10^3$ genomic copies (Fig. 3.6.), whereas the real-time RT-PCR was capable of detecting 25 copies of ARV RNA (Fig. 3.5). Therefore, real-time RT-PCR was about 150 ($3.8x10^3/25$) times more sensitive than conventional RT-PCR.

Reproducibility

Cloned ARV S4 RNA was serially diluted from 5 $x10^{10}$ to 50 copies/μl and subsequently detected by real-time RT-PCR (Fig. 3.7). The assay was repeated three times. Standard curves indicating the linear relationships between the threshold crossing points (Cp) and the logarithms of initial ARV S4 RNA count were constructed. Three replicates of standard curves had an average intercept of 40.86 ± 0.88 and an average slope of -3.237 ± 0.17. Standard curves showed a significant correlation between Cp values and copy number with $R^2 \approx 1$ and average efficiency of 2.040 ± 0.07 (Fig. 3.8, Table 3.4). Serial dilutions were amplified in triplicates in the same run to evaluate the intra-experimental reproducibility. Standard deviations of the Cp values were mostly less than 0.39 (Table 3.3). These data indicated excellent reproducibility.

Correlation between virus genome count and virus titer

Viral titers of ARV strain 2408 were measured using 7-day old chicken embryos and CEK cells. Both EID_{50} and $TCID_{50}$ titrations were repeated 3 times and compared with number of ARV genomic copies determined by the real-time RT-PCR assay. Results

indicated that 1 EID_{50} was equivalent to 3.91 $\pm$0.80 ARV genome copies, and 1 $TCID_{50}$ was equivalent to 2.9 $\pm$0.3 ARV genome copies (Table 3.5 A and B).

3.4 Discussion

ARVs are known to cause multiple disease conditions in chickens, which can lead to economic losses to the poultry industry. Rapid and accurate detection and identification of the pathogen is critical for controlling and prevention of ARV infections. In the current study, a sensitive and specificTaqMan probe based real-time PCR assay based on a conserved region of the ARV S4 genome segment was developed for the qualitative and quantitative detection of ARVs.

Previously, studies developed conventional RT-PCR based detection methods targeting various regions of ARV genome segments (Bruhn et al., 2005; Lee et al., 1998; Liu et al., 1999; Wen et al., 2004). However, these results indicated that the assays could obtain only low sensitivity for detecting ARVs from chicken tissues or cell cultures. Ke and coworkers (2006) reported quantitative real-time RT-PCR assay based on SYBR-Green I chemistry for detection of ARVs. The assay targeted ARV σA-encoding gene (genome segment S2), which resulted in high sensitivity (Ke et al., 2006). However, because of non-specific binding of SYBR-Green I dye to dsDNA molecules, sample RNA required laborious purification process and density gradient precipitation to remove cellular DNAs. In addition, results of the SYBR-Green based PCR can be affected by factors such as the formation of primer-dimers and sample concentration. Therefore, this assay must go through optimization to determine optimal PCR conditions. Furthermore, multiple SYBR-Green dye molecules can simultaneously bind to the same dsDNA fragment, thus the fluorescence intensity generated is proportional to the size of the DNA

molecule. These drawbacks have limited the application of SYBR-Green I based real-time PCR in quantitative detections.

In the current study, we reported the first TaqMan probe based real-time RT-PCR targeting the conserved region of ARV S4 genome segment. The assay achieved additional specificity because of inclusion of a dual-labeled sequence-specific probe. TaqMan probes only emit fluorescence signals upon complementary binding to the target region and subsequent cleavage by exonuclease activity of *Taq* polymerase. Therefore, sample preparation process is simplified. Regular commercial total RNA extraction kits can attain satisfactory results with simpler procedures. In the specificity test, TaqMan real-time RT-PCR has shown high specificity by detecting all eight different ARV strains with no cross-reaction with other avian viruses. TaqMan real-time PCR successfully detected CO8 and ss412, which unlike the other 6 strains belonged to different serological subgroups (BIOMUNE Inc., Lenexa, KS., 2007; Hieronymus et al., 1983).

Our assay was highly sensitive with the capability of detecting and quantifying ARV RNA templates as few as 25 copies per reaction. Considering 5 µl of sample was used in each PCR reaction, the lowest detectable concentration was about 5 copies/µl. TaqMan real-time RT-PCR was highly reproducible. Multiple repeats resulted in nearly identical standard curves, and the statistics indicated only small variations in the intercept (40.86 ± 0.88) and slope (-3.237 ± 0.17) of the regression equation (Fig. 3.7 and Table 3.4). Intra-experimental comparisons resulted in small variations (Table 3.3). Comparing conventional RT-PCR using the same primer set, real-time RT-PCR was about 150 times more sensitive for detecting cloned ARV S4 RNA.

Determination of virus or vaccine titer is critical for successful experiments or vaccination studies. Traditionally, virus titration was performed using standard VI method involving inoculation and incubation of virus in chicken embryos or cell culture, which took up to a week. In the current study, titers of ARV reference strain 2408 were determined (in replicates) in 7-day-old chicken embryos (EID_{50}) and CEK cell culture ($TCID_{50}$), and number of ARV genome copies were simultaneously determined with real-time RT-PCR. Results indicated that for ARV strain 2408, 1 EID_{50} was equivalent to 3.9 ± 0.8 ARV genome copies, and 1 $TCID_{50}$ was equivalent to 2.9 ± 0.3 ARV genome copies. ARV strain 2408 has been propagated in chicken embryos and cell cultures for vaccine development for nearly two decades (Rosenberger et al., 1989). These results indicated that this strain was well adapted to propagate in both chicken embryos and cell culture. Conversion factors provided a simple, rapid mathematical estimation of the viral titer for a particular ARV strain.

In conclusion, TaqMan based real-time RT-PCR reported in this study, can be used for early and rapid detection of ARV infections.

References

Adair, B. M., Burns, K., and McKillop, E. R., 1987. Serological studies with reoviruses in chickens, turkeys and ducks. J. Comp. Pathol. 97, 495-501.

Bains, B. S. and MacKenzie, M., 1974. Reovirus-associated mortality in broiler chickens. Avian Dis. 18, 472-476.

Benavente, J. and Martinez-Costas, J., 2007. Avian reovirus: Structure and biology. Virus Res. 123, 105-119.

BIOMUNE Inc., 2007. REOMUNE ss412 (Avian Reovirus Vaccine). BIOMUNE Inc., Lenexa, KS. USA.

Bruhn, S., Bruckner, L., and Ottiger, H. P., 2005. Application of RT-PCR for the detection of avian reovirus contamination in avian viral vaccines. J. Virol. Meth. 123, 179-186.

Caterina, K. M., Frasca, S., Girshick, T., and Khan, M. I., 2004. Development of a multiplex PCR for detection of avian adenovirus, avian reovirus, infectious bursal disease virus, and chicken anemia virus. Mol.Cell.Probe. 18, 293-298.

Fahey, J. E. and Crawley, J. F., 1954. Studies on chronic respiratory disease of chickens II. Isolation of a virus. Can. J. Comp. Med. Vet. S. 18, 13-21.

Hieronymus, D. R. K., Villegas, P., and Kleven, S. H., 1983. Identification and serological differentiation of several reovirus strains isolated from chickens with suspected malabsorption syndrome. Avian Dis. 27, 246-254.

Joklik,W.K. 1983. The reovirus particle. 9-78pp in The *Reoviridae*. Plenum Press Inc.

Ke, G. M., Cheng, H. L., Ke, L. Y., Ji, W. T., Chulu, J. L. C., Liao, M. H., Chang, T. J., and Liu, H. J., 2006. Development of a quantitative LightCycler real-time RT-PCR for detection of avian reovirus. J. Virol. Meth. 133, 6-13.

Kerr, K. M. and Olson, N. O., 1969. Pathology of chickens experimentally inoculated or contact-infected with an arthritis-producing virus. Avian Dis. 13, 729-745.

Kibenge, F. S. B. and Wilcox, G. E., 1983. Tenosynovitis in chickens. Vet. Bull. 53, 431-443.

Lee, L. H., Shien, J. H., and Shieh, H. K., 1998. Detection of avian reovirus RNA and comparison of a portion of genome segment S3 by polymerase chain reaction and restriction enzyme fragment length polymorphism. Res. Vet. Sci. 65, 11-15.

Liu, H. J., Chen, J. H., Liao, M. H., Lin, M. Y., and Chang, G. N., 1999. Identification of the C-encoded gene of avian reovirus by nested PCR and restriction endonuclease analysis. J. Virol. Meth. 81, 83-90.

Liu, H. J., Giambrone, J. J., and Nielsen, B. L., 1997. Molecular characterization of avian reoviruses using nested PCR and nucleotide sequence analysis. J. Virol. Meth. 65, 159-167.

McFerran, J. B., McCracken, R. M., Connor, T. J., and Evans, R. T., 1976. Isolation of viruses from clinical outbreaks of inclusion body hepatitis. Avian Pathol. 5, 315-324.

Menendez, N. A., Calnek, B. W., and Cowen, B. S., 1975. Localization of avian reovirus (FDO isolant) in tissues of mature chickens. Avian Dis. 19, 112-117.

Mertens, P., 2004. The dsRNA viruses. Virus Res. 101, 3-13.

Nibert, M. L., 1998. Structure of mammalian orthoreovirus particles, reoviruses I. structure, proteins and genetics. Curr. Top. Microbiol. 233, 2-30.

Page, R. K., Fletcher, O. J., Rowland, G. N., Gaudry, D., and Villegas, P., 1982. Malabsorption syndrome in broiler chickens. Avian Dis. 26, 618-624.

Reed,L.J. and Muench,H., 1938. A simple method of estimating fifty percent endpoints. Am.J.Hyg. 27, 493-497.

Robertson, M. D. and Wilcox, G. E., 1986. Avian reovirus. Vet. Bull. 56, 726-733.

Rosenberger, J. K., Sterner, F. J., Botts, S., Lee, K. P., and Margolin, A., 1989. *In vitro* and *in vivo* characterization of avian reoviruses. I. Pathogenicity and antigenic relatedness of several avian reovirus isolates. Avian Dis. 33, 535-544.

Schnitzer, T. J., 1985. Protein coding assignment of the S genes of the avian reovirus S1133. Virology. 141, 167-170.

Slaght, S. S., Yang, T. J., van der Heide, L., and Fredrickson, T. N., 1978. An enzyme-linked immunosorbent assay (ELISA) for detecting chicken anti-reovirus antibody at high sensitivity. Avian Dis. 22, 802-805.

Slaoui, M., Leo, O., Marvel, J., Moser, M., Hiernaux, J., and Urbain, J., 1984. Idiotypic analysis of potential and available repertoires in the arsonate system. J. Exp. Med. 160, 1-11.

Spandidos, D. A. and Graham, A. F., 1976. Nonpermissive infection of L cells by an avian reovirus: restricted transcription of the viral genome. J. Virol. 19, 977-984.

Taswell, C., 1981. Limiting dilution assays for the determination of immunocompetent cell frequencies. I. Data analysis. J. Immunol. 126, 1614-1619.

van der Heide, L. and Page, R. K., 1980. Field experiments with viral arthritis/tenosynovitis vaccination of breeder chickens. Avian Dis. 24, 493-497.

Varela, R. and Benavente, J., 1994. Protein coding assignment of avian reovirus strain S1133. J. Virol. 68, 6775-6777.

Wen, L. S., Ying, J. L., Hung, Y. S., Hung, J. L., and Long, H. L., 2004. Rapid characterization of avian reoviruses using phylogenetic analysis, reverse transcription-polymerase chain reaction and restriction enzyme fragment length polymorphism. Avian Pathol. 33, 171-180.

Table 3.1. Diseases associated with ARV strains tested

ARV Strains	Disease association or characteristics	Literature or origin
S1133	Tenosynovitis	(van der Heide and Page, 1980)
2408	Malabsorption/Tenosynovitis	(Rosenberger et al., 1989)
1733	Malabsorption/Tenosynovitis	(Rosenberger et al., 1989)
CO8	Malabsorption Syndrome	(Hieronymus et al., 1983)
JR1	Unknown, trypsin-resistant	Fort Dodge Animal Health, Inc.
ss412	Malabsorption/proventriculitis	(BIOMUNE Inc., 2007)
V.A.Vac®	Tenosynovitis Vaccine (3-8 wks old)	Fort Dodge Animal Health, Inc.
ChickVac™	Tenosynovitis Vaccine (1-10 day old)	Fort Dodge Animal Health, Inc.

Table 3.2. Real-time and conventional RT-PCR primers and TaqMan probe sequences

RT-PCR	Primers and Probes	Length	Positions
Real-time	R-S4F: ATTATGGCTGGCTTTGTACCT	21	433-453
	S4-P: FAM[a]-CGTGAAGGTGATGACTTTGCTCC-TAMRA[b]	23	454-476
	R-S4R: ACAATCTGAGGACGACCATC	20	572-553
Conventional Full-length	S4-FF: ATGGACAACACCGTGCGT	18	1-18
	S4-FR: CTACGCCATCCTAGCTGGAGA	21	1104-1084

[a] FAM, 6-carboxyfluorescein;
[b] TAMRA, 6-carboxytetramethylrhodamine.

Table 3.3. Intra-experimental reproducibility of real-time RT-PCR assay

Copy number	Mean C_p (cycles)	SD
$5x10^8$	12.68	±0.79
$5x10^7$	17.06	±0.13
$5x10^6$	18.90	±0.12
$5x10^5$	22.66	±0.30
$5x10^4$	25.71	±0.39
$5x10^3$	28.65	±0.08
$5x10^2$	32.44	±0.13
$5x10^1$	34.99	±0.14

Table 3.4. Statistics for standard curve and regression equations[a]

	Repeat 1	Repeat 2	Repeat 3	Mean	SD
Intercept	40.49	40.23	41.86	40.86	±0.88
Slope	-3.115	-3.162	-3.433	-3.237	±0.17
E^b	2.094	2.071	1.955	2.040	±0.07
R^2	0.9977	0.9958	0.9935		

[a] $Cp = slope \times \log(genome\ count) + intercept$

[b] E: Efficiency $= 10^{-1/slope}$

Table 3.5 A. Correlation between strain 2408 viral genome copy number and EID_{50}

	Titration 1[a]	Titration 2[a]	Titration 3[a]		
EID_{50}/ml	$1.26x10^4$	$8.91x10^5$	$1.26X10^6$	Mean	*SD*
Real-time RT-PCR (genome copies/ml)	$3.76x10^4$	$3.83x10^6$	$5.58x10^6$		
Conversion factor[b] (copies/EID_{50})	3.0	4.3	4.4	3.9	±0.8

[a] Titrations were repeated with 3 different virus stock solutions.

[b] 1 $EID_{50} \approx 3.9 \pm 0.8$ ARV 2408 genome copies.

Table 3.5 B. Correlation between strain 2408 viral genome copy number and $TCID_{50}$

	Titration 1[a]	Titration 2[a]	Titration 3[a]		
$TCID_{50}$/ml	$1.02X10^6$	$9.12X10^5$	$1.12X10^6$	Mean	*SD*
Real-time RT-PCR (genome copies/ml)	$2.89x10^6$				
Conversion factor[b] (copies/$TCID_{50}$)	2.8	3.2	2.6	2.9	±0.3

[a] Titration was repeated with the same virus stock solution.

[b] 1 $TCID_{50} \approx 2.9 \pm 0.3$ ARV 2408 genome copies

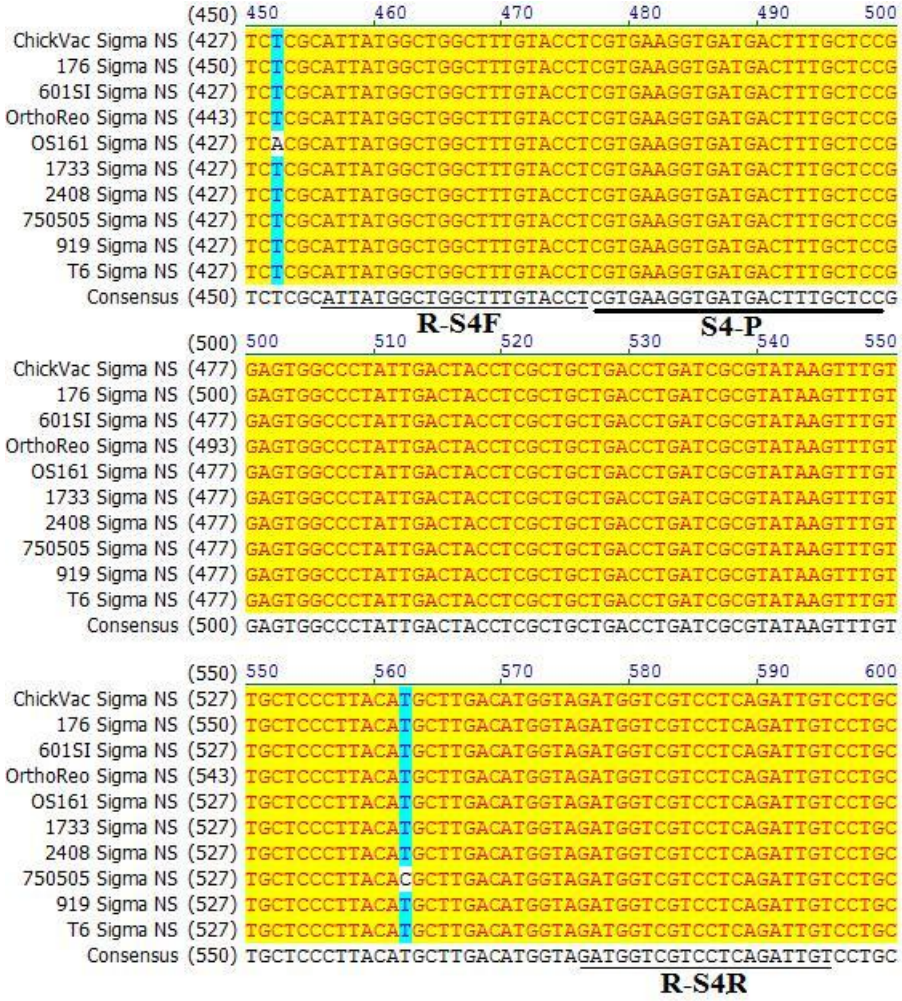

Figure 3.1. Multiple alignment analysis (partial) of ARV S4 genome segments and positions of primers (R-S4F/R-S4R) and TaqMan® probe (S4-P).

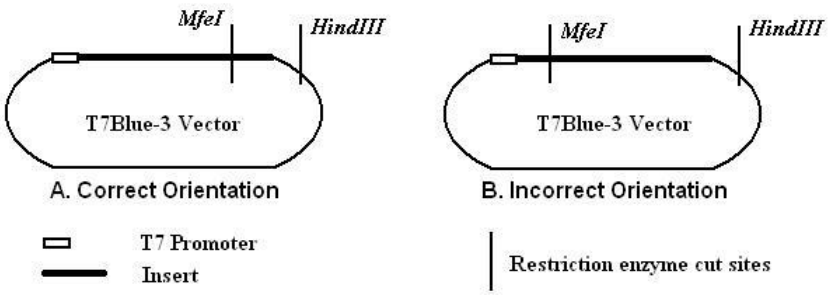

Figure 3.2. Diagram of using restriction enzyme digestion to determine the orientation of blunt-end inserts. A unique restriction site (*MfeI*) within the insert was selected, which divided the insert into two fragments of different length. Another restriction site (*HindIII*), which was located on the vector and close to the insert was chosen, so that with dual enzyme digestion, the insert with correct orientation could be easily identified by size of fragments.

Figure 3.3. Comparison of ARV infected chicken embryos (two hemorrhagic embryos on the right) and uninfected chicken embryos (two embryos on the left)

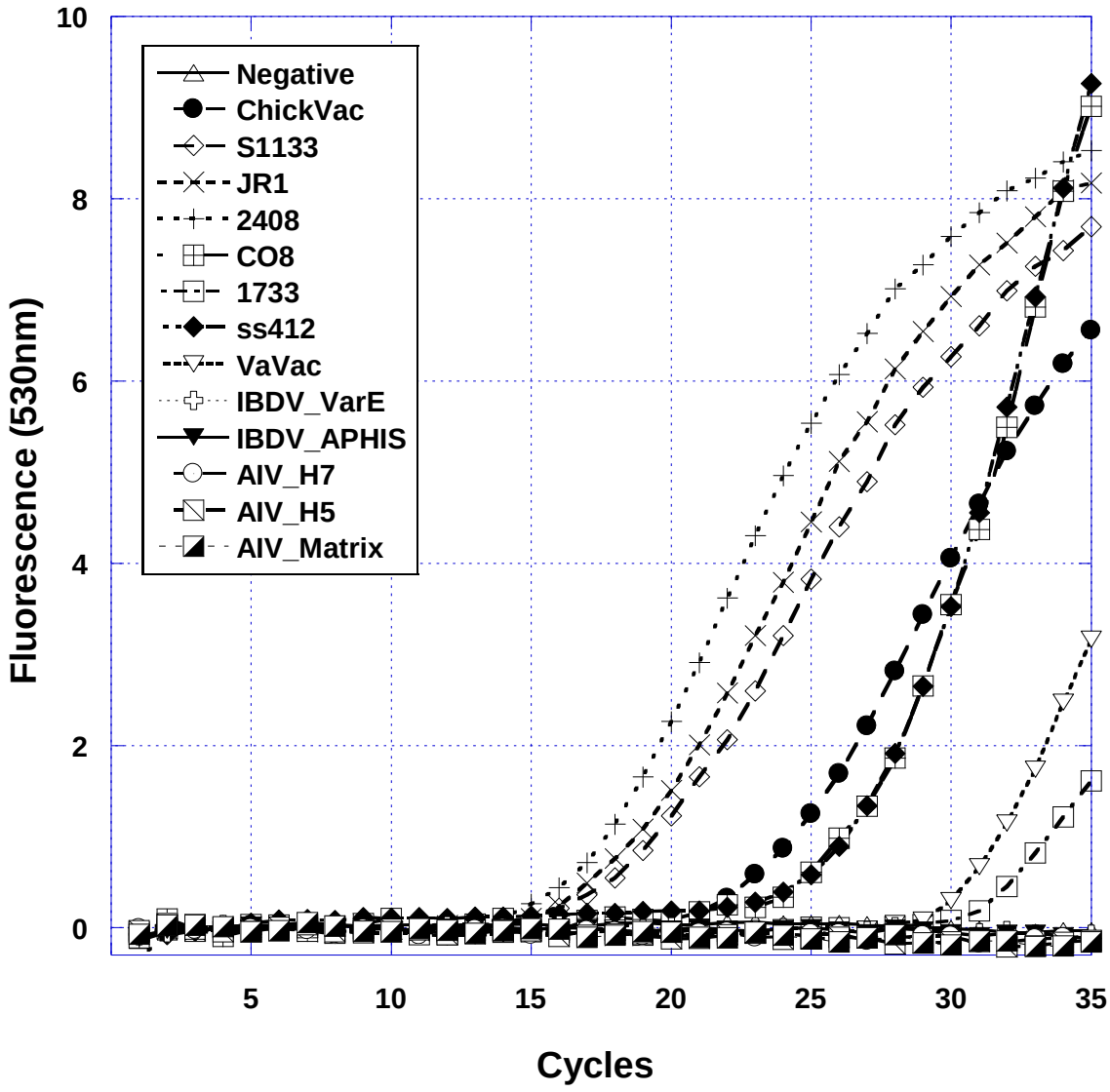

Figure 3.4. Specificity test of real-time RT-PCR. Eight ARV strains: ChickVac, S1133, JR1, 2408, CO8, 1733, ss412 and V.A.Vac and five non-ARV viral RNAs: IBDV VarE, IBDV APHIS, AIVs (H7, H5 and Matrix gene) were tested.

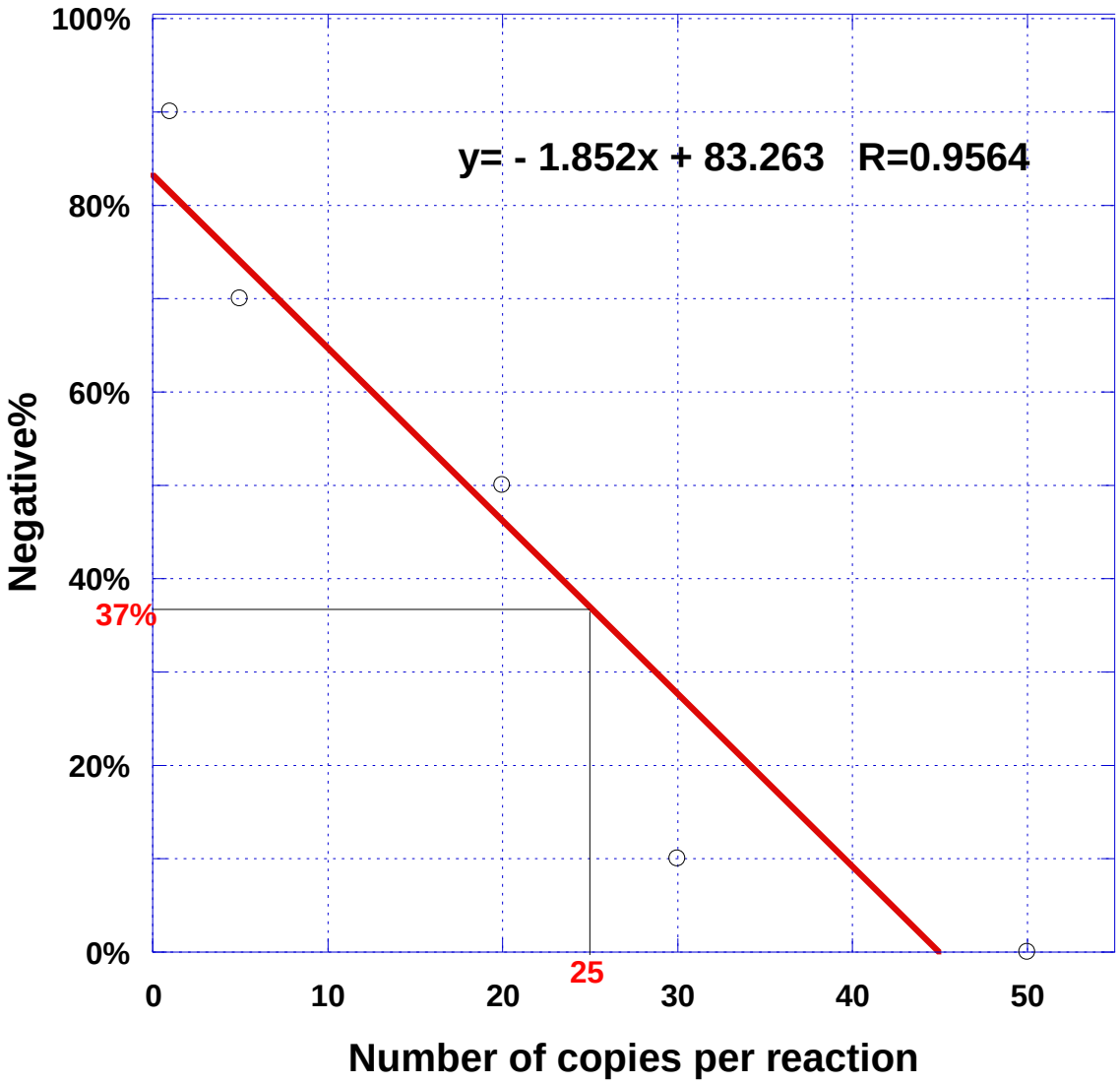

Figure 3.5. Limiting dilution assay indicated that the detection limit of TaqMan real-time RT-PCR was about 25 genome copies per reaction.

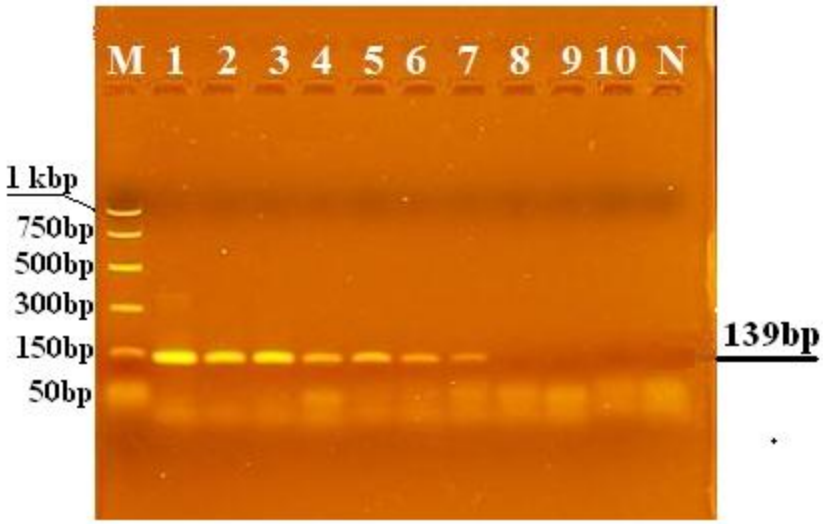

Figure 3.6. Electrophoresis photo of conventional RT-PCR of serial dilution of cloned ARV S4 gene on 1.8% agarose gel indicated the target amplicon of 139 bp. (M: DNA marker; 1: $3.8x10^9$; 2: $3.8x10^8$; 3: $3.8x10^7$; 4: $3.8x10^6$; 5: $3.8x10^5$; 6: $3.8x10^4$; 7: $3.8x10^3$; 8: $3.8x10^2$; 9: 3.8x10; 10: 3.8 genome copies; N: negative control)

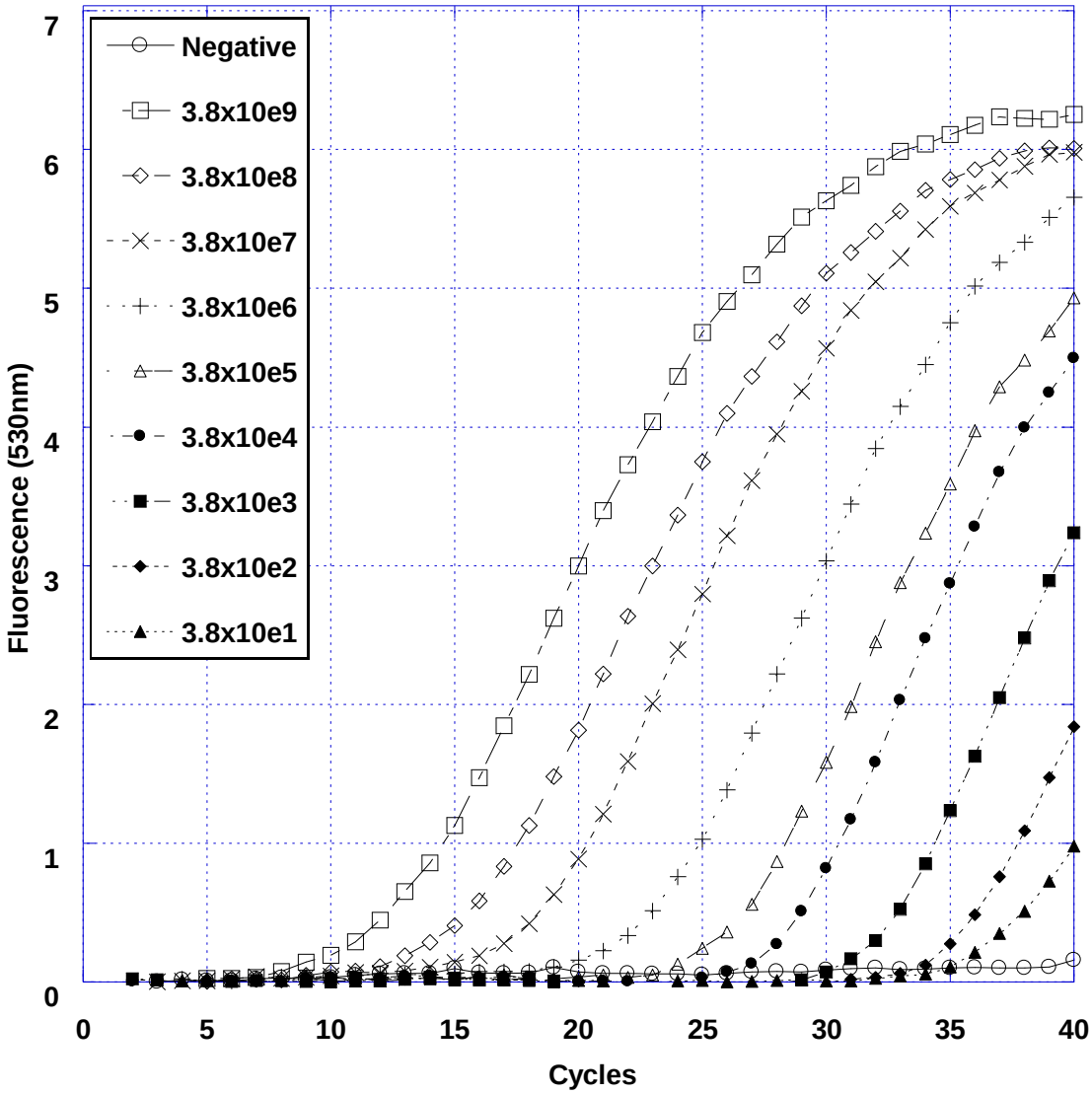

Figure 3.7. Amplification curves of 10-fold serial dilutions of cloned ARV S4 RNA. Legend indicates the number of copies of S4 RNA template.

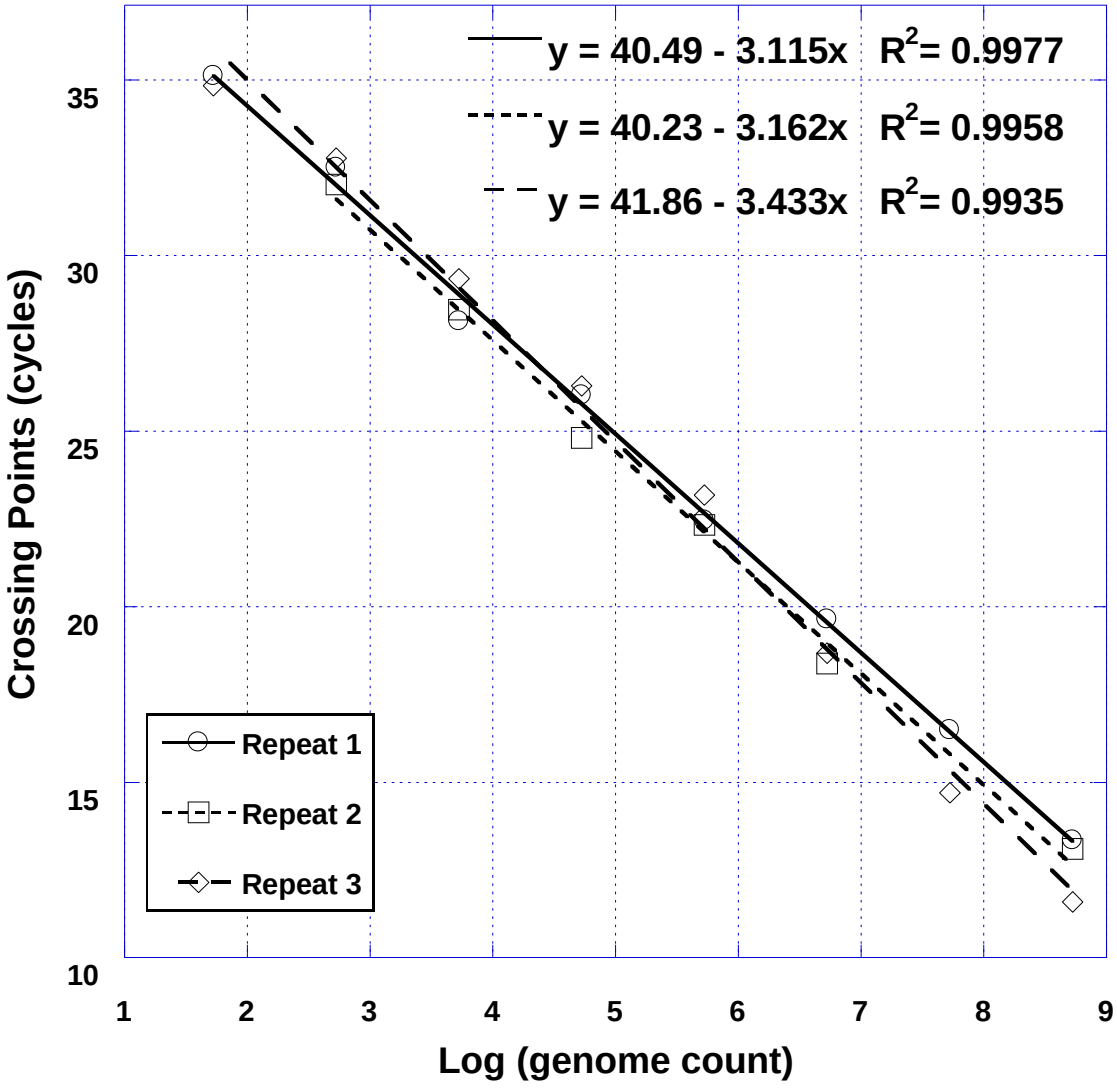

Figure 3.8. Standard curves (three repeats) of the TaqMan real-time RT-PCR assay and regression equations.

CHAPTER IV: DETECTION AND MONITORING OF AVIAN REOVIRUS SHEDDING FROM CLOACAL SWABS USING REAL-TIME RT-PCR

4.1 Introduction

Avian reoviruses belong to the genus of *Orthoreovirus* and the family of *Reoviridae* (Mertens, 2004; Nibert, 1998). They have a non-enveloped, double-layer concentric capsid of 70-80 nm in diameter, which encloses the segmented double-stranded RNA (dsRNA) genome (Spandidos and Graham, 1976). A total of 10 dsRNA segments can be categorized into three groups, which are designated L (large), M (medium), and S (small), based on their size and electrophoretic mobility. The 10 genome segments code for at least 8 structural proteins (λA, λB, λC, μA, μB/μBC, σC, σA and σB) and 4 non-structural proteins (μNS, P10, P17, and σNS) (Benavente and Martinez-Costas, 2007; Varela and Benavente, 1994).

ARVs are associated with tenosynovitis and viral enteritis related malabsorption syndrome, or runting and stunting syndrome, chronic respiratory disease, inclusion body hepatitis, myocarditis, and hydropericardium in young chickens (Bains and MacKenzie, 1974; Fahey and Crawley, 1954; Kerr and Olson, 1969; Kibenge and Wilcox, 1983; McFerran et al., 1976; Page et al., 1982). These diseases cause significant economic losses because of high mortality and morbidity, poor growth, and reduced feed

conversion. Viral arthritis can also increase the condemnation rate of chicken carcasses at slaughter due to the unpleasant appearance of affected hocks.

ARV strain 2408 is associated with malabsorption syndrome in young chicks. ARV infection caused disease in the digestive system, such as enteritis, hepatitis, pancreatitis, and proventriculitis, could disrupt normal feed digestion and nutrient absorption. This resulted in nutrient deficiency signs, such as weight gain depression, abnormal feather development, and increased morbidity and mortality (Songserm et al., 2003; Sterner et al., 1989; van der Heide et al., 1981).

The most effective and practical method of preventing and controlling ARV infections is vaccination. Multiple regimens of vaccines (both live and killed) are given to the breeder flocks to stimulate high antibody titers before sexual maturation. These antibodies in the hen can then be passed into embryos to protect newly hatched chicks from ARV infection (Giambrone, 1985).

ARVs can be transmitted vertically from parents to progeny and horizontally from infected birds via fecal oral route (Jones and Onunkwo, 1978; van der Heide and Kalbac, 1975). ARVs were reisolated from most tissues and organs within a short period post-infection (PI), such as liver in 6 hr PI, plasma, red blood cells, and monocyte fractions in 30 hr PI, bone marrow in 3-5 days PI, hock joint, respiratory, enteric, and reproductive tracts in 4 days PI (Kibenge et al., 1985; Menendez et al., 1975). No study has monitored virus shedding over time, which will provide information on the ARV infection cycle and virus-host interaction.

Monitoring virus shedding after ARV infection requires sampling and detection. Traditional ARV detection methods such as virus isolation (VI) and serological methods

such as virus neutralization (VN) are time-consuming and laborious, which made continuous sampling impractical. Previously, we developed a TaqMan probe based real-time RT-PCR for rapid detection of ARV infections. This assay was specific and sensitive and could detect as few as 25 ARV genome copies. In the current study, real-time RT-PCR successfully detected ARV in swab samples in a short time period.

4.2 Materials and methods

Avian reovirus

The 2408 strain of ARV was used to infect chickens. It was isolated by Rosenberger in late 1980s at the University of Delaware. The 2408 strain can cause malabsorption syndromes and viral arthritis in young chickens. Typical clinical signs are stunting, feather abnormality, weight depression, lameness, and mortality that may reach 84%. Gross and microscopic lesions can be observed in the liver, kidney, and intestines. (Rosenberger et al., 1989).

Experimental design

Fifty 1-day-old commercial broiler chickens, which were obtained from hens that had been vaccinated with multiple live and killed vaccines containing the S1133 virus, and 50 1-day-old specific-pathogen-free (SPF) white leghorn chickens were used. Twenty chicks from each group were sacrificed at one day of age to obtain blood. After centrifugation, serum samples were tested for maternal antibody titer against ARV at Alabama State Diagnostic Laboratory (Auburn, AL). The remaining thirty chickens from each group were separated in 2 modified Horsfall-Bauer isolation units maintained with

filtered air under negative pressure in the biocontainment facility of the Department of Poultry Science at Auburn University. Feed and water were provided *ad libitum*.

Each of the thirty remaining chicks of each group (both commercial and SPF group) received 0.15 ml of ARV 2408 inoculation containing 10^6 EID_{50} via intra-tracheal route at one day of age. Subsequently, cloacal swabs were collected at 1, 2, 3, 5, 7, 10, 14, 16, and 21 days post-infection (DPI). Ten birds were randomly selected from each group for sampling at each time. Each swab was immersed in 2 ml brain heart infusion broth (BHIB), which contained 1% (w/v) streptomycin and 0.6% (w/v) penicillin-G to eliminate bacterial contamination. Swabs were kept on ice during transportation from the biocontainment facility to the laboratory.

The last sampling and necropsy of commercial chickens was conducted on 16 DPI on all chickens. Sample collections from SPF chickens were conducted as planned, except 9 birds died within the first week. Post-mortem examinations were performed the same day as death; the remaining 21 chicks in the SPF group were euthanized and post-mortem examination was performed at 21 DPI.

Post-mortem examination and lesion scoring

Post-mortem examinations were performed on birds that died of acute infection. All remaining chickens were euthanized at the end of the experiment and necropsy exams were carried out to investigate the pathological changes (gross lesions) caused by the infection. Results of the post-mortem examination for each bird were recorded, and the severity of gross lesions was assigned a score as follows: 1, no lesion; 2, minor lesions (mildly congested and swollen) in liver and or kidney; 3, severe congestion, enlargement and discoloration in liver and kidney; and 4, liver and kidney lesions as lesion score 3

with additional lesion foci found in other tissues and organs, such as spleen, pericardium, proventriculus and footpad.

Cloacal swab sample preparation

Cloacal swabs were stirred in BHIB media to release fecal material, mixed well with media, and subsequently discarded. Sample collection tubes containing released fecal material were centrifuged at 2,000xg for 10 min to precipitate fecal material. Supernatants were transferred to 2 ml plastic tubes and stored at -70˚C.

Viral RNA extraction

Viral RNAs were extracted using Qiagen RNeasy® Mini Kit (Valencia, CA) with slight modifications. Briefly, 250 µl of swab sample supernatant were mixed with 3.5 volumes (875 µl) of lysis buffer RLT and 20 U Proteinase K (Sigma-Aldrich, St. Louis, MO) and incubated at 37˚C for 10 min. Two and half volumes (625 µl) of cold 100% ethanol were added and mixed well. Seven hundred microliters of the mixture was transferred to a RNeasy column and centrifuged at 9,000xg for 15 sec, then the flow-through was discarded. Remaining mixture was filtered through the same column and subsequently, the column was washed once with 700 µl of buffer RW1 and twice with 500 µl buffer RPE. The column was transferred to a new 2 ml collection tube and centrifuged at 14,000xg for 2 min to remove excess reagents in the column filter. Finally, total RNA was eluted in 30 µl of nuclease-free water.

Real-time RT-PCR

Real-time RT-PCR was previously developed with primers and TaqMan probes specifically targeting the conserved region in ARV S4 genome segment (Table 4.1).

Real-time RT-PCR was performed on a LightCycler® (Roche Applied Science, Indianapolis, IN) with a 20 µl reaction volume, containing 5 µl RNA prepared from fecal swab samples. The Qiagen One-Step RT-PCR Kit (Valencia, CA) was used to make the reaction mixtures, which contained 4 µl of 5x buffer, 3.75 mM $MgCl_2$, 325 µM dNTPs (each), 0.5 µM of each primer (R-S4F and R-S4R), 20 U of RNase inhibitor, 0.8 µl of Enzyme Mix, and 0.25 µM probe S4-P. Reverse transcription was carried out at 45˚C for 30 min, and subsequently the reverse transcriptase was deactivated at 95˚C for 15 min. PCR stage was subjected to 40 cycles at 95˚C denaturation for 0 sec, 59˚C annealing for 20 sec, and 72˚C extension for 10 sec.

4.3 Results

Effects of experimental infection

The ARV-infected commercial group all survived the 16-day experimental period. During the study, a few birds showed early signs of diarrhea. These signs disappeared within a week. The average serum ARV antibody titer obtained for maternal antibody of the day-old chicks was 5453±42. Post-mortem examinations of commercial chickens revealed that only 9 out of the 30 birds contained mild lesion foci in liver and kidney and the remaining 22 chickens were normal with no lesions. The mean lesion score was 1.3 ± 0.47 for commercial birds (Table 4.2).

In the SPF group, which lacked maternal immunity (Table 4.2), 9 birds died within the first week. This represented the mortality significantly higher than that of the commercial group (P<0.001). These early dead birds showed signs of acute infection with severe lesions and necrotic foci on the liver (Fig. 4.1). The remaining 21 birds showed clinical signs (lethargic with ruffled feathers) of viral infection. Green and white

diarrhea was seen at the bottom of the isolation unit. Birds gathered in the corner most of the time and feed consumption decreased in the first week of the infection. In addition, abnormal feather development was observed with some birds later in the experiment. Necropsy examination revealed all had liver and kidney congestion. Within the remaining 21 SPF birds some also demonstrated at least one of the following gross lesions, such as severe congested and discolored liver, swollen kidney, spleen, pericarditis, and proventriculitis (Fig. 4.2). One of the SPF birds also showed signs of viral arthritis (swollen and reddish) in the footpad and hock joint (Fig. 4.3). Because the 9 early-death birds had different viral infection progression, they were not included in lesion scoring. The mean lesion score for the remaining 21 birds was 3.05 ± 0.59, which was significantly higher than that of the commercial birds ($P<0.001$).

Real-time RT-PCR detection

ARV was detected in cloacal swabs in both the commercial group and SPF groups. They were positive for ARV in fecal excretions at 1 DPI and throughout the experimental period. In the commercial group, 80-90% of chickens were positive for ARV from 1-7 DPI. Detection rate gradually decreased after 7 DPI and only 2 samples out of 10 were positive at 16 DPI. The SPF group followed a similar trend, but with fluctuations. Positive rates remained high during 1-5 DPI ranging from 70% to 90%. Detected samples remained 40- 60% positive 7 through 14 DPI, and then gradually decreased. At 21 DPI, only one sample out of ten was positive for ARV (Fig. 4.4).

Virus shedding quantification

Quantitative detection was performed to estimate the amount of ARV excreted in the feces during the experiment. The ARV levels in the cloacal swabs from commercial

birds were low, ranging from 60 to 90 copies on 1, 7, 10 and 14 DPI, with slight increase between 2 and 5 DPI. In contrast, viral shedding in SPF birds was significantly higher. A peak viral shedding of about 40 times higher than that of the commercial group was observed at 7 DPI. Virus shedding decreased after 7 DPI, and reached a similar level as the commercial group at 14 DPI (Fig. 4.5).

4.4 Discussion

Multiple infection studies evaluating the susceptibilities of chickens at different ages have indicated that chickens were most susceptible to ARV infection at hatch with susceptibility dropping rapidly thereafter. Severity of disease, including gross and microscopic lesion development in the thymus, trachea, intestine, liver, etc. as well as virus shedding in the feces for chickens older than 1 week were less than younger birds. This indicated more resistance for ARV infection in older chicks, which correlated with the maturation of the immune systems (Jones and Georgiou, 1984; Montgomery et al., 1986; Roessler and Rosenberger, 1989). Since chicks are most susceptible to ARV infection, once hatched until at least a week-old, the common practice is to vaccinate breeder flocks so that maternal antibodies are passed passively to the newly hatched chicks via the yolk. Maternal antibodies and their protective capability for progeny were first studied in 1975 using the inactivated ARV Connecticut isolate S1133. Later, Giambrone (1985) proposed a multiple vaccination protocol that used live attenuated vaccine as a primer in the early life of breeders, followed by an inactivated vaccine at 6-weeks of age and again prior to egg production. This primer-booster vaccination scheme resulted in higher, more uniform and longer lasting titers in breeders and has become

common for the protection against many avian infectious diseases (Cessi and Lombardini, 1975; Giambrone, 1985).

In the current study, both commercial and SPF birds were inoculated with high dosage of the ARV 2408 strain at 1-day-old. The severity of disease between the two groups was different. Commercial birds, which contained high ARV antibody titer (5453±42), had no visible clinical signs of ARV infection. Post-mortem examination indicated mild gross lesions in these birds. Results showed that maternal antibodies, passed from breeders, were protective in commercial birds.

The SPF birds, on the other hand, had no detectable ARV antibodies. They developed severe clinical signs such as depression, diarrhea, and abnormal feather development, which are typical in malabsorption syndrome. In addition, 9 birds died (30% mortality) of acute infection within the first week. Necropsy of dead birds and the remaining 21 chickens revealed severe gross lesions in liver, kidney, proventriculus, and other organs. Lesions were consistent with the ARV 2408 strain, which causes malabsorption syndrome (Rosenberger et al., 1989). SPF chickens showed significantly higher lesion scores than those of the commercial birds, indicating more severe disease by the ARV infection.

Previous studies indicated that susceptibility to ARV infection varies among breeds of chickens. Lighter breeds and white leghorn layers were more resistant than heavier breeds, such as broilers. Broilers tended to have more severe gross lesions, longer virus persistence, and virus spread to more tissues and organs. They had delayed seroconversion compared with the lighter breeds and layers infected with the same virus (Jones and Kibenge, 1984). Results of the present study showed severe signs of

malabsorption syndrome in white leghorn SPF birds, whereas no visible clinical signs were observed for commercial broilers. This demonstrated the successful immunization of the breeder flocks and resultant protective effect of maternal antibodies.

Previous studies demonstrated that early pathogenetic progression of ARVs involved a viremic stage, which rapidly distributed the viruses throughout the body. ARVs were isolated from the intestine and bursa of Fabricius within 12 hr PI; in the blood in 24 to 48 hr PI. Viral distribution suggested that the epithelium of the intestine and bursa of Fabricius is a primary site for ARV entry and replication (Jones et al., 1989; Kibenge et al., 1985). Under experimental conditions, usually at 14-15 DPI, most viruses are eliminated from the host or are no longer detectable, except for the hock joint and oviduct, where ARV can persist for at least 285 DPI (Kerr and Olson, 1969). In the present study, viral RNA was detected as early as the first DPI in the feces of both commercial and SPF birds and persisted throughout 16-21 DPI. This agreed with previous studies.

The current study was the first to continuously quantitate ARV shedding through a 3-week period using the newly developed real-time RT-PCR. Although both groups were inoculated with a high dosage (10^6 EID_{50}) of virus, commercial birds excreted lower amount of virus compared to the SPF birds throughout the test period. Viral shedding from the SPF group was higher, and peaked about 40 times higher than the commercial group at 7 DPI. The significant increase in virus shedding during the first week coincided with high mortality. This result was probably due to the absence of maternal antibodies in SPF birds. ARVs rapidly spread within the host and replicated in large numbers during the first week.

The newly developed TaqMan probe based real-time RT-PCR detected and monitored virus shedding in infected commercial and SPF chickens. Cloacal samples were used for viral RNA extraction without propagating in chicken embryos. Subsequently they were tested for viral RNA with the real-time RT-PCR. The process of sampling, RNA extraction, and real-time RT-PCR assay took about 3-4 hours depending on number of samples processed. This is significantly less time compared to traditional VI tests, which can take up to 7 days because of virus propagation in chicken embryos or cell culture. Results indicated that real-time RT-PCR was highly sensitive and suitable for rapid detection of ARVs.

References

Bains, B. S. and MacKenzie, M., 1974. Reovirus-associated mortality in broiler chickens. Avian Dis. 18, 472-476.

Benavente, J. and Martinez-Costas, J., 2007. Avian reovirus: Structure and biology. Virus Res. 123, 105-119.

Cessi, D. and Lombardini, F., 1975. Orientamenti sulla profilassi dell artrite virale aviare. Vaccinazione dei reproduttori, gran parentali e parentali. Clin. Vet. 98, 414-417.

Fahey, J. E. and Crawley, J. F., 1954. Studies on chronic respiratory disease of chickens II. Isolation of a virus. Can. J. Comp. Med. Vet. S. 18, 13-21.

Giambrone, J. J., 1985. Vaccinating pullets to control reovirus associated diseases. Poult. Digest. 44, 96-100.

Jones, R. C., Islam, M. R., and Kelly, D. F., 1989. Early pathogenesis of experimental reovirus infection in chickens. Avian Pathol. 18, 239-253.

Jones, R. C. and Kibenge, F. S. B., 1984. Reovirus-induced tenosynovitis in chickens: The effect of breed. Avian Pathol. 13, 511-528.

Jones, R. C. and Georgiou, K., 1984. Reovirus-induced tenosynovitis in chickens the influence of age at infection. Avian Pathol. 13, 441-457.

Jones, R. C. and Onunkwo, O., 1978. Studies on experimental tenosynovitis in light hybrid chickens. Avian Pathol. 7, 171-181.

Kerr, K. M. and Olson, N. O., 1969. Pathology of chickens experimentally inoculated or contact-infected with an arthritis-producing virus. Avian Dis. 13, 729-745.

Kibenge, F. S. B., Gwaze, G. E., Jones, R. C., Chapman, A. F., and Savage, C., 1985. Experimental reovirus infection in chickens: Observations on early viraemia and virus distribution in bone marrow, liver and enteric tissues. Avian Pathol. 14, 87-98.

Kibenge, F. S. B. and Wilcox, G. E., 1983. Tenosynovitis in chickens. Vet. Bull. 53, 431-443.

McFerran, J. B., McCracken, R. M., Connor, T. J., and Evans, R. T., 1976. Isolation of viruses from clinical outbreaks of inclusion body hepatitis. Avian Pathol. 5, 315-324.

Menendez, N. A., Calnek, B. W., and Cowen, B. S., 1975. Localization of avian reovirus (FDO isolant) in tissues of mature chickens. Avian Dis. 19, 112-117.

Mertens, P., 2004. The dsRNA viruses. Virus Res. 101, 3-13.

Montgomery, R. D., Villegas, P., and Kleven, S. H., 1986. Role of route of exposure, age, sex, and type of chicken on the pathogenicity of avian reovirus strain 81-176. Avian Dis. 30, 460-467.

Nibert, M. L., 1998. Structure of mammalian orthoreovirus particles, reoviruses I. structure, proteins and genetics. Curr. Top. Microbiol. 233, 2-30.

Page, R. K., Fletcher, O. J., Rowland, G. N., Gaudry, D., and Villegas, P., 1982. Malabsorption syndrome in broiler chickens. Avian Dis. 26, 618-624.

Roessler, D. E. and Rosenberger, J. K., 1989. *In vitro* and *in vivo* characterization of avian reoviruses. III. Host factors affecting virulence and persistence. Avian Dis. 33, 555-565.

Rosenberger, J. K., Sterner, F. J., Botts, S., Lee, K. P., and Margolin, A., 1989. *In vitro* and *in vivo* characterization of avian reoviruses. I. Pathogenicity and antigenic relatedness of several avian reovirus isolates. Avian Dis. 33, 535-544.

Songserm, T., van Roozelaar, D., Kant, A., Pol, J., Pijpers, A., and ter Huurne, A., 2003. Enteropathogenicity of Dutch and German avian reoviruses in SPF white leghorn chickens and broilers. Vet. Rec. 34, 285-295.

Spandidos, D. A. and Graham, A. F., 1976. Nonpermissive infection of L cells by an avian reovirus: restricted transcription of the viral genome. J. Virol. 19, 977-984.

Sterner, F. J., Rosenberger, J. K., Margolin, A., and Ruff, M. D., 1989. *In vitro* and *in vivo* characterization of avian reoviruses. II. Clinical evaluation of chickens infected with two avian reovirus pathotypes. Avian Dis. 33, 545-554.

van der Heide, L. and Kalbac, M., 1975. Infectious tenosynovitis (viral arthritis) : Characterization of a connecticut viral isolant as a reovirus and evidence of viral egg transmission by reovirus-infected broiler breeders. Avian Dis. 19, 683-706.

van der Heide, L., Lutticken, D., and Horzinek, M., 1981. Isolation of avian reovirus as a possible etiologic agent of osteoporosis ("brittle bone diseas"; "femoral head necrosis") in broiler chickens. Avian Dis. 25, 847-856.

Varela, R. and Benavente, J., 1994. Protein coding assignment of avian reovirus strain S1133. J. Virol. 68, 6775-6777.

Table 4.1 TaqMan real-time PCR primer and probe sequences for ARV S4 gene

Primers and Probes (5' → 3')
Forward primer: ATTATGGCTGGCTTTGTACCT
Probe: FAM-CGTGAAGGTGATGACTTTGCTCC-TAMRA
Reverse primer: ACAATCTGAGGACGACCATC

Table 4.2 Disease in chickens infected with ARV strain 2408[a]

	1-day serum ARV antibody titer	Mortality[b]	Lesion score
Commercial group	5453 ±42	0	1.30 ±0.47[c]
SPF group	_	9	3.05 ±0.59[d]

[a] For the commercial chickens, necropsy examination was conducted on 16 DPI on all 30 chickens; for 9 early dead SPF chicks, necropsy was performed the same day after death; the remaining 21 SPF birds were euthanized and examined on 21 DPI.

[b] Mortality in the 30 birds of each group. SPF group had 9 chicks died in first week of the experiment. The mortality of the SPF group was significantly higher than that of the commercial group by Chi-square test ($P<0.001$)

[c, d] Means with different lowercase superscripts were significantly different ($P<0.001$) by Wilcoxon Signed Rank test.

Figure 4.1. Liver congestion and necrotic foci observed in an SPF chick, which died in first week of infection with ARV.

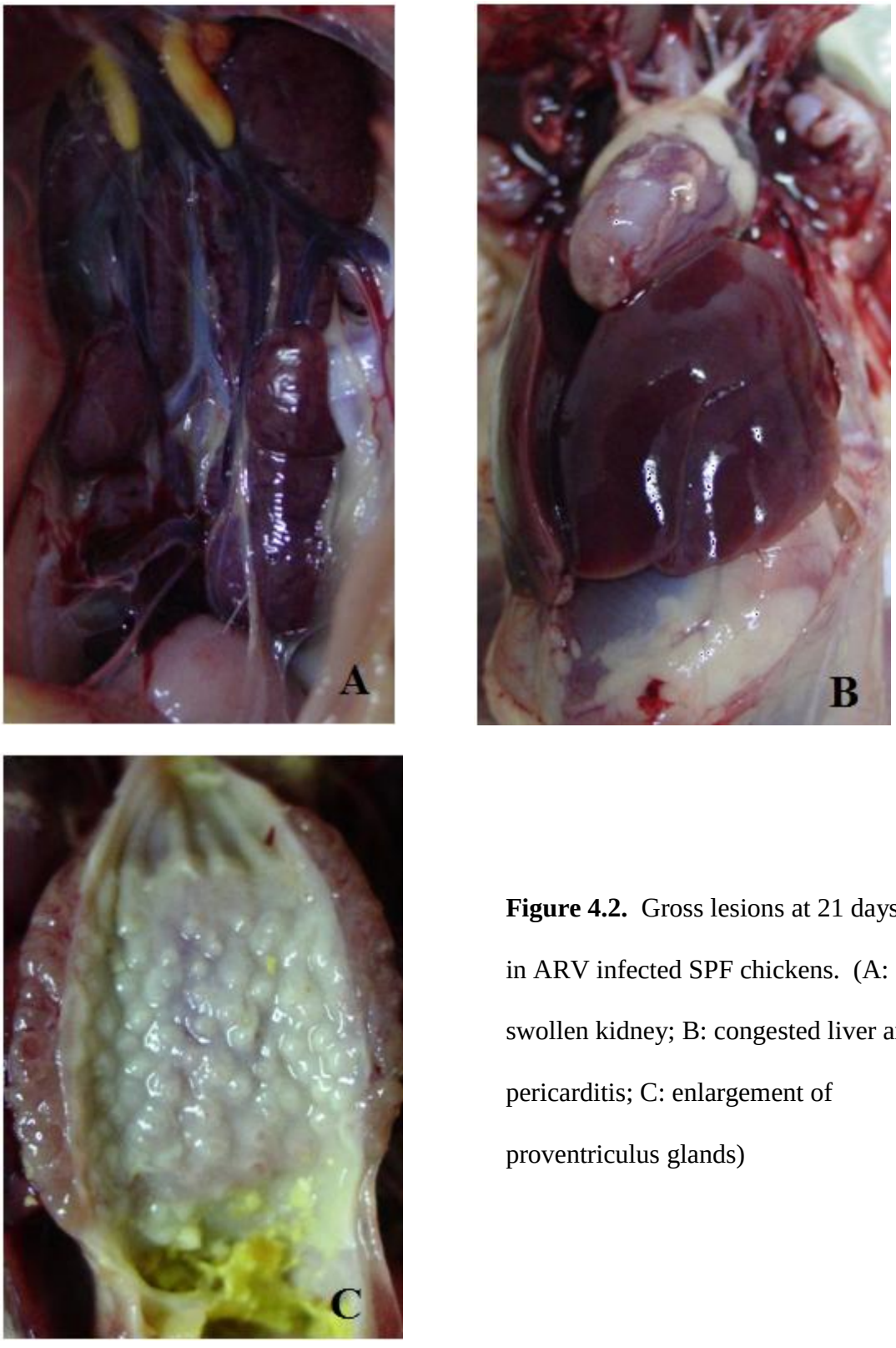

Figure 4.2. Gross lesions at 21 days in ARV infected SPF chickens. (A: swollen kidney; B: congested liver and pericarditis; C: enlargement of proventriculus glands)

Figure 4.3. Comparison of ARV infected footpad (left) in an SPF chicken and a normal chicken (right)

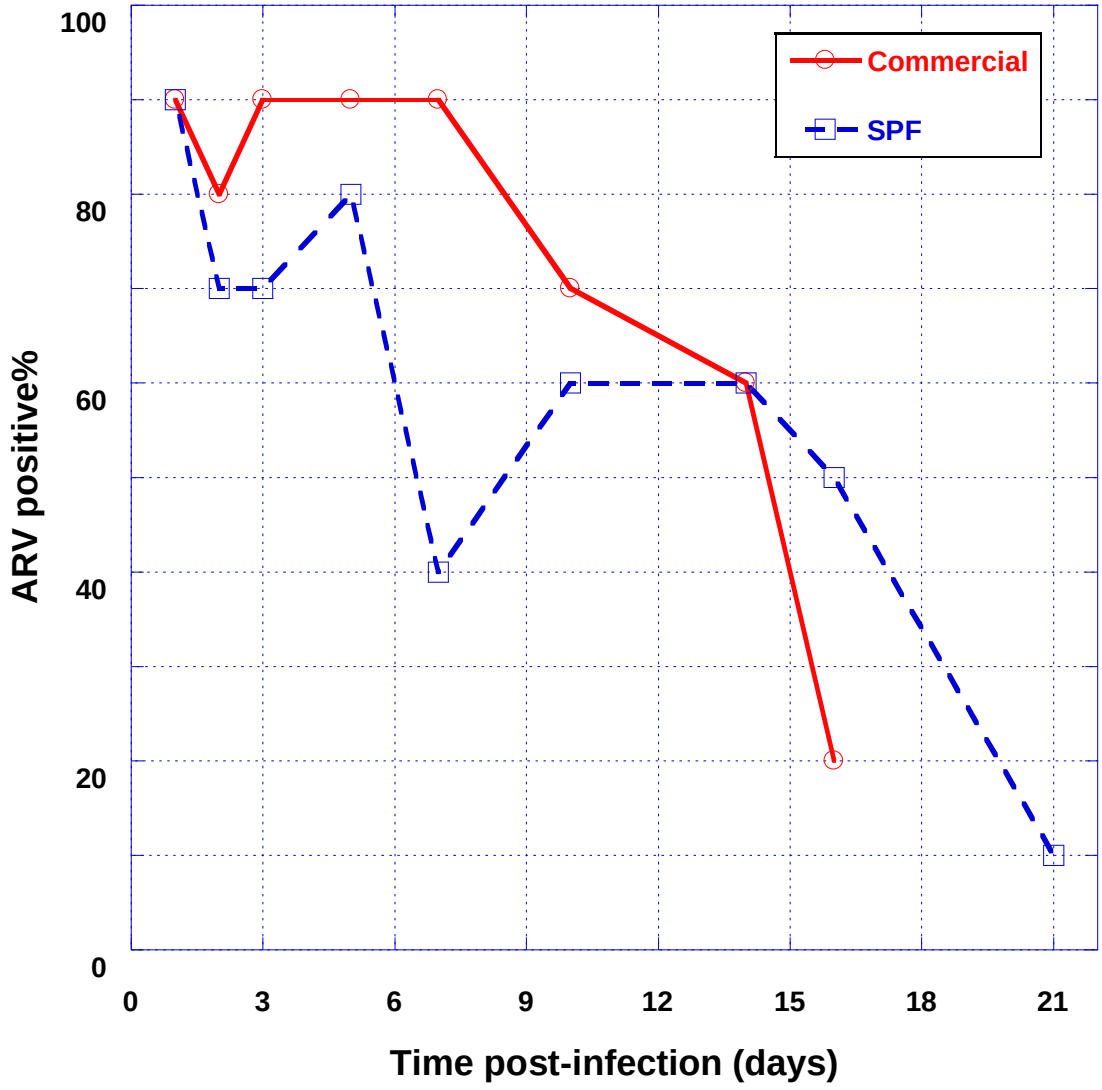

Figure 4.4. Percentage of birds positive for ARV from cloacal swabs detected by real-time RT-PCR of both commercial and SPF chicks.

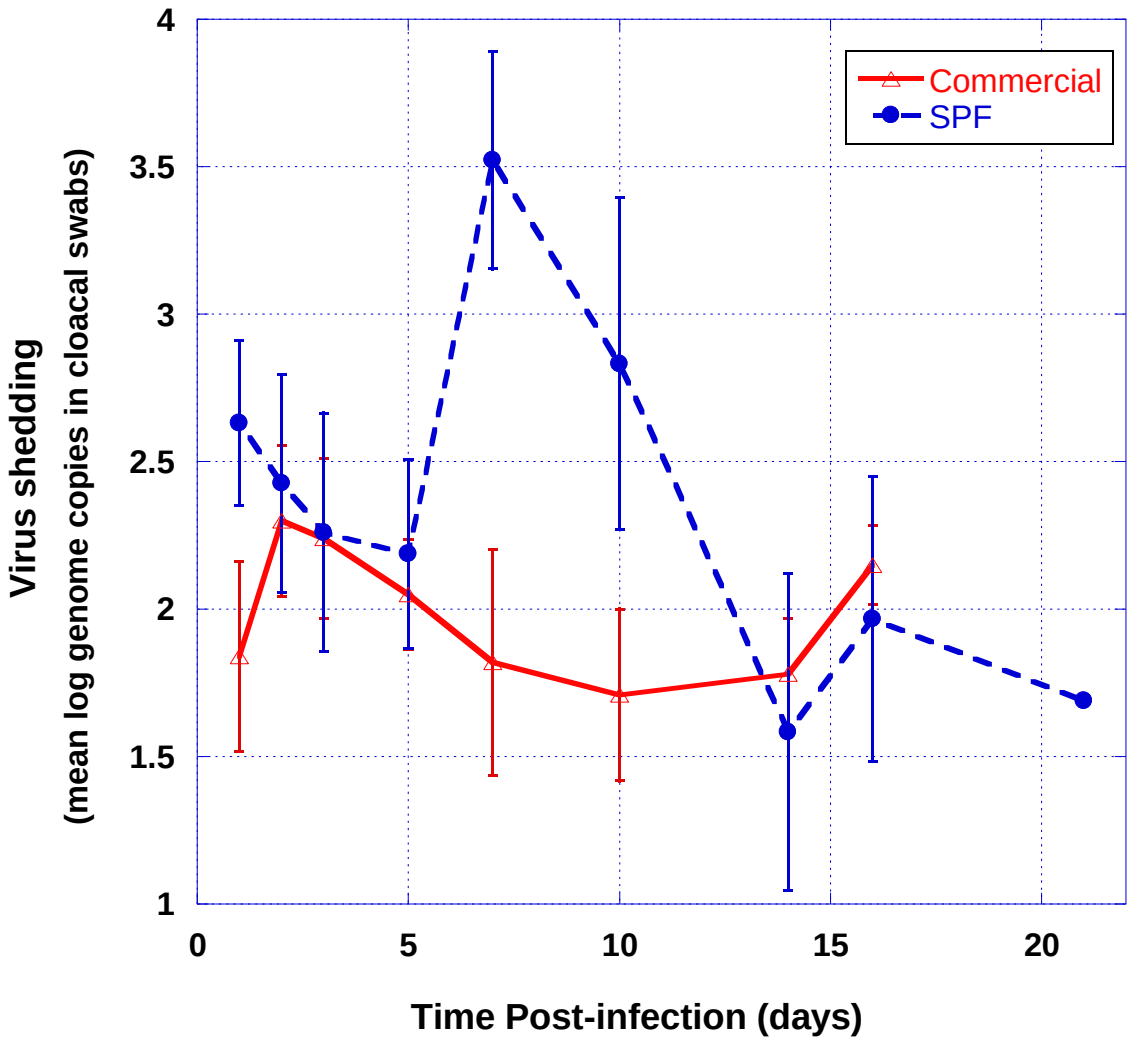

Figure 4.5. Number of ARV RNA copies detected in cloacal swabs after infection monitored by real-time RT-PCR from both commercial and SPF chicks.

CHAPTER V: DIFFERENTIATION OF NORTH AMERICAN AVIAN REOVIRUS STRAINS USING SYBR-GREEN I BASED TWO-STEP REAL-TIME RT-PCR WITH MELTING CURVE ANALYSIS

5.1 Introduction

Avian reovirus belongs to *Orthoreovirus* genus and *Reoviridae* family (Mertens, 2004). ARVs are pathogens associated with multiple conditions in poultry and can cause economical losses (Rosenberger et al., 1989). They were first identified as the cause of tenosynovitis in young chickens, and subsequently were associated with enteritis, respiratory disease, myocarditis, hepatitis, and malabsorption syndrome. However, most disease conditions were subclinical, which caused difficulty in detection and prevention (Bains and MacKenzie, 1974; Fahey and Crawley, 1954; Kerr and Olson, 1969; Kibenge et al., 1985; McFerran et al., 1976; Page et al., 1982).

ARVs are associated with immunosuppression in infected birds, which can enhance the effects of secondary infection by other pathogens, such as infectious bursal disease virus, chicken anemia virus, and Newcastle disease virus *etc*. Co-infection of pathogens can result in synergistic effects, which may lead to more severe diseases and poor immunological response to vaccination (Page et al., 1982; Robertson and Wilcox, 1986).

There are over 40 distinct ARVs that have been isolated and characterized world-wide. They are categorized into 5 subtypes in Japan (Kawamura et al., 1965; Takase et

al., 1987), 3 subtypes in Australia (Robertson et al., 1984), and 11 subtypes in other regions and countries (Wood et al., 1980). A phylogenetic study grouped them into 5 major geographical clusters: the Netherlands, Germany, Taiwan, Australia, and the US, among which Australian and US isolates have a higher uniformity than other regions (Kant et al., 2003). Heterogeneity in sequences and serological classifications may result from high mutation rate of viral RNA and the possible reassortment when 2 strains co-infect the same host (Rekik et al., 1991). Isolated geographical characteristics facilitated exchange of segmented genomes within small numbers of viral strains, which resulted in less genetic variations within the region. In fact, all North American ARV strains belong to the same serotype (van der Heide, 2000). Nevertheless, diversities in serological and phylogenetic classifications did not help scientists find correlations with specific diseases (Kant et al., 2003).

Closely related strains provided ease of detection and prevention. On the other hand, small differences in genotypes affected the vaccination responses. Studies indicated that S1133 attenuated vaccine resulted in poor titer and only partial protection against infection with strain 1733 as compared to the recombinant vaccine developed specifically from 1733 (Vasserman et al., 2004). Therefore, to achieve effective protection against ARVs, it is important to identify the specific pathogenic and antigenic subtype before carrying out vaccination.

To differentiate closely related strains, one must locate the area or region in the viral genome that contains variations. The σC-encoding gene located at the third open reading frame of the S1 genome segment codes for the attachment protein for the virus, which allows its binding with host cells. The σC protein is located on the surface of the outer

layer capsid, induces neutralizing antibody production and is the determinant for ARV serotypes (Martinez-Costas et al., 1997). σC-encoding gene has a higher mutation rate than other ARV genes (Liu et al., 2003). Therefore, we selected it as the target to differentiate ARVs.

We compared σC genes for different strains by melting peak analysis of RT-PCR products using SYBR-Green real-time PCR. SYBR-Green is an asymmetrical cyanine dye, which binds the minor groove of double stranded DNA. Under excitement of a light source (e.g. ultraviolet light), SYBR Green dye can emit a strong fluorescent signal upon binding to double stranded DNA. The intensity of the fluorescent emissions increases during PCR annealing and extension phases (Nygren et al., 1998). As more double stranded amplicons are produced, SYBR Green dye signal will increase. Although, SYBR-Green dye binds dsDNA non-specifically, SYBR-Green real-time PCR has some advantages over TaqMan probe based real-time PCR. It is easy to design, because it has no requirement for probe. Also, it can accommodate a long fragment and most importantly, it allows melting curve analysis, which can provide additional specificity verification.

Melting peak analysis monitors changes in fluorescent signal during a continuous temperature increase. This analysis is based on the fact that each dsDNA has its own specific melting temperature (T_m), which is defined as the temperature at which 50% of DNA becomes single-stranded. The T_m value of a dsDNA molecule is determined by its size (number of nucleotides), G-C content, Watson-Crick pairing and sequence order. As temperature increases, the proportion of dissociated dsDNA increases; therefore, using dsDNA dye, such as SYBR-Green I, when temperature reaches the T_m, the fluorescent

signal will drop (Ririe et al., 1997). A sequence-specific melting peak is calculated as the negative first derivative of fluorescence change, meaning the temperature at which the highest reduction of fluorescence signal strength occurs.

In the current study, a SYBR-Green based real-time PCR scheme was developed to amplify 3 regions of the σC genes of different ARV strains using three primer pairs, which maximize the coverage of mutation sites. Subsequently, melting peak analyses were performed to determine the specific melting peak temperature combination profile for each ARV strain. This method was used to differentiate ARVs.

5.2 Materials and methods

Avian reovirus strains and sample preparation

The ARVs included in the study were S1133, 2408, 1733, CO8, ss412, and JR1, and two vaccine strains (V.A. Vac®, and ChickVac™). All North American ARVs belong to the same serotype; however, the CO8 and ss412 each belongs to a different subtype (BIOMUNE Inc., 2007; Giambrone and Solano, 1988). V.A. Vac® and ChickVac™ were derived from S1133, which is the standard reovirus challenge virus. Strain JR1, which is trypsin-resistant, was kindly provided by Fort Dodge Animal Health (Fort Dodge, IA). Table 5.1 lists ARV strains and their association with disease.

Virus propagation and preparation

All strains were propagated in primary chicken embryo kidney (CEK) cell cultures. Flasks were collected after 48 to 72 hrs of incubation when 75%-85% CPE was observed. Cell culture flasks were frozen and thawed three times to rupture the cell membrane and release virus particles. Subsequently cell culture materials were transferred into 30 ml

centrifugation tubes, which contained 3 ml of 40% sucrose. Centrifugation was at 100,000 xg using Type 30 rotor with Beckman® (Fullerton, CA) ultracentrifuge L8-70 for 1.5 hr. The bottom phase, which contained concentrated virus and cell debris, was collected into cryopreservation vials and stored at -70˚C until use.

Viral RNA extraction

The total RNA was extracted from virus stock using Qiagen RNeasy® Mini Kit (Valencia, CA) with slight modifications. Briefly, 250 µl of virus stock were mixed with 3.5 volumes (875 µl) of lysis buffer RLT and 20 U Proteinase K (Sigma-Aldrich, St. Louis, MO) and incubated at 37˚C for 10 min. Two and half volumes (625 µl) of cold 100% ethanol were added and mixed well. Seven hundred microliters of the mixture was transferred to a RNeasy column and centrifuged at 9,000xg for 15 sec, then the flow-through was discarded. All the remaining mixture was filtered through the same column and subsequently, the column was washed once with 700 µl of buffer RW1 and twice with 500 µl buffer RPE. The column was transferred to a new 2 ml collection tube and centrifuged at 14,000xg for 2 min to remove excess reagents in the column filter. Finally, total RNA was eluted in 30 µl of nuclease-free water.

Concentrations were measured using NanoDrop® ND-1000 UV-Vis Spectrophotometer (Wilmington, DE). RNA samples were diluted to similar concentration (35-40 ng/µl) to minimize concentration effects of the amplification during real-time RT-PCR.

Experiment and primer design

A multiple alignment analysis of available nucleotide sequences of σC gene was conducted using Vector NTI ® v10.3 (Invitrogen , Carlsbad, CA). Three partially overlapping regions (Fig. 5.1), which contain the most differences, were selected. Three primer sets were designed to amplify these regions, which resulted in amplicons of 451 bp, 370 bp and 357 bp in length, respectively, for 5' region, center region, and the 3' region (Fig. 5.1 and Table 5.2). All primers were designed to have similar T_m values, so that 3 sets of PCR amplification could be conducted under the same conditions.

Two-step real-time RT-PCR

Reverse transcription (RT) reaction was performed using QuantiTect® Reverse Transcription Kit (Qiagen, Valencia, CA), according to the manufacturer's instructions with minor adjustments. RNA sample was mixed with 2 µl of 7x gDNA wipeout buffer (included in the kit) and nuclease-free water (a total reaction of 14 µl) and incubated at 42˚C for 2 min to remove contaminating cellular DNA. After incubation, the tube was chilled immediately on ice. Subsequently, 1 µl of Quantiscript Reverse Transcriptase, 4 µl of 5x Quantiscript RT buffer and 1 µl random hexamer primer were added into each tube, which concluded a total reaction of 20 µl. The RT was performed at 42˚C for 15 min in a GeneAmp® PCR System 9700 thermocycler (Applied BioSystems, Foster City, CA).

SYBR-Green real-time PCR was performed in Roche LightCycler® 1.5 with LightCycler® software version 4.05 (Indianapolis, IN). Total reaction of 20 µl consisted of 2 µl finished RT reaction and 18 µl of real-time PCR master mix made from QuantiTect® SYBR® Green PCR Kit (Qiagen, Valencia, CA), including 10 µl of 2x

QiantiTect SYBR Green PCR Master Mix, 1 µl of each primer (final concentration of 0.3 µM) and 6 µl of nuclease-free water. Real-time PCR was carried out at 95˚C for 15 min to activate HotStart Taq DNA polymerase, and 50 cycles at 94˚C denaturation for 15 sec, 55˚C annealing for 20 sec, and 72˚C extension for 22 sec. A single fluorescence signal acquisition was set at the end of each extension step. Melting curve analyses began with 95˚C initial denaturation for 0 sec followed by 65˚C annealing for 15 sec. Then the temperature was gradually increased at the ramp rate of 0.1˚C/sec until it reached 95˚C. Fluorescence detection was set to the continuous acquisition mode to record fluorescence signal intensity changes during the course of temperature increase.

Statistical analyses on T_ms

The SYBR-Green real-time PCRs were repeated 5-6 times for each primer set and ARV strain combination to obtain sufficient data for statistical analyses. All T_ms were transformed to ΔT_ms to exclude the back ground noise by subtracting the mean T_m of the non-template negative control of each corresponding primer set. The mean ΔT_ms of all ARV strains at each of the three regions were compared respectively by using Tukey-Kramer (HSD) multiple comparison method in SAS v9.1 (Cary, NC).

Amplification and sequencing of full-length ARV S1 segment

An extended RT primer "Uni13" (5'- GCTGACGATGAAT-3') was designed to bind with the conserved 5 bases "UCAUC" at 3' end of positive strands of all ARV genome segments (Nibert and Schiff, 2001). Two more bases (AU) to the 5' end of the 5 conserved bases were included, because multiple alignment analyses indicated that they are conserved in S1, S4, L1, and M2 genome segments (data not shown). Additionally,

a pair of extended PCR primers ES1F (5'- CTGACGATGCCGCTTTTTCAAT-3') and ES1R (5'-GACAGTGCTGACGATGAATAACCAAT-3'), were constructed to recognize both the conserved 7 bases and 5 bases at the 5' and 3' end of S1 segment, respectively.

Two-step RT-PCR (Hoffman, et al., 2001) was employed to amplify the S1 genome segment. Briefly, 4 µl of ARV RNA was transcribed into cDNA using AMV reverse transcriptase (Promega, Madison, WI) according to the manufacturer's instruction by using 500 ng of primer Uni13 in 30 µl. The RT step was performed at 42 ℃ for 60 min. Subsequently, 4 µl of RT-reaction was used in PCR amplification using the Expanded High-Fidelity PCR system (Roche Diagnostics, Mannheim, Germany) according to the provided protocol. The final concentrations of primer (ES1F/ES1R) were 0.6 µM. The PCR program consisted of a 4-min period of 94 ℃ followed by 50 cycles with following conditions: 94 ℃ for 30 sec, 57 ℃ for 45 sec, and 72 ℃ for 7 min. The program ended with a final extension at 72 ℃ for 7 min.

The PCR products were gel purified using Wizard® PCR Preps DNA Purification System (Promega, Madison, WI) and subsequently sequenced using combinations of external primers ES1F/ES1R with internal primers 2408LF/2408LR on the automated ABI PRISM® 3100 Genetic Analyzer at Auburn University Genetic Analysis Lab. Results were used for reconstructing full-length ARV S1 genome segments. A phylogenetic tree was generated by AlignX program from Vector NTI® v10.3 sequence analysis program package (Invitrogen, Carlsbad, CA) using Neighbor Joining method of Saitou and Nei (1987).

5.3 Results

The melting peak temperature profiles

The three regions of σC gene of each ARV were tested with their corresponding primer sets in separate reactions in replicates, and the melting peak temperatures were transformed to obtain ΔT_ms. In figure 5.2 and 5.3 (A to C), the mean ΔT_ms were grouped by ARV strains and regions, respectively, indicating distinct ΔT_m combination profiles of each ARV strain and the ΔT_m variations among ARV strains at each regions. Multiple comparison analyses of the mean ΔT_ms of all ARV strains at each region were performed and results indicated that at the 5' region (Fig. 5.3 A), ARV 1733 had the highest ΔT_m and there were no differences in ΔT_m between strain S1133 and its derivatives (V.A. Vac® and ChickVac™), and the trypsin-resistant strain JR1. Additionally, ARV strains CO8 and ss412 had significant lower ΔT_m than all other strains at the 5' region. In the center region (Fig. 5.3 B), both strains 2408 and 1733 had higher ΔT_m than other strains and ss412 was the lowest. No significant differences in ΔT_ms were found between the remaining 5 ARV strains in this region. In the 3' region (Fig. 5.3 C), ARV strains S1133, 2408, CO8, JR1 and VaVac® all showed similar ΔT_m. On the other hand, strains ChickVac™, 1733, and ss412 had significantly lower ΔT_m with ss412 having the lowest.

Phylogenetic analyses

Nucleotide sequences of σC genes were extracted from full-length S1 segments for 2408, CO8, and ss412 and compared with the σC genes of S1133, 1733, 2408, ChickVac™ [which were previously sequenced in our lab (not published)], JR1 (GenBank accession number: EF122836) and VaVac® (EF122837) (both were

previously sequenced in our lab), S1133 (AF330703), and 2408 (AF204945). The ARV strain S1133, JR1, and the two vaccine strains (ChickVac™and V.A.Vac®) had the identical pattern at all mutations sites at all three regions, except ChickVac™ had a G at position 791 in the 3' region. All other ARV strains displayed different point mutations patterns within all three SYBR-Green real-time PCR tested regions (Table 5.3 A to C). Phylogenetic analyses (Fig. 5.4) indicated that the σC genes of viral arthritis inducing strain S1133 and its derivatives VaVac® and ChickVac™ were closely related. Trypsin-resistant strain JR1 was also closely related to S1133. On the other hand, all remaining MAS associated ARV strains 1733, 2408, ss412, and CO8 were clustered in a separate branch showing their closeness with each other in their σC genes.

5.4 Discussion

Traditionally, ARV strains were differentiated by cross virus neutralization assays, which measured the percentage of plaque-reduction in primary chicken kidney cell culture (Wood et al., 1980). In contrast, the genotypical classification of ARVs was performed using conventional RT-PCR in combination with phylogenetic analysis and/or other molecular techniques, such as restriction fragment length polymorphism (Kant et al., 2003; Lee et al., 1998; Liu et al., 1999; Wen et al., 2004). However, serological classification of ARVs has not been successful, because of high cross-reactivity of the neutralizing antibodies. It is puzzling that no correlation was found between genotypes, serotypes and pathotypes, given the detectable genetic differences of different ARV strains (Kant et al., 2003). Discrepancies between genotypes, serotypes, and

pathogenicity suggested the involvement of multiple genes/proteins in serological and pathogenic determination.

To develop a real-time RT-PCR to distinguish among American ARV strains, all published σC nucleotide sequences of North American ARV strains were compared and found to have at least 96.6% sequence similarity. Moreover, mutation sites were scattered across the whole gene. Therefore, the σC gene had no short (20-30 bp in length) strain-specific regions, which could be used for designing probes for probe based real-time PCR. However, utilizing melting peak analysis of DNA dye – SYBR-Green based real-time RT-PCR was a viable option for differentiation of isolates.

In the current study, 3 sets of primers were designed to encompass 3 partially overlapping regions in ARV σC gene, which included the majority of mutation sites. This scheme then utilized the melting curve aspect of the SYBR-Green based real-time PCR to analyze differences in mean ΔT_ms in these regions of all tested ARVs. Results demonstrated that each ARV had a unique ΔT_m combination of the three regions (Fig. 5.3 A to C). Therefore, it was possible to differentiate ARV strains based on their ΔT_m profile.

It is noteworthy that both ARV strains CO8 and ss412 were different from the other strains (Fig. 5.3). Mean ΔT_m of CO8 was the lowest in the 5' region (Fig. 5.3 A) and multiple alignment analyses indicated that it contained A→T, G→C and C→A transversions at positions 179, 317 and 405 as compared to S1133, respectively. C→T, T→C and A→G transitions were also observed at positions 84, 212, 338, and 376 (Table 5.3 A). On the other hand, the 5' region of ARV strain 1733 when compared with S1133, contains A→C (positions 71 and 213) and T→G (234) transversions and T→C (338) and

A→G (376, 397, and 405) transitions. Together they may contribute to its high mean ΔT_ms in the 5' region. ARV strain ss412 also displayed a significantly lower mean ΔT_m, which may correspond to its variations at 6 out of 14 of the common mutation sites discovered in this region.

Although all mutation sites in the center region were included in the 5' region (Table 5.3 B), with removal of mutation sites 46, 54 and 71 and different surrounding sequences, the mean ΔT_m profile in this region displayed a different pattern (Fig. 5.3 B). The mean ΔT_m of strain ss412 was the lowest, and the mean ΔT_m of strain CO8 was similar to those of JR1, VaVac® and ChickVac™. The differences in sequence composition and the ΔT_m change in the 5' region and the center region may indicate that the T at position 84 was critical for the low T_m of CO8 in the 5' region. In contrast, strain 1733 and 2408 remained the highest in 5' region.

There were 6 point mutation sites in the 3' region (Table 5.3 C). Compared to strain S1133, strain ss412 had Ts (at 495, 726, and 778) and A (at 695) at positions where strain S1133 had Gs or Cs. These may result in lower mean ΔT_m of ss412 in this region (Fig. 5.3 C). Similarly, strain 1733, which was the second lowest mean ΔT_m, had three Ts at positions 495, 726, and 781, where S1133 had Gs or Cs.

It is known that ARV strains CO8 and ss412 are the only North American ARVs studied belonging to their own serological subtypes (BIOMUNE Inc., 2007; Giambrone and Solano, 1988). In the current study, the mean ΔT_m profiles of CO8 in the 5' region and ss412 in all three regions were significantly lower than all other strains. In contrast, another newly isolated trypsin-resistant strain JR1 appeared similar to other ARVs (except CO8 and ss412). Sequencing of the σC gene of the JR1 strain revealed that it had

96.6% nucleotide sequence similarity with other North American strains. In addition, phylogenetic analysis also confirmed that JR1 was closely related to S1133 and its derivatives. On the other hand, a phylogenetic tree grouped CO8 and ss412 with other MAS associated North American ARV strains. Furthermore, the sequence differences between strains 1733 and S1133 in all three regions may explain the partial protection of S1133 based vaccine against strain 1733 (Vasserman et al., 2004). In the current study, these sequence differences were also reflected in different ΔT_m profiles.

5.5 Conclusion

SYBR-Green I real-time RT-PCR was developed for subtyping of ARVs based on ΔT_m profiles of 3 different regions of ARV σC gene. This assay utilized SYBR-Green chemistry and real-time PCR. It provided an alternative means of characterizing the σC gene, which was capable of differentiating closely related North American ARVs.

References

Bains, B. S. and MacKenzie, M., 1974. Reovirus-associated mortality in broiler chickens. Avian Dis. 18, 472-476.

BIOMUNE Inc., 2007. REOMUNE ss412 (Avian Reovirus Vaccine). BIOMUNE Inc., Lenexa, KS, USA. http://www.biomunecompany.com/chickens/reomuness412.html

Fahey, J. E. and Crawley, J. F., 1954. Studies on chronic respiratory disease of chickens II. Isolation of a virus. Can. J. Comp. Med. Vet. S. 18, 13-21.

Giambrone, J. J. and Solano, W., 1988. Serologic comparison of avian reovirus isolates using virus neutralization and an enzyme-linked immunosorbent assay. Avian Dis. 32, 678-680.

Hieronymus, D. R. K., Villegas, P., and Kleven, S. H., 1983. Identification and serological differentiation of several reovirus strains isolated from chickens with suspected malabsorption syndrome. Avian Dis. 27, 246-254.

Hoffmann, E., Stech, J., Guan, Y., Webster, R. G., Perez, D. R., 2001. Universal primer set for the full-length amplification of all influenza A viruses. Arch. Virol. 146, 2275-2289.

Kant, A., Balk, F., Born, L., van Roozelaar, D., Heijmans, J., Gielkens, A., and ter Huurne, A., 2003. Classification of Dutch and German avian reoviruses by sequencing the σC protein. Vet. Rec. 34, 203-212.

Kawamura, H., Shimizu, F., Maeda, M., and Tsubahara, H., 1965. Avian reovirus: Its properties and serological classification. Natl. Inst. Anim. Hlth. Q. 5, 124

Kerr, K. M. and Olson, N. O., 1969. Pathology of chickens experimentally inoculated or contact-infected with an arthritis-producing virus. Avian Dis. 13, 729-745.

Kibenge, F. S. B., Gwaze, G. E., Jones, R. C., Chapman, A. F., and Savage, C., 1985. Experimental reovirus infection in chickens: Observations on early viraemia and virus distribution in bone marrow, liver and enteric tissues. Avian Pathol. 14, 87-98.

Lee, L. H., Shien, J. H., and Shieh, H. K., 1998. Detection of avian reovirus RNA and comparison of a portion of genome segment S3 by polymerase chain reaction and restriction enzyme fragment length polymorphism. Res. Vet. Sci. 65, 11-15.

Liu, H. J., Chen, J. H., Liao, M. H., Lin, M. Y., and Chang, G. N., 1999. Identification of the σC-encoded gene of avian reovirus by nested PCR and restriction endonuclease analysis. J. Virol. Meth. 81, 83-90.

Liu, H. J., Lee, L. H., Hsu, H. W., Kuo, L. C., and Liao, M. H., 2003. Molecular evolution of avian reovirus:: evidence for genetic diversity and reassortment of the S-class genome segments and multiple cocirculating lineages. Virology. 314, 336-349.

Martinez-Costas, J., Grande, A., Varela, R., Garcia-Martinez, C., and Benavente, J., 1997. Protein architecture of avian reovirus S1133 and identification of the cell attachment protein. J. Virol. 71, 59-64.

McFerran, J. B., McCracken, R. M., Connor, T. J., and Evans, R. T., 1976. Isolation of viruses from clinical outbreaks of inclusion body hepatitis. Avian Pathol. 5, 315-324.

Mertens, P., 2004. The dsRNA viruses. Virus Res. 101, 3-13.

Nibert, M. L. and Schiff, L. A. 2001. Reoviruses and their replication. Pp.1679-1728 in Fields virology. Knipe, D. M. and Hooley, P. M. Lippincott Williams & Wilkins, Philadelphia, PA.

Nygren, J., Svanvik, N., and Kubista, M., 1998. The interactions between the fluorescent dye thiazole orange and DNA. Biopolymers. 46, 39-51.

Page, R. K., Fletcher, O. J., Rowland, G. N., Gaudry, D., and Villegas, P., 1982. Malabsorption syndrome in broiler chickens. Avian Dis. 26, 618-624.

Rekik, M. R., Silim, A., and Bernier, G., 1991. Serological and pathogenic characterization of avian reoviruses isolated in Quebec. Avian Pathol. 20, 607-617.

Ririe, K. M., Rasmussen, R. P., and Wittwer, C. T., 1997. Product differentiation by analysis of DNA melting curves during the polymerase chain reaction. Anal. Biochem. 245, 154-160.

Robertson, M. D. and Wilcox, G. E., 1986. Avian reovirus. Vet. Bull. 56, 726-733.

Robertson, M. D., Wilcox, G. E., and Kibenge, F. S. B., 1984. Prevalence of reoviruses in commercial chickens. Aust. Vet. J. 61, 319-322.

Rosenberger, J. K., Sterner, F. J., Botts, S., Lee, K. P., and Margolin, A., 1989. *In vitro* and *in vivo* characterization of avian reoviruses. I. Pathogenicity and antigenic relatedness of several avian reovirus isolates. Avian Dis. 33, 535-544.

Saitou, N.; and Nei, M., 1987. The neighbor-joining method: a new method for reconstructing Guide Trees. Mol. Biol. Evol. 4, 406-425.

Takase, K., Nonaka, F., Yamamoto, M., and Yamada, S., 1987. Serological and pathogenetic studies on avian reoviruses isolated in Japan. Avian Dis. 31, 464-469.

van der Heide, L., 2000. The history of avian reovirus. Avian Dis. 44, 638-641.

van der Heide, L. and Page, R. K., 1980. Field experiments with viral arthritis/tenosynovitis vaccination of breeder chickens. Avian Dis. 24, 493-497.

Vasserman, Y., Eliahoo, D., Hemsani, E., Kass, N., Ayali, G., Pokamunski, S., and Pitcovski, J., 2004. The influence of reovirus sigma C protein diversity on vaccination efficiency. Avian Dis. 48, 271-278.

Wen,L. S., Ying, J. L., Hung, Y. S., Hung, J. L., and Long, H. L., 2004. Rapid characterization of avian reoviruses using phylogenetic analysis, reverse transcription-polymerase chain reaction and restriction enzyme fragment length polymorphism. Avian Pathol. 33, 171-180.

Wood, G. W., Nicholas, R. A. J., Hebert, C. N., and Thornton, D. H., 1980. Serological comparisons of avian reoviruses. J. Comp. Pathol. 90, 29-38.

Table 5.1. Disease association of different ARV strains

ARV Strains	Disease association or characteristics	Literature or origin
S1133	Tenosynovitis	(van der Heide and Page, 1980)
2408	Malabsorption/Tenosynovitis	(Rosenberger et al., 1989)
1733	Malabsorption/Tenosynovitis	(Rosenberger et al., 1989)
CO8	Malabsorption Syndrome	(Hieronymus et al., 1983)
JR1	Unknown, trypsin-resistant	Fort Dodge Animal Health, Inc
ss412	Malabsorption/proventriculitis	(BIOMUNE Inc., 2007)
V.A.Vac®	Tenosynovitis Vaccine (3-8 wks old)	Fort Dodge Animal Health, Inc.
ChickVac™	Tenosynovitis Vaccine (1-10 day old)	Fort Dodge Animal Health, Inc.

Table 5.2. SYBR-Green based real-time PCR primer sequences

Primers	Sequence	Length	Positions
5’ region			
2408L-F	5’-TCA ATC CAT CGC AGC GAA GAG-3’	21	11-31
2408L-R	5’-GAC TCC AAT GAT TTA ACA CGA TCC TG -3’	26	461-436
Center region			
2408C-F	5’-GCG TCT ACG GAG TTA TTA CAT CGC T-3’	25	124-148
2408C-R	5’-AGG CGA AAA AGA TAG ACC ATG AC-3’	23	493-471
3’ region			
2408R-F	5’-TGG AGT CTA CCG CGA GTC A-3’	19	455-473
2408R-R	5’-TTG GAA TCC CGC ACT GG-3’	17	811-795

Table 5.3. Sites of point mutations of different ARV strains discovered by multiple alignment analyses of the σC genes

A. Point mutations in 5' region (primer set:2408L-F/2408L-R) of σC gene

ARV Strains	Positions of point mutations (ARV σC gene)														
	46	**54**	**71**	**84**	**179**	**212**	**213**	**234**	**317**	**338**	**376**	**382**	**397**	**403**	**405**
S1133	A	A	A	C	A	C	A	T	G	T	A	A	A	A	C
2408	A	A	C	C	A	C	C	T	C	C	A	A	A	G	A
CO8	A	A	A	T	T	T	A	A	C	C	G	A	A	A	A
ss412	T	A	C	G	A	T	C	T	C	T	A	A	A	A	A
1733	A	T	C	C	A	T	C	G	C	C	G	T	G	G	A
JR1	A	A	A	C	A	C	A	T	G	T	A	A	A	A	C
VaVac	A	A	A	C	A	C	A	T	G	T	A	A	A	A	C
ChickVac	A	A	A	C	A	C	A	T	G	T	A	A	A	A	C

B. Point mutations in Center region (primer set:2408C-F/2408C-R) of σC gene

ARV Strains	Positions of point mutations (ARV σC gene)										
	179	**212**	**213**	**234**	**317**	**338**	**376**	**382**	**397**	**403**	**405**
S1133	A	C	A	T	G	T	A	A	A	A	C
2408	A	C	C	T	C	C	A	A	A	G	A
CO8	T	T	A	A	C	C	G	A	A	A	A
ss412	A	T	C	T	C	T	A	A	A	A	A
1733	A	T	C	G	C	C	G	T	G	G	A
JR1	A	C	A	T	G	T	A	A	A	A	C
VaVac	A	C	A	T	G	T	A	A	A	A	C
ChickVac	A	C	A	T	G	T	A	A	A	A	C

C. Point mutations in 3' region (primer set:2408R-F/2408R-R) of σC gene

ARV Strains	Positions of point mutations (ARV σC gene)					
	495	**695**	**726**	**778**	**781**	**789**
S1133	G	C	C	C	G	T
2408	G	C	T	C	G	T
CO8	G	C	C	C	G	T
ss412	T	A	T	T	G	T
1733	T	C	T	T	T	T
JR1	G	C	C	C	G	T
VaVac	G	C	C	C	G	T
ChickVac	G	C	C	C	G	G

Figure 5.1. Schematic diagram of the experimental design. Three pairs of primers were designed to amplify three regions of ARV 2408 sigma C gene, which cover regions that contain the most genetic variations. The 5' region, center region and the 3' region result in PCR production of 451 bp, 370 bp and 357 bp in length, respectively.

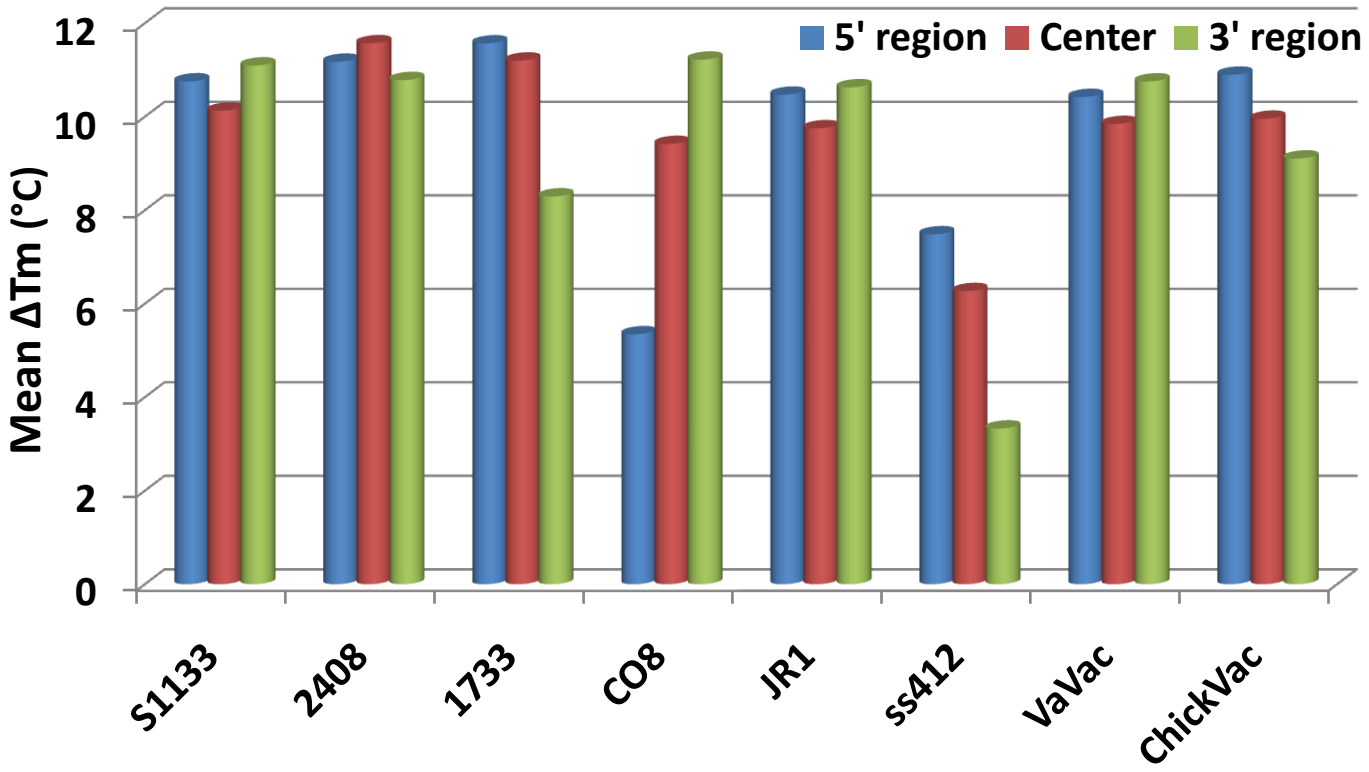

Figure 5.2. Combination profiles of mean ΔT_m (mean sample melting peak temperature – mean negative control melting peak temperature) at all 3 regions of different ARV strains.

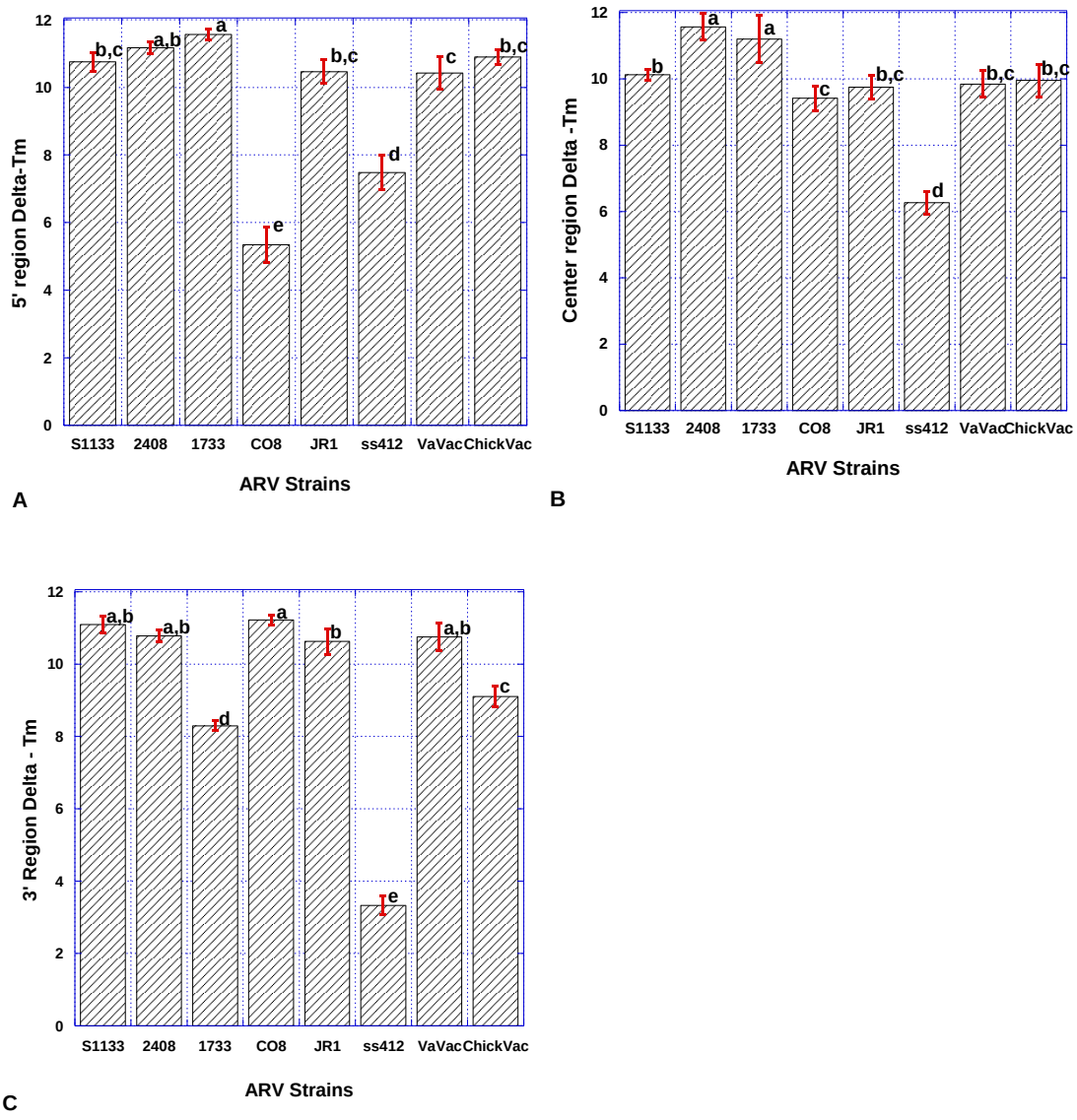

Figure 5.3 Multiple comparisons of mean ΔT_m of different ARV strains at each of the 3 regions using Tukey-Kramer HSD. A). Mean ΔT_m of different strains at 5' region; B). Mean ΔT_m of different strains at Center region; C). Mean ΔT_m of different strains at 3' region.

Note: columns with different alphabetical superscripts indicate significant differences ($p<0.05$) in T_ms between each other.

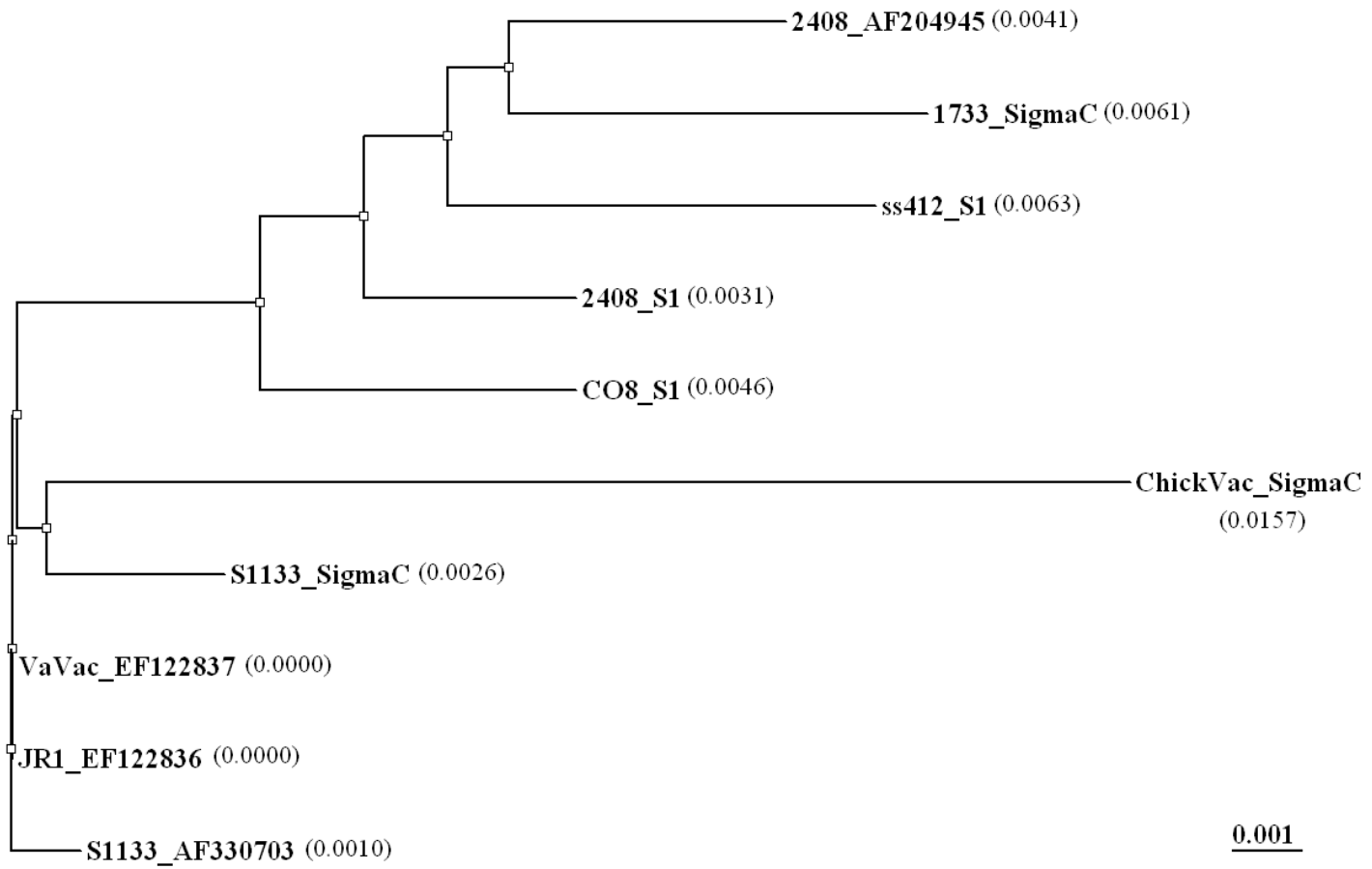

Figure 5.4. The phylogenetic tree of the σC genes of North American ARV strains used in the current study. The numbers in the parentheses indicate the relative distance of the branch to its nearest node.

DISSERTATION CONCLUSIONS

Avian reoviruses (ARVs) belong to the *Orthoreovirus* genus of the *Reoviridae* family. Their genome consists of 10 segmented double-stranded RNAs, which can be divided into three groups based on their sizes: Large (L1, L2, and L3), Medium (M1, M2, and M3), and Small (S1, S2, S3, and S4).

ARVs can cause tenosynovitis, proventriculitis, malabsorption syndrome, chronic respiratory disease, and immunosuppression in chickens. All can cause severe economic losses. Early detection and proper vaccination are the most effective control and prevention means. Virus isolation (VI) is time-consuming, and can take up to 7 days. Serological testing such as enzyme-linked immunosorbent assay (ELISA), although fast, has cross reactions and lacks sensitivity for ARV detection. Therefore, it is necessary to develop a simple, rapid, and highly sensitive and specific method to detect ARVs.

We developed a TaqMan probe based real-time PCR for qualitative and quantitative detection of ARVs. The primer-probe set was designed from the conserved region of ARV S4 genome segment. ARV strains S1133, 2408, CO8, 1733, JR1, ss412, and two vaccine strains: ChickVac™ and V.A. Vac® were tested. Specificity testing indicated that this real-time RT-PCR had high specificity. It could detect these 8 ARVs with no cross-reaction with other avian viruses. TaqMan real-time PCR successfully detected CO8 and ss412, which belonged to a different serological subgroup from the other 6 strains. The full-length ARV S4 gene was cloned and *in vitro* transcription

was performed to produce a pure ARV S4 RNA standard. This was used for sensitivity testing. TaqMan real-time RT-PCR was highly reproducible. Multiple repeated experiments resulted in nearly identical standard curves, and statistical analysis indicated only small variations in the intercept (40.86 ± 0.88) and slope (-3.237 ± 0.17) of the regression equation. Intra-experimental comparisons resulted in small variations. Comparing conventional RT-PCR using the same primer set, real-time RT-PCR was about 150 times more sensitive for detecting cloned ARV S4 RNA.

Traditionally, virus titration was performed using the standard VI method involving inoculation and incubation of virus in chicken embryos or cell culture. It took up to a week to perform. In the current study, EID_{50} and $TCID_{50}$ titers of ARV strain 2408 were determined (in replicates) using the VI method. The number of ARV genome copies was then simultaneously determined with real-time RT-PCR. Results indicated that 3-4 ARV particles were needed to achieve 1 EID_{50}, and similarly 3 ARV particles were needed to achieve 1 $TCID_{50}$. Results indicated that this strain was well adapted to propagate in both chicken embryos and cell culture. Conversion factors provided a simple, rapid mathematical estimation of viral titer for a particular ARV strain.

We used the real-time RT-PCR assay we developed to continuously monitor ARV shedding in feces of commercial and specific-pathogen-free chickens infected with the 2408 virus. ARV was detected in the cloacal swabs as early as 1 DPI and throughout the tested period. Commercial chickens, which had high maternal antibody against AIV, showed no mortality, minimal clinical signs, and low ARV excretion. In contrast, SPF chickens had 30% mortality within the first week and severe clinical signs and gross lesions during the experiment. SPF chickens demonstrated high virus shedding, which

peaked at 7 DPI. Therefore, maternal antibodies in commercial chickens were protective against the effects of ARV infection.

The process of cloacal swabbing, RNA extraction, and real-time RT-PCR took about 3-4 hours depending on the number of samples processed. This is significantly less time than traditional VI tests. Results indicated that real-time RT-PCR was highly sensitive and was suitable for rapid detection of ARVs. In addition, measuring ARV shedding quantitatively may provide important information on the life cycle of ARV in live host under normal conditions.

A SYBR-Green I based real-time RT-PCR was developed to differentiate closely related ARV strains. Three primers sets were designed to amplify three partially overlapping regions of σC encoding gene, which covered a majority of mutation sites. Subsequently, melting curve analyses were performed to determine the unique melting peak temperature (T_m) of each of these regions. Results indicated that each of the ARV strains had a specific profile of ΔT_m combination of the three regions. The T_m profiles of ARV strains CO8 and ss412 were more divergent than the other strains indicating that they may belong to different subgroups. Therefore, this assay can be used to differentiate specific ARV strains, so that appropriate vaccines can be applied to protect chickens from ARV infection.

The TaqMan probe real-time RT-PCR presented here provided a useful tool, which can be used to rapidly and accurately detect ARVs. The SYBR-Green I real-time PCR can identify specific ARV strains, which can indicate when variant ARV strains are present and thus provide critical information for selecting a proper vaccination plan.

BIBLIOGRAPHY

Adair, B. M., Burns, K., and McKillop, E. R., 1987. Serological studies with reoviruses in chickens, turkeys and ducks. J. Comp. Pathol. 97, 495-501.

Al-Afaleq, A. I. and Jones, R. C., 1990. Localisation of avian reovirus in the hock joints of chicks after entry through broken skin. Res. Vet. Sci. 48, 381-382.

Al-Muffarej, S. I., Savage, C. E., and Jones, R. C., 1996. Egg transmission of avian reoviruses in chickens: Comparison of a trypsin-sensitive and a trypsin-resistant strain. Avian Pathol. 25, 469-480.

Bagust, T. J. and Westbury, H. A., 1975. Isolation of avian reoviruses associated with diseases of chickens in victoria. Aust. Vet. J. 51, 406-407.

Bains, B. S. and MacKenzie, M., 1974. Reovirus-associated mortality in broiler chickens. Avian Dis. 18, 472-476.

Banyai, K., Palya, V., Benko, M. A., Bene, J., Havasi, V., Melegh, B. A., and Szucs, G., 2005. The goose reovirus genome segment encoding the minor outer capsid protein, □ 1/□ Çis bicistronic and shares structural similarities with its counterpart in Muscovy duck reovirus. Virus Genes. 31, 285-291.

Barton, E. S., Forrest, J. C., Connolly, J. L., Chappell, J. D., Liu, Y., Schnell, F. J., Nusrat, A., Parkos, C. A., and Dermody, T. S., 2001. Junction adhesion molecule is a

receptor for reovirus. Cell. 104, 441-451.

Benavente, J. and Martinez-Costas, J., 2007. Avian reovirus: Structure and biology. Virus Res. 123, 105-119.

Bodelon, G., Labrada, L., Martinez-Costas, J., and Benavente, J., 2001. The avian reovirus genome segment S1 is a functionally tricistronic gene that expresses one structural and two nonstructural proteins in infected cells. Virology. 290, 181-191.

Bodelon, G., Labrada, L., Martinez-Costas, J., and Benavente, J., 2002. Modification of late membrane permeability in avian reovirus-infected cells. Viroporin activity of the S1-encoded nonstructural P10 protein. J. Biol. Chem. 277, 17789-17796.

Bruhn, S., Bruckner, L., and Ottiger, H. P., 2005. Application of RT-PCR for the detection of avian reovirus contamination in avian viral vaccines. J. Virol. Meth. 123, 179-186.

Bustin, S. A., Gyselman, V. G., Williams, N. S., and Dorudi, S., 1999. Detection of cytokeratins 19/20 and guanylyl cyclase C in peripheral blood of colorectal cancer patients. Br. J. Cancer. 79, 1813-1820.

Carrasco, L., 1994. Entry of animal viruses and macromolecules into cells. FEBS Letters. 350, 151-154.

Caterina, K. M., Frasca, S., Girshick, T., and Khan, M. I., 2004. Development of a multiplex PCR for detection of avian adenovirus, avian reovirus, infectious bursal disease virus, and chicken anemia virus. Mol. Cell. Probe. 18, 293-298.

Cessi, D. and Lombardini, F., 1975. Orientamenti sulla profilassi dell artrite virale aviare. Vaccinazione dei reproduttori, gran parentali e parentali. Clin. Vet. 98, 414-417.

Clemens, M. J., 1997. PKR--A protein kinase regulated by double-stranded RNA. Int. J. Biochem. Cell Biol. 29, 945-949.

Costas, C., Martinez-Costas, J., Bodelon, G., and Benavente, J., 2005. The second open reading frame of the avian reovirus S1 gene encodes a transcription-dependent and CRM1-independent nucleocytoplasmic shuttling protein. J. Virol. 79, 2141-2150.

Day, J., Pantin-Jackwood, M., and Spackman, E., 2007. Sequence and phylogenetic analysis of the S1 genome segment of turkey-origin reoviruses. Virus Genes. 32, 235-242.

Deshmukh, D. R., Sayed, H. I., and Pomeroy, B. S., 1969. Avian reoviruses. IV relationship to human reoviruses. Avian Dis. 13, 16-22.

Duncan, R., 1999. Extensive sequence divergence and phylogenetic relationships between the fusogenic and nonfusogenic orthoreoviruses: A species proposal. Virology. 260, 316-328.

Duncan, R., 1996. The low pH-dependent entry of avian reovirus is accompanied by two specific cleavages of the major outer capsid protein μ2C. Virology. 219, 179-189.

Duncan, R., Chen, Z., Walsh, S., and Wu, S., 1996. Avian reovirus-induced syncytium formation is independent of infectious progeny virus production and enhances the rate, but is not essential, for virus-induced cytopathology and virus egress. Virology. 224, 453-464.

Duncan, R. and Sullivan, K., 1998. Characterization of two avian reoviruses that exhibit strain-specific quantitative differences in their syncytium-inducing and pathogenic capabilities. Virology. 250, 263-272.

Duncan, R., Murphy, F. A., and Mirkovic, R. R., 1995. Characterization of a novel syncytium-inducing baboon reovirus. Virology. 212, 752-756.

Dutta, S. K. and Pomeroy, B. S., 1969. Isolation and characterisation of an enterovirus from baby chicks having an enteric infection. II. physical and chemical characterisation and ultrastructure. Avian Dis. 11, 9-15.

Eidson, C. S., Page, R. K., Fletcher, O. J., and Kleven, S. H., 1979. Vaccination of broiler breeders with a tenosynovitis virus vaccine. Poultry Sci. 58, 1490-1497.

Endo-Munoz, L. B., 1990. A western blot to detect antibody to avian reovirus. Avian Pathol. 19, 477-487.

Espy, M. J., Cockerill III, F. R., Meyer, R. F., Bowen, M. D., Poland, G. A., Hadfield, T. L., and Smith, T. F., 2002. Detection of smallpox virus DNA by LightCycler PCR. J. Clin. Microbiol. 40, 1985-1988.

Fahey, J. E. and Crawley, J. F., 1954. Studies on chronic respiratory disease of chickens II. Isolation of a virus. Can. J. Comp. Med. Vet. S. 18, 13-21.

Fields, B. N., Raine, C. S., and Baum, S. G., 1971. Temperature-sensitive mutants of reovirus type 3: Defects in viral maturation as studied by immunofluorescence and electron microscopy. Virology. 43, 569-578.

Freeman, W. M. and Vrana, S. L., 1996. Use of elevated reverse transcription reaction temperatures in RT-PCR. BioTechniques. 20, 782-783.

Gerard, G., Fox, D., Nathan, M., and D'Alessio, J., 1997. Reverse transcriptase. Mol. Biotechnol. 8, 61-77.

Giambrone, J. J., 1985. Vaccinating pullets to control reovirus associated diseases. Poult. Digest. 44, 96-100.

Giambrone, J. J., Dormitorio, T., and Lockaby, S. B., 1992. Coarse-spray immunization of one-day-old broilers against enteric reovirus infections. Avian Dis. 36, 364-368.

Giambrone, J. J. and Hathcock, T. L., 1991. Efficacy of coarse-spray administration of a reovirus vaccine in young chickens. Avian Dis. 35, 204-209.

Glass, S. E., Naqui, S. A., Hall, C. F., and Kerr, K. M., 1973. Isolation and characterization of virus associated with arthritis of chickens. Avian Dis. 17, 415-424.

Gonzalez-Lopez, C., Martinez-Costas, J., Esteban, M., and Benavente, J., 2003. Evidence that avian reovirus □ A protein is an inhibitor of the double-stranded RNA-dependent protein kinase. J. Gen. Virol. 84, 1629-1639.

Goodwin, M. A., Davis, J. F., McNulty, M. S., Brown, J., and Player, E. C., 1993. Enteritis (so-called runting stunting syndrome) in Georgia broiler chicks. Avian Dis. 37, 451-458.

Gouvea, V. S. and Schnitzer, T. J., 1982. Polymorphism of the migration of double-stranded RNA genome segments of avian reoviruses. J. Virol. 43, 465-471.

Grande, A., Costas, C., and Benavente, J., 2002. Subunit composition and conformational stability of the oligomeric form of the avian reovirus cell-attachment protein σC. J. Gen. Virol. 83, 131-139.

Grande, A., Rodriguez, E., Costas, C., Everitt, E., and Benavente, J., 2000. Oligomerization and cell-binding properties of the avian reovirus cell-attachment protein σC. Virology. 274, 367-377.

Guardado Calvo, P., Fox, G. C., Hermo Parrado, X. L., Llamas-Saiz, A. L., Costas, C., Martinez-Costas, J., Benavente, J., and van Raaij, M. J., 2005. Structure of the carboxy-terminal receptor-binding domain of avian reovirus fibre σC. J. Mol. Biol. 354, 137-149.

Guneratne, J. R. M., Jones, R. C., and Georgiou, K., 1982. Some observations on the isolation and cultivation of avian reoviruses. Avian Pathol. 11, 453-462.

Guo, Z. Y., Giambrone, J. J., Dormitorio, T. V., and Wu, H., 2003a. Influence of a reovirus-antibody complex vaccine on efficacy of Marek's Disease Vaccine administered *in ovo.* Avian Dis. 47, 1362-1367.

Guo, Z. Y., Giambrone, J. J., Wu, H., and Dormitorio, T., 2003b. Safety and efficacy of an experimental reovirus vaccine for *in ovo* administration. Avian Dis. 47, 1423-1428.

Gut, M., Leutenegger, M., Huder, B., Pedersen, C., and Lutz, H., 1999. One-tube fluorogenic reverse transcription-polymerase chain reaction for the quantitation of feline coronaviruses. J. Virol. Meth. 77, 37-46.

Heggen-Peay, C. L., Cheema, M. A., Ali, R. A., Schat, K. A., and Qureshi, M. A., 2002. Interactions of poult enteritis and mortality syndrome-associated reovirus with various cell types in vitro. Poultry Sci. 81, 1661-1667.

Heid, C. A., Stevens, J., Livak, K. J., and Williams, P. M., 1996. Real time quantitative PCR. Genome Res. 6, 986-994.

Hieronymus, D. R. K., Villegas, P., and Kleven, S. H., 1983. Identification and serological differentiation of several reovirus strains isolated from chickens with suspected malabsorption syndrome. Avian Dis. 27, 246-254.

Hill, J. E., Rowland, G. N., Steffens, W. L., and Ard, M. B., 1989. Ultrastructure of the gastrocnemius tendon and sheath from broiler infected with reovirus. Avian Dis. 33, 79-85.

Hsiao, J., Martinez-Costas, J., Benavente, J., and Vakharia, V. N., 2002. Cloning, expression, and characterization of avian reovirus guanylyltransferase. Virology. 296, 288-299.

Hsu, H. W., Su, H. Y., Huang, P., Lee, L. H., and Liu, H. J., 2005. Sequence and phylogenetic analysis of P10- and P17-encoding genes of avian reovirus. Avian Dis. 49, 36-42.

Huang, D. D., 1995. Restriction of avian reovirus in primary chicken embryo tendon cells. Virology. 207, 117-126.

Huang, L. K., Liao, S. C., Chang, C. C., and Liu, H. J., 2006. Expression of avian reovirus σC protein in transgenic plants. J. Virol. Meth. 134, 217-222.

Ide, P. R., 1982. Avian reovirus antibody assay by indirect immunofluorescence using plastic microculture plates. Can. J. Comp. Med. 46, 39-42.

Johnson, D. C. and van der Heide, L., 1971. Incidence of tenosynovitis in Maine broilers. Avian Dis. 15, 829-834.

Joklik, W. K. 1983. The reovirus particle. pp9-78 in The *Reoviridae*. Plenum Press.

Jones, R. C., 2000. Avian reovirus infections. Rev. Sci. Tech. 19, 614-625.

Jones, R. C., Islam, M. R., and Kelly, D. F., 1989. Early pathogenesis of experimental reovirus infection in chickens. Avian Pathol. 18, 239-253.

Jones, R. C., Jordan, F. T. W., and Lioupis, S., 1975. Characterization of reovirus isolated from ruptured gastrocnemius tendons of chickens. Vet. Rec. 96, 153-154.

Jones, R. C. and Kibenge, F. S. B., 1984. Reovirus-induced tenosynovitis in chickens: The effect of breed. Avian Dis. 13, 511-528.

Jones, R. C., 1976. Reoviruses from chickens with hydropericardium. Vet. Rec. 99, 458-45a.

Jones, R. C. and Georgiou, K., 1984. Reovirus-induced tenosynovitis in chickens the influence of age at infection. Avian Pathol. 13, 441-457.

Jones, R. C. and Guneratne, J. R. M., 1984. The pathogenicity of some avian reoviruses with particular reference to tenosynovitis. Avian Pathol. 13, 173-189.

Jones, R. C. and Onunkwo, O., 1978. Studies on experimental tenosynovitis in light hybrid chickens. Avian Pathol. 7, 171-181.

Kant, A., Balk, F., Born, L., van Roozelaar, D., Heijmans, J., Gielkens, A., and ter Huurne, A., 2003. Classification of Dutch and German avian reoviruses by sequencing the σC protein. Vet. Res. 34, 203-212.

Kapczynski, D., Sellers, H., Simmons, V., and Schultz-Cherry, S., 2002. Sequence analysis of the S3 gene from a turkey reovirus. Virus Genes. 25, 95-100.

Kawamura, H., Shimizu, F., Maeda, M., and Tsubahara, H., 1965. Avian reovirus: Its properties and serological classification. Natl. Inst. Anim. Hlth. Q. 5, 124-

Kawamura, H. and Tsubahara, H., 1966. Common antigenicity of avian reoviruses. Natl. Inst. Anim. Hlth. Q.(Tokyo). 6, 187-193.

Ke, G. M., Cheng, H. L., Ke, L. Y., Ji, W. T., Chulu, J. L. C., Liao, M. H., Chang, T. J., and Liu, H. J., 2006. Development of a quantitative Light Cycler real-time RT-PCR for detection of avian reovirus. J. Virol. Meth. 133, 6-13.

Kerr, K. M. and Olson, N. D., 1964. Control of infectious synovitis: the effect of age of chickens on the susceptibility to three agents. Avian Dis. 8, 256-263.

Kerr, K. M. and Olson, N. O., 1969. Pathology of chickens experimentally inoculated or contact-infected with an arthritis-producing virus. Avian Dis. 13, 729-745.

Kibenge, F. S. B., Gwaze, G. E., Jones, R. C., Chapman, A. F., and Savage, C., 1985. Experimental reovirus infection in chickens: Observations on early viraemia and virus distribution in bone marrow, liver and enteric tissues. Avian Pathol. 14, 87-98.

Kibenge, F. S. B., Jones, R. C., and Savage, C. E., 1987. Effects of experimental immunosuppression on reovirus-induced tenosynovitis in light-hybrid chickens. Avian Pathol. 16, 73-92.

Kibenge, F. S. B. and Wilcox, G. E., 1983. Tenosynovitis in chickens. Vet. Bull. 53, 431-443.

Kisary, J., Nagy, B., and Bitay, Z., 1984. Presence of parvoviruses in the intestine of chickens showing stunting syndrome. Avian Pathol. 13, 339-343.

Kouwenhoven, B., Davelaar, F. G., and Van Walsum, J., 1978a. Infectious proventriculitis causing runting in broilers. Avian Pathol. 7, 183-187.

Kouwenhoven, B., Vertommen, M. H., and van Eck, J. H. H., 1978b. Runting and leg weakness in broilers: Involvement of infectious factors. Vet. Sci. Commun. 2, 253-259.

Kozak, M., 1991. Structural features in eukaryotic mRNAs that modulate the initiation of translation. J. Biol. Chem. 266, 19867-19870.

Kutyavin, I. V., Afonina, I. A., Mills, A., Gorn, V. V., Lukhtanov, E. A., Belousov, E. S., Singer, M. J., Walburger, D. K., Lokhov, S. G., Gall, A. A., Dempcy, R., Reed, M. W., Meyer, R. B., and Hedgpeth, J., 2000. 3'-Minor groove binder-DNA probes increase sequence specificity at PCR extension temperatures. Nucl. Acids Res. 28, 655-661.

Lee, L. H., Shien, J. H., and Shieh, H. K., 1998. Detection of avian reovirus RNA and comparison of a portion of genome segment S3 by polymerase chain reaction and restriction enzyme fragment length polymorphism. Res. Vet. Sci. 65, 11-15.

Li, Q., Luan, G., Guo, Q., and Liang, J., 2002. A new class of homogeneous nucleic acid probes based on specific displacement hybridization. Nucl. Acids Res. 30, e5-

Lin, H. Y., Chuang, S. T., Chen, Y. T., Shih, W. L., Chang, C. D., and Liu, H. J., 2007. Avian reovirus-induced apoptosis related to tissue injury. Avian Pathol. 36, 155-159.

Lin, P.-Y., Liu, H.-J., Lai, M.-J., Yu, F.-L., Hsu, H.-Y., Lee, J.-W., and Wen-Ling, S., 2006. Avian reovirus activates a novel proapoptotic signal by linking Src to p53. Apoptosis. 11, 2179-2193.

Liu, H. J., Lee, L. H., Hsu, H. W., Kuo, L. C., and Liao, M. H., 2003. Molecular evolution of avian reovirus: evidence for genetic diversity and reassortment of the S-class genome segments and multiple cocirculating lineages. Virology. 314, 336-349.

Liu, H. J., Liao, M. H., Chang, C. D., Chen, J. H., Lin, M. Y., and Tung, M. C., 1999. Comparison of two molecular techniques for the detection of avian reoviruses in formalin-fixed, paraffin-embedded chicken tissues. J. Virol. Meth. 80, 197-201.

Liu, H. J., Giambrone, J. J., and Nielsen, B. L., 1997. Molecular characterization of avian reoviruses using nested PCR and nucleotide sequence analysis. J. Virol. Meth. 65, 159-167.

Liu, H. J. and Huang, P. H., 2001. Sequence and phylogenetic analysis of the □ A-encoding gene of avian reovirus. J. Virol. Meth. 98, 99-107.

Liu, H. J., Lin, P. Y., Lee, J. W., Hsu, H. Y., and Shih, W. L., 2005. Retardation of cell growth by avian reovirus p17 through the activation of p53 pathway. Biochem. Biophys. Res. Commun. 336, 709-715.

Liu, H.-J. and Giambrone, J. J., 1997. *In situ* detection of reovirus in formalin-fixed, paraffin-embedded chicken tissues using a digoxigenin-labeled cDNA probe. Avian Dis. 41, 447-451.

Luftig, R. B., Kilham, S. S., Hay, A. J., Zweerink, H. J., and Joklik, W. K., 1972. An ultrastructural study of virions and cores of reovirus type 3. Virology. 48, 170-181.

Lyamichev, V., Brow, M. A., and Dahlberg, J. E., 1993. Structure-specific endonucleolytic cleavage of nucleic acids by eubacterial DNA polymerases. Science. 260, 778-783.

Mandelli, G., Rampin, T., and Finazzi, M., 1978. Experimental reovirus hepatitis in newborn chicks. Vet. Path. 15, 531-543.

Marquardt, J., Hermans, W., Schulz, L. C., Leibold, W. 1983. A persistent reovirus infection of chickens as a possible model of human rheumatoid arthritis (RA). Zentralbl. Veterinarmed., 30, 274-282.

Martinez-Costas, J., Grande, A., Varela, R., Garcia-Martinez, C., and Benavente, J., 1997. Protein architecture of avian reovirus S1133 and identification of the cell attachment protein. J. Virol. 71, 59-64.

Martinez-Costas, J., Gonzalez-Lopez, C., Vakharia, V. N., and Benavente, J., 2000. Possible involvement of the double-stranded RNA-binding core protein □ A in the resistance of avian reovirus to interferon. J. Virol. 74, 1124-1131.

Martinez-Costas, J., Varela, R., and Benavente, J., 1995. Endogenous enzymatic activities of the avian reovirus S1133: Identification of the viral capping enzyme. Virology. 206, 1017-1026.

McCrae, M. A. and Joklik, W. K., 1978. The nature of the polypeptide encoded by each of the 10 double-stranded RNA segments of reovirus type 3. Virology. 89, 578-593.

McFerran, J. B., McCracken, R. M., Connor, T. J., and Evans, R. T., 1976a. Isolation of Viruses from Clinical Outbreaks of Inclusion Body Hepatitis. Avian Pathol. 5, 315-324.

McFerran, J. B., McCracken, R. M., Connor, T. J., and Evans, R. T., 1976b. Isolation of viruses from clinical outbreaks of inclusion body hepatitis. Avian Pathol. 5, 315-324.

McNulty, M. S. 1993. Reovirus. 181-193 in Virus infections in birds. McFerran, J. B. and McNulty, M. S. Elsevier Science Publishers, BV, Amsterdam.

McNulty, M. S., Allan, G. M., Connor, T. J., McFerran, J. B., and McCracken, R. M., 1984. An entero-like virus associated with the runting syndrome in broiler chickens. Avian Pathology. 13, 429-439.

Menendez, N. A., Calnek, B. W., and Cowen, B. S., 1975a. Localization of avian reovirus (FDO isolant) in tissues of mature chickens. Avian Dis. 19, 112-117.

Menendez, N. A., Calnek, B. W., and Cowen, B. S., 1975b. Experimental egg-transmission of avian reovirus. Avian Dis. 19, 104-111.

Mertens, P., 2004. The dsRNA viruses. Virus Res. 101, 3-13.

Meulemans, G. and Halen, P., 1982. Efficacy of some disinfectants against infectious bursal diseases virus and avian reovirus. Vet. Rec. 111, 412-413.

Montgomery, R. D., Villegas, P., and Kleven, S. H., 1986. Role of route of exposure, age, sex, and type of chicken on the pathogenicity of avian reovirus strain 81-176. Avian Dis. 30, 460-467.

Mukiibi-Muka, G. and Jones, R. C., 1999. Local and systemic IgA and IgG response of chicks to avian reoviruses: Effects of age of chick, route of infection and virus strain. Avian Pathol. 28, 54-60.

Nazarenko, I., Lowe, B., Darfler, M., Ikonomi, P., Schuster, D., and Rashtchian, A., 2002. Multiplex quantitative PCR using self-quenched primers labeled with a single fluorophore. Nucl. Acids Res. 30, e37-

Ni, Y. and Kemp, M. C., 1995. A comparative study of avian reovirus pathogenicity: virus spread and replication and induction of lesions. Avian Dis. 39, 554-566.

Nibert, M. L. and Fields, B. N., 1992. A carboxy-terminal fragment of protein mu 1/mu 1C is present in infectious subvirion particles of mammalian reoviruses and is proposed to have a role in penetration. J. Virol. 66, 6408-6418.

Nibert, M. L. and Schiff, L. A. 2001. Reoviruses and their replication. Pp.1679-1728 in Fields virology. Knipe, D. M. and Hooley, P. M. Lippincott Williams & Wilkins, Philadelphia, PA.

Nibert, M. L., 1998. Structure of mammalian orthoreovirus particles, reoviruses I. structure, proteins and genetics. Curr. Top. Microbiol. 233, 2-30.

Nwajei, B. N. C., Afaleq, A. A., and Jones, R. C., 1988. Comparison of chick embryo liver and vero cell cultures for the isolation and growth of avian reoviruses. Avian Pathol. 17, 759-766.

Nygren, J., Svanvik, N., and Kubista, M., 1998. The interactions between the fluorescent dye thiazole orange and DNA. Biopolymers. 46, 39-51.

Olson, N. D. 1978. Reovirus infections. 641-647 in Diseases of poultry. Hofstad, M. S. Iowa State University Press, Ames, Iowa.

Olson, N. O. and Kerr, K. M., 1966. Some characteristics of an avian arthritis viral agent. Avian Dis. 10, 470-476.

Olson, N. O., Shelton, D. C., and Munro, D. A., 1957. Infectious synovitis control by medication: Effect of strain differences and pleuro-pneumonia-like organisms. Am. J. Vet. Res. 18, 735-739.

Olson, N. O. and Weiss, R., 1972. Similarity between arthritis virus and Fahey-Crawley virus. Avian Dis. 16, 535-540.

Page, R. K., Fletcher, O. J., Rowland, G. N., Gaudry, D., and Villegas, P., 1982a. Malabsorption syndrome in broiler chickens. Avian Dis. 26, 618-624.

Page, R. K., Fletcher, O. J., and Villegas, P., 1982b. Infectious tenosynovitis in young turkeys. Avian Dis. 26, 924-927.

Pass, D. A., Robertson, D. M., and Villegas, P., 1982. Runting syndrome in broiler chickens in Australia. Vet. Rec. 110, 386-387.

Pertile, T. L., Walser, M. M., Sharma, J. M., and Shivers, J. L., 1996. Immunohistochemical detection of lymphocyte subpopulations in the tarsal joints of chickens with experimental viral arthritis. Vet. Path. 33, 303-310.

Petek, M., Felluga, B., Borghi, G., and Baroni, A., 1967. The Crawley agent: An avian reovirus. Arch. Ges. Virusforsch. 21, 413-424.

Pradhan, H. K., Mohanty, G. C., Kataria, J. M., Pattnaik, B., and Verma, K. C., 1987. Antinuclear antibody in chickens with reoviral arthritis. Avian Dis. 31, 249-253.

Rabinow, P. 1996. Introduction. pp.1-18 in Making PCR: A story of biotechnology. The University of Chicago Press.

Rau, W. E., van der Heide, L., Kalbac, M., and Girshick, T., 1980. Oneset of progeny immunity against viral arthritis/tenosynovitis after experimental vaccination of parent breeder chickens and cross-immunity against six reovirus isolates. Avian Dis. 24, 648-657.

Rebouillat, D. and Hovanessian, A. G., 1999. The human 2', 5'-oligoadenylate synthetase family: Interferon-induced proteins with unique enzymatic properties. J. Interferon. Cytokine. Res. 19, 295-308.

Rekik, M. R., Silim, A., and Bernier, G., 1991. Serological and pathogenic characterization of avian reoviruses isolated in Quebec. Avian Pathol. 20, 607-617.

Ririe, K. M., Rasmussen, R. P., and Wittwer, C. T., 1997. Product differentiation by analysis of DNA melting curves during the polymerase chain reaction. Anal. Biochem. 245, 154-160.

Robertson, M. D. and Wilcox, G. E., 1986. Avian reovirus. Vet. Bull. 56, 726-733.

Robertson, M. D., Wilcox, G. E., and Kibenge, F. S. B., 1984. Prevalence of reoviruses in commercial chickens. Aust. Vet. J. 61, 319-322.

Roessler, D. E. and Rosenberger, J. K., 1989. *In vitro* and *in vivo* characterization of avian reoviruses. III. Host factors affecting virulence and persistence. Avian Dis. 33, 555-565.

Roner, M. R., Sutphin, L. A., and Joklik, W. K., 1990. Reovirus RNA is infectious. Virology. 179, 845-852.

Rosenberger, J. K., Sterner, F. J., Botts, S., Lee, K. P., and Margolin, A., 1989. *In vitro* and *in vivo* characterization of avian reoviruses. I. Pathogenicity and antigenic relatedness of several avian reovirus isolates. Avian Dis. 33, 535-544.

Rutledge, R. G. and Cote, C., 2003. Mathematics of quantitative kinetic PCR and the application of standard curves. Nucl. Acids Res. 31, e93-

Sahu, S. P. and Olson, N., 1975. Comparison of the characteristics of avian reoviruses isolated from the digestive and respiratory tract, with viruses isolated from the synoviae. Am. J. Vet. Res. 36, 847-850.

Salsman, J., Top, D., Boutilier, J., and Duncan, R., 2005. Extensive syncytium formation mediated by the reovirus FAST proteins triggers apoptosis-induced membrane instability. J. Virol. 79, 8090-8100.

Schnitzer, T. J., Ramos, T., and Gouvea, V., 1982. Avian reovirus polypeptides: Analysis of intracellular virus-specified products, virions, top component, and cores. J. Virol. 43, 1006-1014.

Schwartz, L. D., Gentry, R. F., and Rothenbacher, H., 1976. Infectious tenosynovitis in commercial white Leghorn chickens. Avian Dis. 20, 769-773.

Sellers, H. S., Linnemann, E. G., Pereira, L., and Kapczynski, D. R., 2004. Phylogenetic analysis of the σ2 protein gene of turkey reoviruses. Avian Dis. 48, 651-657.

Shapouri, M. R. S., Kane, M., Letarte, M., Bergeron, J., Arella, M., and Silim, A., 1995. Cloning, sequencing and expression of the S1 gene of avian reovirus. J. Gen. Virol. 76, 1515-1520.

Shih, W. L., Hsu, H. W., Liao, M. H., Lee, L. H., and Liu, H. J., 2004. Avian reovirus C protein induces apoptosis in cultured cells. Virology. 321, 65-74.

Shmulevitz, M., Corcoran, J., Salsman, J., and Duncan, R., 2004. Cell-cell fusion induced by the avian reovirus membrane fusion protein is regulated by protein degradation. J. Virol. 78, 5996-6004.

Shmulevitz, M. and Duncan, R., 2000. A new class of fusion-associated small transmembrane (FAST) proteins encoded by the non-enveloped fusogenic reoviruses. EMBO J. 19, 902-912.

Shmulevitz, M., Yameen, Z., Dawe, S., Shou, J., O'Hara, D., Holmes, I., and Duncan, R., 2002. Sequential partially overlapping gene arrangement in the tricistronic S1 genome segments of avian reovirus and Nelson Bay reovirus: implications for translation initiation. J. Virol. 76, 609-618.

Silverstein, S. C. and Schur, P. H., 1970. Immunofluorescent localization of double-stranded RNA in reovirus-infected cells. Virology. 41, 564-566.

Songserm, T., van Roozelaar, D., Kant, A., Pol, J., Pijpers, A., and ter Huurne, A., 2003. Enteropathogenicity of Dutch and German avian reoviruses in SPF white leghorn chickens and broilers. Vet. Res. 34, 285-295.

Songserm, T., Zekarias, B., van Roozelaar, D. J., Kok, R. S., Pol, J. M. A., Pijpers, A., and ter Huurne, A. A. H. M., 2002. Experimental reproduction of malabsorption syndrome with different combinations of reovirus, *Escherichia coli*, and treated homogenates obtained from broilers. Avian Dis. 46, 87-94.

Spandidos, D. A. and Graham, A. F., 1976. Physical and chemical characterization of an avian reovirus. J. Virol. 19, 968-976.

Sterner, F. J., Rosenberger, J. K., Margolin, A., and Ruff, M. D., 1989. *In vitro* and *in vivo* characterization of avian reoviruses. II. Clinical evaluation of chickens infected with two avian reovirus pathotypes. Avian Dis. 33, 545-554.

Su, Y. P., Su, B. S., Shien, J. H., Liu, H. J., and Lee, L. H., 2006. The sequence and phylogenetic analysis of avian reovirus genome segments M1, M2, and M3 encoding the minor core protein μA, the major outer capsid protein μB, and the nonstructural protein μNS. J. Virol. Meth. 133, 146-157.

Svanvik, N., Westman, G., Wang, D., and Kubista, M., 2000. Light-Up probes: Thiazole orange-conjugated peptide nucleic acid for detection of target nucleic acid in homogeneous solution. Anal. Chem. 281, 26-35.

Takase, K., Nonaka, F., Yamamoto, M., and Yamada, S., 1987. Serological and pathogenetic studies on avian reoviruses isolated in Japan. Avian Dis. 31, 464-469.

Tang, K. N., Fletcher, O. J., and Villegas, P., 1987. The effect on newborn chicks of oral inoculation of reovirus isolated from chickens with tenosynovitis. Avian Dis. 31, 584-590.

Timinskas, A., Butkus, V., and Janulaitis, A., 1995. Sequence motifs characteristic for DNA [cytosine-N4] and DNA [adenine-N6] methyltransferases. Classification of all DNA methyltransferases. Gene. 157, 3-11.

Toro, H., Tang, D. C., Suarez, D. L., Sylte, M. J., Pfeiffer, J., and Van Kampen, K. R., 2007. Protective avian influenza in ovo vaccination with non-replicating human adenovirus vector. Vaccine. 25, 2886-2891.

Touris-Otero, F., Cortez-San Martin, M., Martinez-Costas, J., and Benavente, J., 2004a. Avian reovirus morphogenesis occurs within viral factories and begins with the selective recruitment of σNS and λA to μNS inclusions. J. Mol. Biol. 341, 361-374.

Touris-Otero, F., Martinez-Costas, J., Vakharia, V. N., and Benavente, J., 2004b. Avian reovirus nonstructural protein μNS forms viroplasm-like inclusions and recruits protein μNS to these structures. Virology. 319, 94-106.

Touris-Otero, F., Martinez-Costas, J., Vakharia, V. N., and Benavente, J., 2005. Characterization of the nucleic acid-binding activity of the avian reovirus non-structural protein μNS. J. Gen. Virol. 86, 1159-1169.

Uehara, H., Nardone, G., Nazarenko, I., and Hohman, R. J., 1999. Detection of telomerase activity utilizing energy transfer primers: Comparison with gel- and ELISA-based detection. BioTechniques. 26, 552-558.

van der Heide, L., 1977. Viral arthritis/tenosynovitis: A review. Avian Pathol. 6, 271-284.

van der Heide, L., 2000. The history of avian reovirus. Avian Dis. 44, 638-641.

van der Heide, L. and Kalbac, M., 1975. Infectious tenosynovitis (viral arthritis) : Characterization of a connecticut viral isolant as a reovirus and evidence of viral egg transmission by reovirus-infected broiler breeders. Avian Dis. 19, 683-706.

van der Heide, L., Kalbac, M., and Brustolon, M., 1983. Development of an attenuated apathogenic reovirus vaccine against viral arthritis/tenosynovitis. Avian Dis. 27, 698-706.

van der Heide, L., Kalbac, M., and Hall, W. C., 1976. Infectious tenosynovitis (viral arthritis) influence of maternal antibodies on the development of tenosynovitis lesions after experimental infection by day-old chickens with tenosynovitis virus. Avian Dis. 20, 641-648.

van der Heide, L., Lutticken, D., and Horzinek, M., 1981. Isolation of avian reovirus as a possible etiologic agent of osteoporosis ("brittle bone diseas"; "femoral head necrosis") in broiler chickens. Avian Dis. 25, 847-856.

van der Heide, L. and Page, R. K., 1980. Field experiments with viral arthritis/tenosynovitis vaccination of breeder chickens. Avian Dis. 24, 493-497.

Varela, R. and Benavente, J., 1994. Protein coding assignment of avian reovirus strain S1133. J. Virol. 68, 6775-6777.

Varela, R., Martinez-Costas, J., Mallo, M., and Benavente, J., 1996. Intracellular posttranslational modifications of S1133 avian reovirus proteins. J. Virol. 70, 2974-2981.

Vertommen, M., van Eck, J. H. H., Kouwenhoven, B., and van Kol, N., 1980. Infectious stunting and leg weakness in broilers: I. pathology and biochemical changes in blood plasma. Avian Pathol. 9, 133-142.

Walker, E. R., Friedman, M. H., and Olson, N. O., 1972. Electron microscopic study of an avian reovirus that causes arthritis. J. Ultra. Struct. R. 41, 67-79.

Whitcombe, D., Theaker, J., Guy, S. P., Brown, T., and Little, S., 1999. Detection of PCR products using self-probing amplicons and fluorescence. Nat Biotech. 17, 804-807.

Wittwer, C. T., Ririe, K. M., Andrew, R. V., David, D. A., Gundry, R. A., and Balis, U. J., 1997. The LightCycler™: A microvolume multisample fluorimeter with rapid temperature control. BioTechniques. 22, 176-181.

Wood, G. W., Nicholas, R. A. J., Hebert, C. N., and Thornton, D. H., 1980. Serological comparisons of avian reoviruses. J. Comp. Pathol. 90, 29-38.

Wu, H., Williams, Y., Gunn, K. S., Singh, N. K., Locy, R. D., and Giambrone, J. J., 2005. Yeast-derived σC protein-induced immunity against avian reovirus. Avian Dis. 49, 281-284.

Wyeth, J. P., Chettle, N. J., and Labram, J., 1981. Avian calicivirus. Vet. Rec. 109, 477-

Xu, W., Patrick, M. K., Hazelton, P. R., and Coombs, K. M., 2004. Avian reovirus temperature-sensitive mutant tsA12 has a lesion in major core protein σA and is defective in assembly. J. Virol. 78, 11142-11151.

Yin, H. S., Shien, J. H., and Lee, L. H., 2000. Synthesis in *Escherichia coli* of avian reovirus core protein σA and Its dsRNA-binding activity. Virology. 266, 33-41.

Zhang, X., Tang, J., Walker, S. B., O'Hara, D., Nibert, M. L., Duncan, R., and Baker, T. S., 2005. Structure of avian orthoreovirus virion by electron cryomicroscopy and image reconstruction. Virology. 343, 25-35.

Zipper, H., Brunner, H., Bernhagen, J., and Vitzthum, F., 2004. Investigations on DNA intercalation and surface binding by SYBR Green I, its structure determination and methodological implications. Nucl. Acids Res. 32, e103-

APPENDIX

Multiple alignment of ARV σC gene (1-820bp)

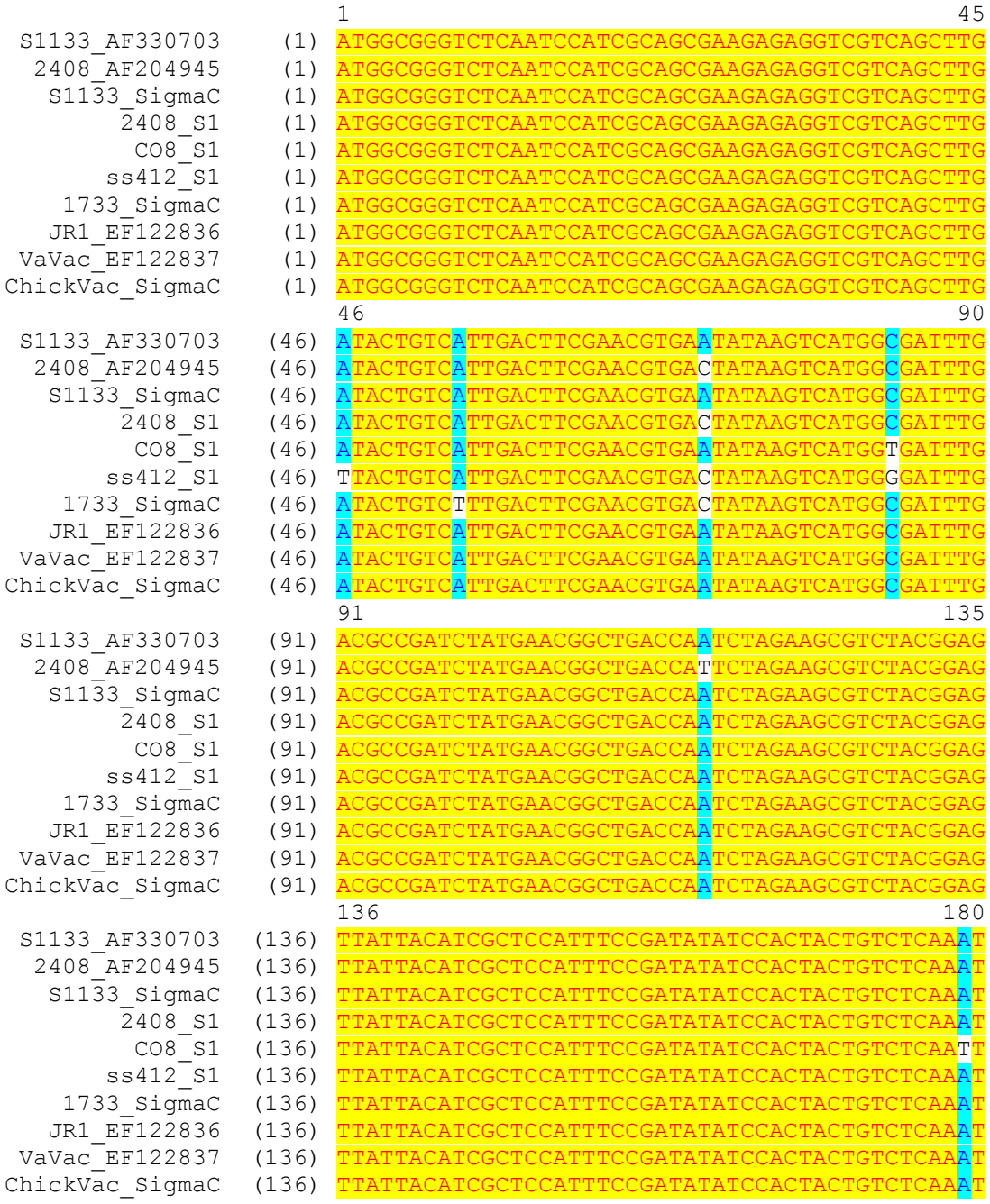

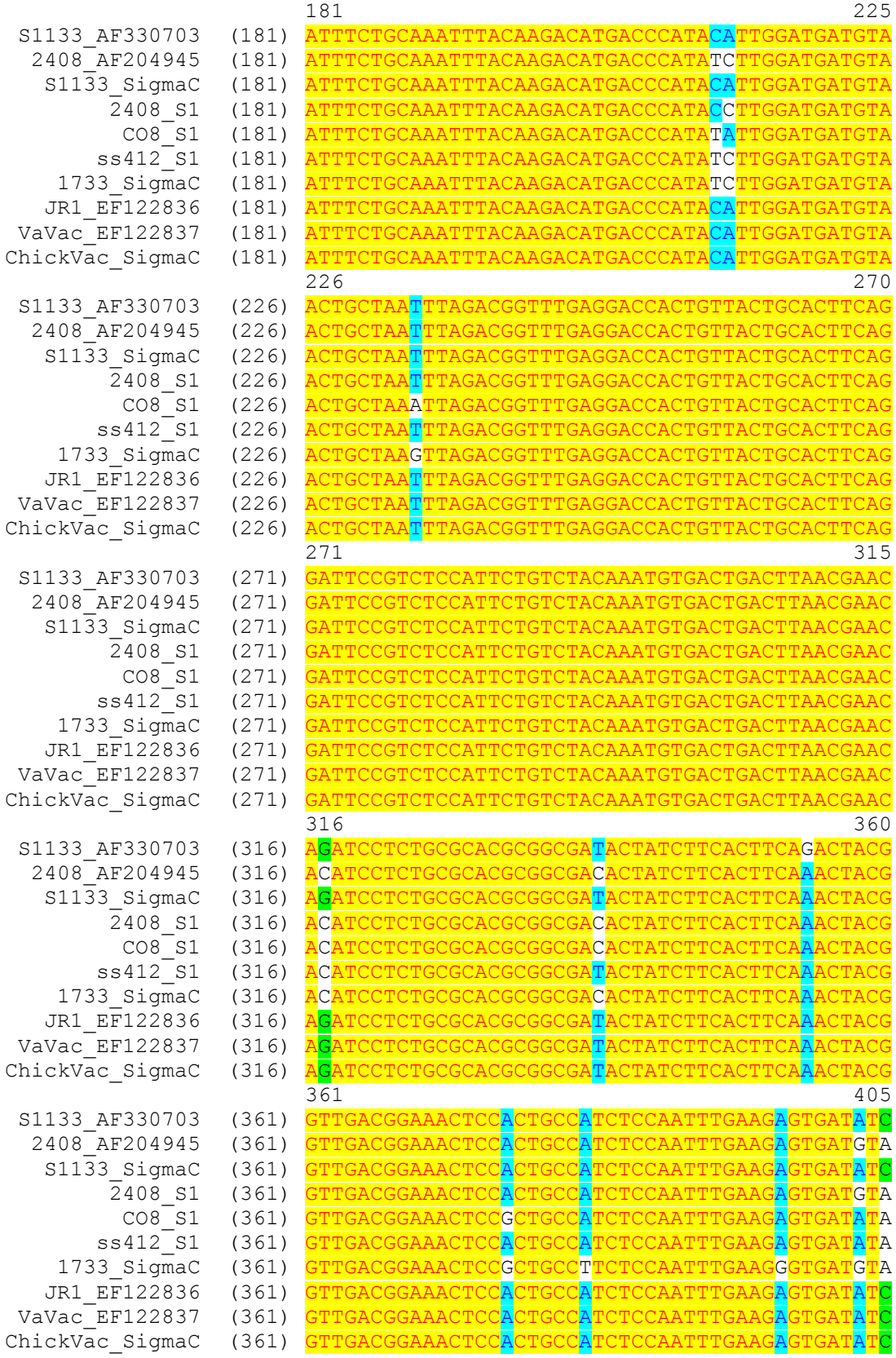
181 225
S1133_AF330703 (181) ATTTCTGCAAATTTACAAGACATGACCCATACATTGGATGATGTA
2408_AF204945 (181) ATTTCTGCAAATTTACAAGACATGACCCATATCTTGGATGATGTA
S1133_SigmaC (181) ATTTCTGCAAATTTACAAGACATGACCCATACATTGGATGATGTA
2408_S1 (181) ATTTCTGCAAATTTACAAGACATGACCCATACCTTGGATGATGTA
CO8_S1 (181) ATTTCTGCAAATTTACAAGACATGACCCATATATTGGATGATGTA
ss412_S1 (181) ATTTCTGCAAATTTACAAGACATGACCCATATCTTGGATGATGTA
1733_SigmaC (181) ATTTCTGCAAATTTACAAGACATGACCCATATCTTGGATGATGTA
JR1_EF122836 (181) ATTTCTGCAAATTTACAAGACATGACCCATACATTGGATGATGTA
VaVac_EF122837 (181) ATTTCTGCAAATTTACAAGACATGACCCATACATTGGATGATGTA
ChickVac_SigmaC (181) ATTTCTGCAAATTTACAAGACATGACCCATACATTGGATGATGTA
226 270
S1133_AF330703 (226) ACTGCTAATTTAGACGGTTTGAGGACCACTGTTACTGCACTTCAG
2408_AF204945 (226) ACTGCTAATTTAGACGGTTTGAGGACCACTGTTACTGCACTTCAG
S1133_SigmaC (226) ACTGCTAATTTAGACGGTTTGAGGACCACTGTTACTGCACTTCAG
2408_S1 (226) ACTGCTAATTTAGACGGTTTGAGGACCACTGTTACTGCACTTCAG
CO8_S1 (226) ACTGCTAAATTAGACGGTTTGAGGACCACTGTTACTGCACTTCAG
ss412_S1 (226) ACTGCTAATTTAGACGGTTTGAGGACCACTGTTACTGCACTTCAG
1733_SigmaC (226) ACTGCTAAGTTAGACGGTTTGAGGACCACTGTTACTGCACTTCAG
JR1_EF122836 (226) ACTGCTAATTTAGACGGTTTGAGGACCACTGTTACTGCACTTCAG
VaVac_EF122837 (226) ACTGCTAATTTAGACGGTTTGAGGACCACTGTTACTGCACTTCAG
ChickVac_SigmaC (226) ACTGCTAATTTAGACGGTTTGAGGACCACTGTTACTGCACTTCAG
271 315
S1133_AF330703 (271) GATTCCGTCTCCATTCTGTCTACAAATGTGACTGACTTAACGAAC
2408_AF204945 (271) GATTCCGTCTCCATTCTGTCTACAAATGTGACTGACTTAACGAAC
S1133_SigmaC (271) GATTCCGTCTCCATTCTGTCTACAAATGTGACTGACTTAACGAAC
2408_S1 (271) GATTCCGTCTCCATTCTGTCTACAAATGTGACTGACTTAACGAAC
CO8_S1 (271) GATTCCGTCTCCATTCTGTCTACAAATGTGACTGACTTAACGAAC
ss412_S1 (271) GATTCCGTCTCCATTCTGTCTACAAATGTGACTGACTTAACGAAC
1733_SigmaC (271) GATTCCGTCTCCATTCTGTCTACAAATGTGACTGACTTAACGAAC
JR1_EF122836 (271) GATTCCGTCTCCATTCTGTCTACAAATGTGACTGACTTAACGAAC
VaVac_EF122837 (271) GATTCCGTCTCCATTCTGTCTACAAATGTGACTGACTTAACGAAC
ChickVac_SigmaC (271) GATTCCGTCTCCATTCTGTCTACAAATGTGACTGACTTAACGAAC
316 360
S1133_AF330703 (316) AGATCCTCTGCGCACGCGGCGATACTATCTTCACTTCAGACTACG
2408_AF204945 (316) ACATCCTCTGCGCACGCGGCGACACTATCTTCACTTCAAACTACG
S1133_SigmaC (316) AGATCCTCTGCGCACGCGGCGATACTATCTTCACTTCAAACTACG
2408_S1 (316) ACATCCTCTGCGCACGCGGCGACACTATCTTCACTTCAAACTACG
CO8_S1 (316) ACATCCTCTGCGCACGCGGCGACACTATCTTCACTTCAAACTACG
ss412_S1 (316) ACATCCTCTGCGCACGCGGCGATACTATCTTCACTTCAAACTACG
1733_SigmaC (316) ACATCCTCTGCGCACGCGGCGACACTATCTTCACTTCAAACTACG
JR1_EF122836 (316) AGATCCTCTGCGCACGCGGCGATACTATCTTCACTTCAAACTACG
VaVac_EF122837 (316) AGATCCTCTGCGCACGCGGCGATACTATCTTCACTTCAAACTACG
ChickVac_SigmaC (316) AGATCCTCTGCGCACGCGGCGATACTATCTTCACTTCAAACTACG
361 405
S1133_AF330703 (361) GTTGACGGAAACTCCACTGCCATCTCCAATTTGAAGAGTGATATC
2408_AF204945 (361) GTTGACGGAAACTCCACTGCCATCTCCAATTTGAAGAGTGATGTA
S1133_SigmaC (361) GTTGACGGAAACTCCACTGCCATCTCCAATTTGAAGAGTGATATC
2408_S1 (361) GTTGACGGAAACTCCACTGCCATCTCCAATTTGAAGAGTGATGTA
CO8_S1 (361) GTTGACGGAAACTCCGCTGCCATCTCCAATTTGAAGAGTGATATA
ss412_S1 (361) GTTGACGGAAACTCCACTGCCATCTCCAATTTGAAGAGTGATATA
1733_SigmaC (361) GTTGACGGAAACTCCGCTGCCTTCTCCAATTTGAAGGGTGATGTA
JR1_EF122836 (361) GTTGACGGAAACTCCACTGCCATCTCCAATTTGAAGAGTGATATC
VaVac_EF122837 (361) GTTGACGGAAACTCCACTGCCATCTCCAATTTGAAGAGTGATATC
ChickVac_SigmaC (361) GTTGACGGAAACTCCACTGCCATCTCCAATTTGAAGAGTGATATC

```
                          406                                                450
 S1133_AF330703   (406)  TCGTCGAACGGTTTAGCTATTACAGATCTGCAGGATCGTGTTAAA
  2408_AF204945   (406)  TCGTCGAACGGTTTAGCTATTACAGATCTGCAGGATCGTGTTAAA
   S1133_SigmaC   (406)  TCGTCGAACGGTTTAGCTATTACAGATCTGCAGGATCGTGTTAAA
        2408_S1   (406)  TCGTCGAACGGTTTAGCTATTACAGATCTGCAGGATCGTGTTAAA
         CO8_S1   (406)  TCGTCGAACGGTTTAGCTATTACAGATCTGCAGGATCGTGTTAAA
       ss412_S1   (406)  TCGTCGAACGGTTTAGCTATTACAGATCTGCAGGATCGTGTTAAA
    1733_SigmaC   (406)  TCGTCGAACGGTTTAGCTATTACAGATCTGCAGGATCGTGTTAAA
   JR1_EF122836   (406)  TCGTCGAACGGTTTAGCTATTACAGATCTGCAGGATCGTGTTAAA
 VaVac_EF122837   (406)  TCGTCGAACGGTTTAGCTATTACAGATCTGCAGGATCGTGTTAAA
ChickVac_SigmaC   (406)  TCGTCGAACGGTTTAGCTATTACAGATCTGCAGGATCGTGTTAAA
                          451                                                495
 S1133_AF330703   (451)  TCATTGGAGTCTACCGCGAGTCATGGTCTATCTTTTTCGCCTCCG
  2408_AF204945   (451)  TCATTGGAGTCTACCGCGAGTCATGGTCTATCTTTTTCGCCTCC
   S1133_SigmaC   (451)  TCATTGGAGTCTACCGCGAGTCATGGTCTATCTTTTTCGCCTCCG
        2408_S1   (451)  TCATTGGAGTCTACCGCGAGTCATGGTCTATCTTTTTCGCCTCCG
         CO8_S1   (451)  TCATTGGAGTCTACCGCGAGTCATGGTCTATCTTTTTCGCCTCCG
       ss412_S1   (451)  TCATTGGAGTCTACCGCGAGTCATGGTCTATCTTTTTCGCCTCCT
    1733_SigmaC   (451)  TCATTGGAGTCTACCGCGAGTCATGGTCTATCTTTTTCGCCTCCT
   JR1_EF122836   (451)  TCATTGGAGTCTACCGCGAGTCATGGTCTATCTTTTTCGCCTCCG
 VaVac_EF122837   (451)  TCATTGGAGTCTACCGCGAGTCATGGTCTATCTTTTTCGCCTCCG
ChickVac_SigmaC   (451)  TCATTGGAGTCTACCGCGAGTCATGGTCTATCTTTTTCGCCTCCG
                          496                                                540
 S1133_AF330703   (496)  CTTAGTGTCGCTGACGGCGTGGTTTCATTAGACATGGACCCCTAC
  2408_AF204945   (496)  CTTAGTGTCGCTGACGGCGTGGTTTCATTAGACATGGACCCCTAC
   S1133_SigmaC   (496)  CTTAGTGTCGCTGACGGCGTGGTTTCATTAGACATGGACCCCTAC
        2408_S1   (496)  CTTAGTGTCGCTGACGGCGTGGTTTCATTAGACATGGACCCCTAC
         CO8_S1   (496)  CTTAGTGTCGCTGACGGCGTGGTTTCATTAGACATGGACCCCTAC
       ss412_S1   (496)  CTTAGTGTCGCTGACGGCGTGGTTTCATTAGACATGGACCCCTAC
    1733_SigmaC   (496)  CTTAGTGTCGCTGACGGCGTGGTTTCATTAGACATGGACCCCTAC
   JR1_EF122836   (496)  CTTAGTGTCGCTGACGGCGTGGTTTCATTAGACATGGACCCCTAC
 VaVac_EF122837   (496)  CTTAGTGTCGCTGACGGCGTGGTTTCATTAGACATGGACCCCTAC
ChickVac_SigmaC   (496)  CTTAGTGTCGCTGACGGCGTGGTTTCATTAGACATGGACCCCTAC
                          541                                                585
 S1133_AF330703   (541)  TTCTGTTCTCAACGAGTTTCTTTAACATCATACTCGGCGGAGGCT
  2408_AF204945   (541)  TTCTGTTCTCAACGAGTTTCTTTAACATCATACTCGGCGGAGGCT
   S1133_SigmaC   (541)  TTCTGTTCTCAACGAGTTTCTTTAACATCATACTCGGCGGAGGCT
        2408_S1   (541)  TTCTGTTCTCAACGAGTTTCTTTAACATCATACTCGGCGGAGGCT
         CO8_S1   (541)  TTCTGTTCTCAACGAGTTTCTTTAACATCATACTCGGCGGAGGCT
       ss412_S1   (541)  TTCTGTTCTCAACGAGTTTCTTTAACATCATACTCGGCGGAGGCT
    1733_SigmaC   (541)  TTCTGTTCTCAACGAGTTTCTTTAACATCATACTCGGCGGAGGCT
   JR1_EF122836   (541)  TTCTGTTCTCAACGAGTTTCTTTAACATCATACTCGGCGGAGGCT
 VaVac_EF122837   (541)  TTCTGTTCTCAACGAGTTTCTTTAACATCATACTCGGCGGAGGCT
ChickVac_SigmaC   (541)  TTCTGTTCTCAACGAGTTTCTTTAACATCATACTCGGCGGAGGCT
                          586                                                630
 S1133_AF330703   (586)  CAACTAATGCAATTTCGGTGGATGGCACGGGGTACTAACGGATCA
  2408_AF204945   (586)  CAACTAATGCAATTTCGGTGGATGGCACGGGGTACTAACGGATCA
   S1133_SigmaC   (586)  CAACTAATGCAATTTCGGTGGATGGCACGGGGTACTAACGGATCA
        2408_S1   (586)  CAACTAATGCAATTTCGGTGGATGGCACGGGGTACTAACGGATCA
         CO8_S1   (586)  CAACTAATGCAATTTCGGTGGATGGCACGGGGTACTAACGGATCA
       ss412_S1   (586)  CAACTAATGCAATTTCGGTGGATGGCACGGGGTACTAACGGATCA
    1733_SigmaC   (586)  CAACTAATGCAATTTCGGTGGATGGCACGGGGTACTAACGGATCA
   JR1_EF122836   (586)  CAACTAATGCAATTTCGGTGGATGGCACGGGGTACTAACGGATCA
 VaVac_EF122837   (586)  CAACTAATGCAATTTCGGTGGATGGCACGGGGTACTAACGGATCA
ChickVac_SigmaC   (586)  CAACTAATGCAATTTCGGTGGATGGCACGGGGTACTAACGGATCA
```

```
                          631                                       675
S1133_AF330703   (631) TCTGATACCATTGACATGACCGTTAACGCTCACTGTCATGGAAGA
 2408_AF204945   (631) TCTGATACCATTGACATGACCGTTAACGCTCACTGTCATGGAAGA
  S1133_SigmaC   (631) TCTGATACCATTGACATGACCGTTAACGCTCACTGTCATGGAAGA
       2408_S1   (631) TCTGATACCATTGACATGACCGTTAACGCTCACTGTCATGGAAGA
        CO8_S1   (631) TCTGATACCATTGACATGACCGTTAACGCTCACTGTCATGGAAGA
     ss412_S1   (631) TCTGATACCATTGACATGACCGTTAACGCTCACTGTCATGGAAGA
    1733_SigmaC   (631) TCTGATACCATTGACATGACCGTTAACGCTCACTGTCATGGAAGA
   JR1_EF122836   (631) TCTGATACCATTGACATGACCGTTAACGCTCACTGTCATGGAAGA
 VaVac_EF122837   (631) TCTGATACCATTGACATGACCGTTAACGCTCACTGTCATGGAAGA
ChickVac_SigmaC   (631) TCTGATACCATTGACATGACCGTTAACGCTCACTGTCATGGAAGA
                          676                                       720
S1133_AF330703   (676) CGCACTGATTATATGATGTCGTCCACGGGAAATCTCACGGTCACT
 2408_AF204945   (676) CGCACTGATTATATGATGTCGTCCACGGGAAATCTCACGGTCACT
  S1133_SigmaC   (676) CGCACTGATTATATGATGTCGTCCACGGGAAATCTCACGGTCACT
       2408_S1   (676) CGCACTGATTATATGATGTCGTCCACGGGAAATCTCACGGTCACT
        CO8_S1   (676) CGCACTGATTATATGATGTCGTCCACGGGAAATCTCACGGTCACT
     ss412_S1   (676) CGCACTGATTATATGATGTAGTCCACGGGAAATCTCACGGTCACT
    1733_SigmaC   (676) CGCACTGATTATATGATGTCGTCCACGGGAAATCTCACGGTCACT
   JR1_EF122836   (676) CGCACTGATTATATGATGTCGTCCACGGGAAATCTCACGGTCACT
 VaVac_EF122837   (676) CGCACTGATTATATGATGTCGTCCACGGGAAATCTCACGGTCACT
ChickVac_SigmaC   (676) CGCACTGATTATATGATGTCGTCCACGGGAAATCTCACGGTCACT
                          721                                       765
S1133_AF330703   (721) AGTAACGTCGTGTTATTAACCTTCGATTTAAGTGACATAACGCAT
 2408_AF204945   (721) AGTAATGTCGTGTTATTAACCTTCGATTTAAGTGACATAACGCAT
  S1133_SigmaC   (721) AGTAACGTCGTGTTATTAACCTTCGATTTAAGTGACATAACGCAT
       2408_S1   (721) AGTAACGTCGTGTTATTAACCTTCGATTTAAGTGACATAACGCAT
        CO8_S1   (721) AGTAACGTCGTGTTATTAACCTTCGATTTAAGTGACATAACGCAT
     ss412_S1   (721) AGTAATGTCGTGTTATTAACCTTCGATTTAAGTGACATAACGCAT
    1733_SigmaC   (721) AGTAATGTCGTGTTATTAACCTTCGATTTAAGTGACATAACGCAT
   JR1_EF122836   (721) AGTAACGTCGTGTTATTAACCTTCGATTTAAGTGACATAACGCAT
 VaVac_EF122837   (721) AGTAACGTCGTGTTATTAACCTTCGATTTAAGTGACATAACGCAT
ChickVac_SigmaC   (721) AGTAACGTCGTGTTATTAACCTTCGATTTAAGTGACATAACGCAT
                          766                                       810
S1133_AF330703   (766) ATCCCATCAGACCTAGCACGTCTTGTTCCCAGTGCGGGATTCCAA
 2408_AF204945   (766) ATCCCATCAGACCTAGCACGTCTTGTTCCCAGTGCGGGATTCCAA
  S1133_SigmaC   (766) ATCCCATCAGACCTAGCACGTCTTGTTCCCAGTGCGGGATTCCAA
       2408_S1   (766) ATCCCATCAGACCTAGCACGTCTTGTTCCCAGTGCGGGATTCCAA
        CO8_S1   (766) ATCCCATCAGACCTAGCACGTCTTGTTCCCAGTGCGGGATTCCAA
     ss412_S1   (766) ATCCCATCAGACTTAGCACGTCTTGTTCCCAGTGCGGGATTCCAA
    1733_SigmaC   (766) ATCCCATCAGACTTATCACGTCTTGTTCCCAGTGCGGGATTCCAA
   JR1_EF122836   (766) ATCCCATCAGACCTAGCACGTCTTGTTCCCAGTGCGGGATTCCAA
 VaVac_EF122837   (766) ATCCCATCAGACCTAGCACGTCTTGTTCCCAGTGCGGGATTCCAA
ChickVac_SigmaC   (766) ATCCCATCAGACCTAGCACGTCTGGTTCCCAGTGCGGGATTCCAA
                          811
S1133_AF330703   (811) GCTGCGTCGT
 2408_AF204945   (811) GCTGCGTCGT
  S1133_SigmaC   (811) GCTGCGTCGT
       2408_S1   (811) GCTGCGTCGT
        CO8_S1   (811) GCTGCGTCGT
     ss412_S1   (811) GCTGCGTCGT
    1733_SigmaC   (811) GCTGCGTCGT
   JR1_EF122836   (811) GCTGCGTCGT
 VaVac_EF122837   (811) GCTGCGTCGT
ChickVac_SigmaC   (811) GCTGCGTCGT
```